Electromagnetic Interference of Equipment in Power Supply Networks

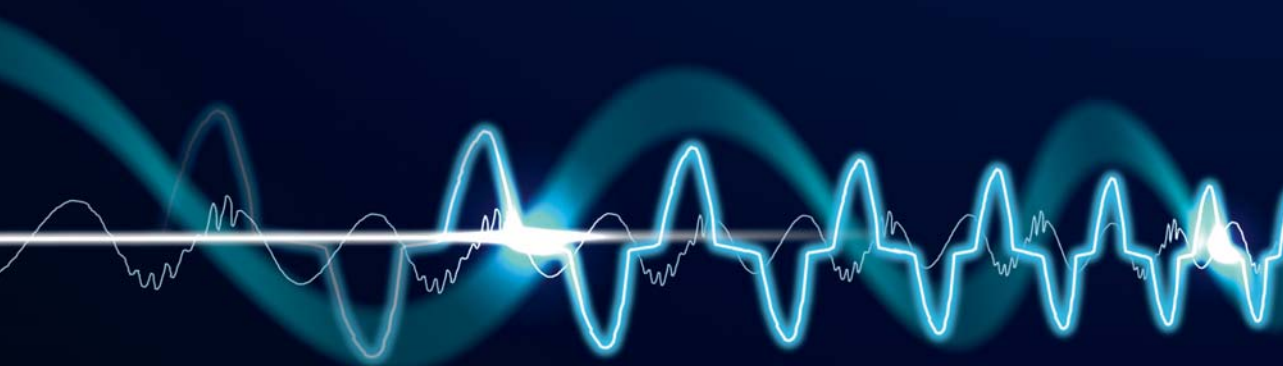

Roelof Bernardus Timens

Electromagnetic Interference of Equipment in Power Supply Networks

by

Roelof Bernardus Timens

Samenstelling van de promotiecommissie:

prof.dr.ir.	A.J. Mouthaan	Universiteit Twente (voorzitter & secretaris)
prof.dr.ir.	F.B.J. Leferink	Universiteit Twente (promotor)
prof.dr.ir.	J.F.G. Cobben	Technische Universiteit Eindhoven (co-promotor)
prof.dr.ir.	G.J.M. Smit	Universiteit Twente
dr.ir.	M.J. Bentum	Universiteit Twente
prof.ir.	M. Antal	Technische Universiteit Eindhoven
prof.dr.	F.G. Canavero	Politecnico di Torino, Italië
prof.dr.	D.W.P. Thomas	The University of Nottingham, Verenigd Koninkrijk

Het onderzoek beschreven in dit proefschrift is uitgevoerd in de leerstoel Telecommunication Engineering, die deel uitmaakt van de Faculteit Elektrotechniek, Wiskunde en Informatica aan de Universiteit Twente, Enschede.

Ministerie van Economische Zaken

De promotieplaats van de auteur is mede gefinancierd door Agentschap NL in het kader van het Innovatiegerichte Onderzoeksprogramma Elektromagnetische Vermogenstechniek (project 08113).

CTIT

CTIT Ph.D. Thesis Series No. 13-265
Centre for Telematics and Information Technology
P.O. Box 217
7500 AE Enschede, The Netherlands

ISBN: 978-90-365-0719-6
ISSN: 1381-3617 (CTIT Ph.D. Thesis Series No. 13-265)
DOI: 10.3990/1.9789036507196

Printed by Gildeprint Drukkerijen, Enschede, The Netherlands
Cover designed by Wieneke Breed in GIMP
Typeset in LaTeX 2ε

Electromagnetic Interference of Equipment in Power Supply Networks

Proefschrift

ter verkrijging van
de graad van doctor aan de Universiteit Twente,
op gezag van de rector magnificus,
prof.dr. H. Brinksma,
volgens besluit van het College voor Promoties
in het openbaar te verdedigen
op vrijdag 08 november 2013 om 16.45 uur

door

Roelof Bernardus Timens

geboren op 11 oktober 1984
te Meppel

Dit proefschrift is goedgekeurd door:

De promotor:	Prof.dr.ir. F.B.J. Leferink
De co-promotor:	Prof.dr.ir. J.F.G. Cobben (Technische Universiteit Eindhoven)

Summary

Electromagnetic Compatibility (EMC) is defined by the European Directive on EMC as the 'ability of an equipment or system to function satisfactorily in its electromagnetic environment without producing intolerable electromagnetic disturbances to anything in that environment'. EMC means that equipment, which can be a single device or a system existing of connected devices, shall be designed and manufactured in such a way that:

- the electromagnetic disturbance generated by the equipment does not exceed the level above which radio and telecommunications equipment or other equipment cannot operate as intended, and
- the equipment has a level of immunity to the electromagnetic disturbance to be expected in its intended use which allows it to operate without unacceptable degradation of its intended use.

The area within EMC focusing on the operation of power distribution systems including connected equipment is called Power Quality (PQ). It involves the supply and the use of electrical power and is therefore about the interaction between voltage and current. This thesis studies this interaction for the distribution network inside large user installations. It analyzes conducted interference and models the distribution network including connected equipment. A pragmatic approach is used for the analysis which is to a large extent based on insitu measurements. The modeling approach for equipment is gray box as the modeling is based on the behavior using knowledge of the design.

The thesis starts with an overview of the description of power distribution systems. An analysis of standards related to supply and consumption of electrical power is made as these define the requirements on supplier and user of electrical power. The grid operator is responsible for the voltage quality and the consumer for the current quality, but both are strongly related. The voltage quality requirements and the equipment Electromagnetic Interference (EMI) requirements are weakly connected. Voltage quality standards cover the electrical power network of the network operator or grid. Standards with equipment EMI requirements cover single devices. No requirements on the power network of the user, Power Distribution User Network (PDUN), are defined. The PDUN interconnects all devices and the grid. Moreover, the standards do not anticipate the shift from linear to nonlinear electronic equipment.

An increasing risk of conducted EMI in modern PDUNs is resulting as more interaction will occur via the PDUN.

The fundamentals when dealing with harmonic distortion in the PDUN are analyzed by using Fourier series to describe steady state voltage and current waveforms. Not only apparent power, being equal to the product of Root Mean Square (RMS) voltage and current, but also the repetitive peaks of the current occurring as function of the power frequency has to be taken into account. The deviations of voltage waveform are a function of impedance of PDUN and equipment, and current. As the current waveform is also a function of voltage, current synchronization effects of electronic equipment can result.

Case studies are used to analyze the existent challenges for the PDUN. They illustrate the interaction between voltage waveform deviations and current waveform, and that a higher grid impedance results in a weaker coupling between PDUN and grid.

Modeling interference requires models for the equipment and PDUN. In power engineering the conventional approach is to split the impedance of cables into a Direct Current (DC) component and fundamental power frequency component. The generic network impedance in IEC 60725 is defined for the fundamental frequency only as $0.24 + j0.15\ \Omega$ for phase and $0.16 + j0.1\ \Omega$ for neutral. For interference measurements an Artificial Mains Network (AMN) or Line Impedance Stabilization Network (LISN) is used to provide a defined impedance at the terminals of the Device Under Test (DUT). The covered frequency bands start at about 9 kHz and ends between 10 to 100 MHz. The equivalent impedance of these networks is a single circuit with lumped components. To model electrical long cables, distributed lumped element circuits are used to account for propagation delay and reflection. Each circuit of the distributed circuits is electrical small. The lumped elements are extracted from transmission line equations for describing the propagation of voltage and current along the axis of the line as function of time.

Transients and surges inside PDUNs can be generated, for instance by disconnecting cables feeding equipment drawing high current. Laboratory measurements using a transient generator, extension cables and varistors representing electronic equipment show that fast transients propagate inside the PDUN. Parameters for propagation and reflection are extracted from transmission line equations. The propagation of fast transients inside the PDUN could not be evaluated as the PQ analyzers used are unsuitable for detection of high frequency phenomena with rise and durations time shorter than 1 μs. A design for high-speed multichannel data logger is proposed for future measurements.

To reduce the complexity in the design of PDUNs for large installations or large high-tech systems and to simulate large PDUNs feeding thousands of small electronic devices, gray box models are developed. The developed models describe the steady state behavior of nonlinear loads and take into account synchronous switching effects. A load without active Power Factor Correction (PFC) and a load with active PFC are used for model development. The models contain the electrical components commonly found in loads similar to

these Device Under Modeling (DUM). Current sources controlled by prototype current waveforms represent the active PFC. All parameter values of the model are determined by measurements of current and voltage waveforms at the supply terminals of the DUM.

The key result of the work presented is that conducted emission is not properly covered in the current design approaches and standardizations regarding the PDUN. This does not only yield to harmonic frequencies, but also include the frequency range above 2 kHz. The work in this thesis provides a distributed broadband description for cables and behavior models for devices. The behavior models are based on the behavior of devices and electrical components commonly found in devices. These can be used for developing new design approaches and standards. This also means that the currently uncovered area between the grid and the terminals of the equipment, the PDUN, has to be included.

Samenvatting

Elektromagnetische Compatibiliteit (EMC) wordt in de Europese EMC Richtlijn gedefinieerd als 'het vermogen van uitrusting om op bevredigende wijze in haar elektromagnetische omgeving te functioneren zonder zelf elektromagnetische storingen te veroorzaken die ontoelaatbaar zijn voor andere uitrusting in die omgeving'. Hierin wordt onder uitrusting 'elk apparaat of vaste installatie' verstaan. In de rest van deze tekst worden de termen 'apparaat' of 'apparatuur' gebruikt.

EMC betekent dat een apparaat op een zodanige manier ontworpen en gebouwd moet worden dat:

- De opgewekte elektromagnetische storing het niveau waarop radio en telecommunicatie apparatuur of andere apparatuur niet meer naar behoren kan functioneren, niet overschrijdt, en
- Deze een immuniteitsniveau ten opzichte van de te verwachten elektromagnetische storing in zijn omgeving heeft die het in staat stelt zonder ontoelaatbaar prestatieverlies zijn bedoelde functie te vervullen.

De discipline die zich binnen het vakgebied EMC bezig houdt met de werking van energie distributie netwerken inclusief de daarop aangesloten apparaten, heet Power Quality (PQ). Het gaat over levering en verbruik van elektrische energie en daarmee over de interactie tussen spanning en stroom. Dit proefschrift bestudeert deze interactie op het distributie netwerk binnen grote installaties van gebruikers. Het analyseert geleide storingen aan de hand van modellen van het netwerk en de aangesloten apparatuur. De analyses volgen een pragmatische aanpak, grotendeels gebaseerd op 'in situ' metingen. Bij de modellering wordt deels gebruikgemaakt van kennis van de apparaten ('gray-box' modellen).

Het proefschrift begint met een overzicht van energie distributie systemen. Daarbij worden normen geanalyseerd die gerelateerd zijn aan de levering en gebruik van elektrische energie, omdat deze de eisen definiëren die aan leverancier en gebruiker gesteld worden. De netwerk beheerder is verantwoordelijk voor de 'spannings-kwaliteit' terwijl de gebruiker de 'stroom-kwaliteit' bepaalt. Beiden zijn sterk van elkaar afhankelijk. De spannings-kwaliteits eisen en de eisen die aan Elektromagnetische Interferentie (EMI) worden gesteld, zijn slechts in

geringe mate met elkaar verweven. De kwaliteits-normen ten aanzien van de spanning gaan over het distributie netwerk van de netwerk beheerder. Normen over EMI gaan over individuele apparaten. Daarin worden geen eisen gesteld aan het energie distributie netwerk van de gebruiker, in dit proefschrift Power Distribution User Network (PDUN) genoemd. Dit PDUN verbindt alle apparaten op het netwerk. Daar komt bij dat de normen geen rekening houden met de transitie van lineaire naar niet lineaire elektronische apparatuur. Het resultaat is een toenemende kans op geleide EMI in de moderne PDUN's, omdat er meer interactie in de PDUN is.

Het verschijnsel harmonische vervorming tijdens normaal bedrijf wordt beschreven met Fourier reeksen van de spannings- en stroom-golfvormen. Daarbij wordt niet alleen het schijnbare vermogen, het product van de Root Mean Square (RMS) spanning en stroom, maar ook de terugkerende stroom-pieken meegenomen die in het ritme van de netfrequentie optreden. De afwijkingen op de spannings-golfvorm zijn het gevolg van stromen in het netwerk, PDUN, en de impedantie van dit netwerk en de aangesloten apparaten. Daar de stroomgolfvorm ook weer een functie is van de spanning kunnen de stromen van elektronische apparatuur synchronisatie effecten vertonen.

Voorbeelden uit de dagelijkse praktijk worden gebruikt om de uitdagingen te analyseren die tegenwoordig aan het PDUN worden gesteld. Ze illustreren de interactie tussen spanning- en stroom-golfvorm afwijkingen. Een hogere netwerk impedantie heeft tot gevolg dat de koppeling tussen het PDUN en het netwerk van de netwerk beheerder afneemt.

Om de interferenties te kunnen simuleren zijn modellen nodig van zowel het PDUN alsook van de apparatuur. Bij het ontwerp van energie distributienetten is het gangbaar de impedanties van kabels op te splitsen in een Direct Current (DC) component en een Alternating Current (AC) component die rekening houdt met de fundamentele netfrequentie. De basis netwerk impedantie, uitsluitend op de netfrequentie, wordt in de norm IEC 60725 gedefinieerd als 0.24 + j0.15 Ω voor de fase-lijnen en 0.16 + j0.1 Ω voor de neutrale lijn. Voor interferentie metingen wordt een 'Artificial Mains Network (AMN)' of 'Line Impedance Stabilization Network (LISN)' gebruikt welke een gedefinieerde impedantie heeft naar het te onderzoeken apparaat, het 'Device Under Test (DUT)', toe. De bruikbare frequentie-band begint bij ongeveer 9 kHz en eindigt tussen 10 en 100 MHz. De equivalente impedantie van deze netwerken bestaan uit een enkel circuit met discrete componenten. Als ook elektrisch lange leidingen voorkomen, worden vervangende netwerken, opgebouwd uit discrete componenten, gebruikt om looptijd vertraging en reflecties te modelleren. Elk vervangend netwerk is elektrisch klein. De component waarden worden afgeleid uit de transmissielijn vergelijkingen die de propagatie van spannings- en stroom-golven langs de lijn beschrijven.

Transiënten en overspanningen kunnen worden veroorzaakt door grote belastingen, gevoed via een kabel, aan en uit te schakelen. Met behulp van een transiënt-generator, lange kabels en varistors om de ingangen van apparatuur te simuleren, is aangetoond dat snelle transiënten zich voortplanten in een

PDUN. De propagatie parameters voor deze voortplanting en bijbehorende reflecties zijn afgeleid uit de transmissielijn vergelijkingen. Deze analyses konden niet worden gevalideerd met behulp van beschikbare commerciële PQ analysers. Deze zijn namelijk ongeschikt om verschijnselen te registreren met stijg- of periode tijden korter dan 1 μs. Om dit type metingen in de toekomst te kunnen doen, wordt er een meer-kanaals 'High-speed Data logger' ontwerp voorgesteld.

Om de complexiteit van het ontwerp van zeer grote installaties en/of grote high-tech systemen te reduceren en grote distributie netwerken te simuleren met duizenden kleine maar niet-lineaire gebruikers, zijn 'gray-box' modellen ontwikkeld. Deze modellen beschrijven het nominale gedrag van deze niet-lineaire belastingen, rekening houdend met de synchronisatie effecten. Voor de ontwikkeling van deze modellen zijn twee type belastingen gebruikt: een niet-lineaire belasting zonder actieve Power Factor Correction (PFC) en een niet-lineaire belasting mét actieve PFC. Deze modellen bevatten de electronische componenten die gewoonlijk in vergelijkbare 'apparatuur onder modellering', in het Engelse Device Under Modeling (DUM) genoemd, worden aangetroffen. Als model voor de actieve PFC worden stroombronnen gebruikt die worden gestuurd met prototype stroomgolfvormen. Alle parameter waarden van het model zijn vastgesteld door stroom- en spanningsmetingen aan de voedingsaansluitingen van de DUM.

De belangrijkste conclusie van het hier gepresenteerde werk is dat geleide emissie onvoldoende wordt meegenomen in de huidige normen en ontwerp benaderingen met betrekking tot het PDUN. Dit geldt niet alleen voor de emmissie op harmonische frequenties, maar voor de emmissie boven de 2 kHz. Het werk dat in dit proefschrift gepresenteerd wordt biedt een gedistribueerde breedband beschrijving voor kabels en gedragsmodellen voor apparatuur. De gedragsmodellen zijn gebaseerd op het gedrag van apparatuur en elektrische componenten die gewoonlijk te vinden zijn in apparatuur. Deze kunnen worden gebruikt voor de ontwikkeling van nieuwe ontwerp benaderingen en normen. Dit betekent ook dat het op dit moment niet afgedekte deel tussen het netwerk van de netwerkbeheerder en de aansluitpunten van de apparaten, het PDUN, wordt meegenomen.

Contents

List of acronyms

AC Alternating Current

ADC Analog to Digital Converter

AECTP Allied Environmental Conditions and Test Publication

AMN Artificial Mains Network

ANSI American National Standards Institute

CE Conformité Européenne

CENELEC Comité Européen de Normalisation Electrotechnique

CF Crest Factor

CFL Compact Fluorescent Light

CISPR International Special Committee on Radio Interference

CM Common Mode

COTS Commercial Off the Shelf

DC Direct Current

DDR Double Data Rate

DM Differential Mode

DoC Declaration of Conformity

DPF Displacement Power Factor

DUM Device Under Modeling

DUT Device Under Test

EMC Electromagnetic Compatibility

EMI Electromagnetic Interference

EN European Norm

FCC Federal Communications Commission

FPGA Field Programmable Gate Array

HSMC High Speed Mezzanine Card

I-THD Current Total Harmonic Distortion

IBIS Input/Output Buffer Information Specification

ICT Information and Communication Technology

IEC International Electrotechnical Commission

IEEE Institute of Electrical and Electronics Engineers

IT Insulation Terre

ITI Information Technology Industry Council

LCL Longitudinal Conversion Loss

LED Light Emitting Diode

LISN Line Impedance Stabilization Network

LVDS Low Voltage Differential Signaling

MIL-HDBK Military Handbook

MIL-STD Military Standard

NATO North Atlantic Treaty Organization

NEN Nederlandse Norm

PC Personal Computer

PCB Printed Circuit Board

PCI Peripheral Component Interconnect

PDS Power Drive System

PDUN Power Distribution User Network

PEN Protective Earth Neutral

PF Power Factor

PFC Power Factor Correction

POI Point of Interface

PQ Power Quality

PV Photovoltaic

RCD Residual Current Device

RF Radio Frequency

RMS Root Mean Square

SATA Serial Advanced Technology Attachment

SD Secure Digital

SMPS Switched Mode Power Supply

SODIMM Small Outline Dual Inline Memory Module

SSD Solid State Disk

STANAG Standardization Agreement

TC Technical Committee

THD Total Harmonic Distortion

UPS Uninterruptible Power Supply

US United States

USA United States of America

USB Universal Serial Bus

V-THD Voltage Total Harmonic Distortion

Chapter 1

Introduction

Electrical equipment is exposed to electromagnetic phenomena in its environment. In essence, three parts are involved in the coupling of electromagnetic energy as illustrated by Figure 1.1. By proper managing the production of and susceptibility to electromagnetic emission disturbance of electrical equipment can be avoided. Malfunctioning or disturbance of electrical equipment due to unwanted or unintended emission is called Electromagnetic Interference (EMI).

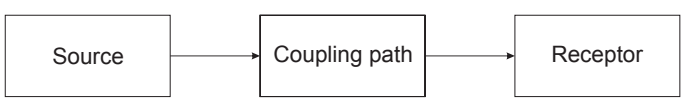

Figure 1.1: Coupling of electromagnetic energy

Electromagnetic Compatibility (EMC) is defined in the European Directive on EMC as 'the ability of equipment to function satisfactorily in its electromagnetic environment without introducing intolerable electromagnetic disturbances to other equipment in that environment', where equipment is defined as 'any apparatus or fixed installation' and electromagnetic disturbance as 'any electromagnetic phenomenon which may degrade the performance of equipment' [1]. In other words, equipment should be able to function without:

- being affected by electromagnetic emission from its environment, and
- generating electromagnetic emission affecting electrical equipment.

This can also be seen from Article 5 in the European Directive on EMC defining two essential protection requirements on the design and manufacture of equipment [1]:

- 'the electromagnetic disturbance generated does not exceed the level above which radio and telecommunications equipment or other equipment cannot operate as intended', and

- 'it has a level of immunity to the electromagnetic disturbance to be expected in its intended use which allows it to operate without unacceptable degradation of its intended use'.

Article 6 in the European Directive on EMC defines harmonized standards [1]. If equipment is compliant with the applicable harmonized standards then the equipment is presumed to be in conformity with the essential requirements. This means that a large office building containing lots of electrical equipment is presumed to fulfill the essential requirements as long as each individual piece of equipment fulfills the applicable harmonized standards. Compliance with a harmonized standard is not compulsory. However, even when there are no applicable harmonized standards defined, the equipment still has to be in compliance with the essential requirements. A graphical representation of the equipment's electromagnetic environment and coupling paths of electromagnetic energy is shown in Figure 1.2. The equipment in this figure can be a small device like a mobile phone or a large office building.

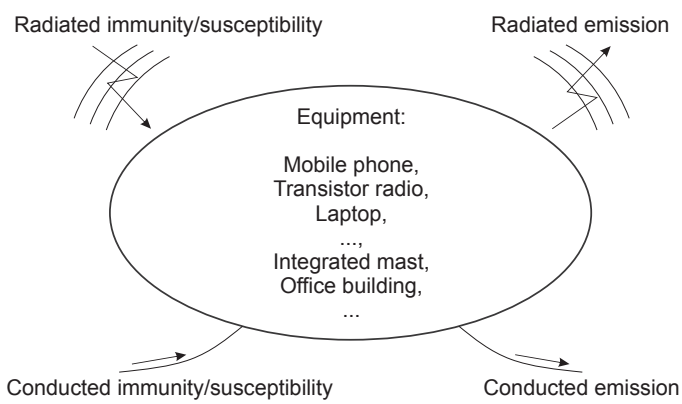

Figure 1.2: Graphical representation of equipment's electromagnetic environment and coupling paths of electromagnetic energy

The area within EMC focusing on the operation of power distribution systems including connected equipment without any malfunctioning is called Power Quality (PQ). Two entities are involved in PQ:

- the grid operator, and
- the user of electrical power.

The grid operator is responsible for the quality of the supplied voltage and the user is responsible for the quality of consumed or produced current. This is schematically shown in Figure 1.3 in which the Point of Interface (POI) is the physical connection between user and grid. The POI is also referred to as Point of Connection (POC). As at this point the user and grid operator are facing each other, POI is used in this thesis for referring to this point. Seen from

the grid, PQ is considered as a quality of supply at the POI. Voltage supply standards describe the supply of voltage and deviations. The user is supposed to fulfill the EMC standards describing the immunity and emission parameters of the connected user. Before 2003 the International Electrotechnical Commission (IEC) did not define Power Quality, but used the term EMC. Then PQ is mentioned in IEC 61000-4-30 standard 'Testing and measurement techniques - Power quality measurement methods EMC standard on Power Quality measurement methods'.

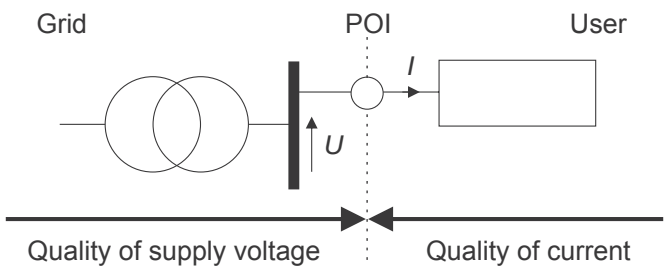

Figure 1.3: Entities involved in PQ

There is a mismatch between the voltage supply standards and the EMC standards describing the immunity and emission parameters of the connected user. The problem is that the POI is the end point of the grid operator, but the starting point for the electrical engineer of the user network. Electrical engineers of grids and installations are used to design the power distribution network using current consumption as reference. This is not valid anymore, especially not in modern grids and installations with a variety of consumers and devices. Product design engineers have to include the actual behavior of the power supply, also during abnormal situations. Examples are production plants, large buildings, offshore platforms but also the residential environment. Users in complex systems are in development phase and specific EMC measures have to be included, not to fulfill EMC standards but just for proper functioning of products. Traditional power system analysis methods are based on models that do not capture interferences from power electronics.

Many PQ problems are observed in professional applications, with many different products and systems in a complex environment. More intelligent components and dispersed generation will be implemented. All these components have to be compatible with the delivered quality of the supply voltage and may not interfere with other components. New limits on the quality of voltage and quality of currents will have an economic impact on either networks or devices and installations. Problems nowadays are solved on a case by case basis, and sometimes by huge over-design like shielding all cables, filtering all power lines, separation of cables. The economical perspective is obvious as in most cases the huge overkill in EMC measures is not needed. But the often less than 1% is creating many problems. Considering the increased complexity of

houses and buildings, and from discussion with engineers active in installation, a rapid increasing need in methodology, models and tools is foreseen. Many users within the Netherlands can be defined from students in the installation area, to industries active in off-shore, and naval engineering to electrical engineering for buildings. Furthermore, design engineers of complex systems and products are users. According [2], the annual waste in 2007 due to inadequate power quality management was € 150 billion in Europe, the majority of which is avoidable.

1.1 Research project

The research is part of the IOP EMVT program [3]. IOP stands for 'Innovatiegerichte Onderzoeksprogramma' or 'Innovation aimed Research Program' and EMVT stands for 'Elektromagnetische Vermogenstechniek' or 'Electromagnetic Power Technology'. The IOP EMVT program is financed by Agentschap NL an agency of the Dutch Ministry of Economic Affairs. EMVT is considered as a technology discipline which encompass integrated electromagnetic systems characterized by high power density, high frequency and a high efficiency thereby taking into account electric, magnetic, thermal and mechanical design aspects. As 'enabling technology', it is relevant for generation, transportation, distribution and utilization of electrical power.

The research presented in this thesis focus on the interaction between equipment via conducted interference in the Power Distribution User Network (PDUN). The PDUN is the network of the user connecting the user's equipment to the POI. Examples of PDUN are the electrical installations in office, factory and hospital buildings. Figure 1.4 shows that the PDUN is neither covered in voltage supply standards nor in EMC standards describing the immunity and emission parameters of the connected user. In The Netherlands the voltage supply standard for public supply grids is part of the law and is based on the European Norm (EN) 50160 'Voltage characteristics of electricity supplied by public distribution systems' [4]. The immunity and emission parameters of the connected user are covered by harmonized EMC standards. These standards describe the immunity and emission parameters on equipment level only.

The goal of the research is to investigate the impact of modern equipment on large and complex PDUNs. The emphasis is on interaction between equipment connected to the PDUN via conducted interference in the PDUN, schematically shown in Figure 1.4. This determines the voltage quality inside the PDUN as well as at the POI of other users. The following tasks can be identified:

- analyze and model equipment as source and victim of interference,
- analyze and model the PDUN as conducting medium (coupling path), and
- analyze propagation of transients in PDUN.

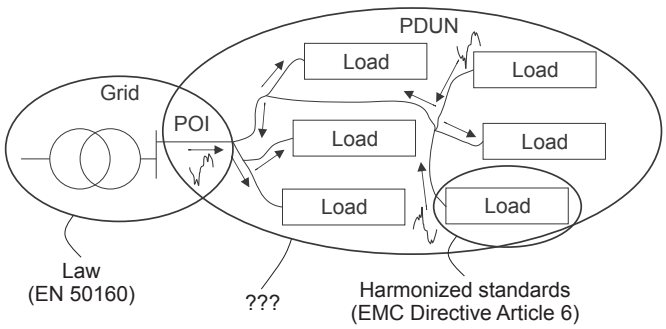

Figure 1.4: Interaction between equipment via conducted interference in the PDUN, where the PDUN is neither covered in voltage supply standards (= law) nor in EMC standards describing the immunity and emission parameters of the connected user (= harmonized standards)

The work will be used for defining a system engineering methodology which will enable power distribution network designers and product designers to prevent interference, to define proper cost-effective EMC measures, and to guarantee a minimum quality of supply to all users.

1.2 Outline of the thesis

After this introduction in the first chapter, the thesis starts in Chapter 2 with an overview of the basics of power distribution systems and conducted interference phenomena resulting from connected equipment. It introduces the main definitions, the parties involved in supply and consumption of electrical power and standards related to supply and consumption of electrical power on land and offshore.

The deployment on large scale of electronic equipment results in new challenges and revision of design approach. Chapter 3 discuss the critical fundamentals of conducted EMI resulting from modern electronic equipment. It starts with the basic description of voltage, current and power in the sinusoidal steady state. Then a shift is made to non sinusoidal periodic steady state and conventional concepts are reconsidered and put into new modern perspective. This shift in concepts has not been made in the base of the standards for supply and consumption of electrical power and design approaches. The resulting harmonic distortion in the PDUN is explained and discussed as well.

In Chapter 4 the evaluation inside the PDUN of PQ in terms of continuous and intermittent events is illustrated. The basic input circuit of low power equipment and the effect of aggregation of low power equipment on the power supply is discussed. One of the great benefits of power electronics is the very efficient power conversion resulting in a reduction of the overall active power

consumption. Besides application of power electronics in equipment consuming electrical power, power electronics are also applied in equipment for generating power. The great disadvantage of the application of power electronics is the conducted emission, due to the switching transistors, resulting in conducted EMI. Case studies of a recently constructed modern office building, farms with recently installed Photovoltaic (PV) systems and a recently constructed modern naval vessel show the resulting challenges for the PDUN which will be encountered nowadays.

As propagation path the PDUN conducts emission from and to the connected equipment. Chapter 5 introduces transmission lines equations for describing the PDUN transmission parameters. Furthermore it reviews the approach applied in power distribution engineering and Radio Frequency (RF) engineering for describing the impedance of the PDUN. In the field of power distribution engineering the typical description of PDUN impedance is limited to Direct Current (DC) component and fundamental power frequency component. In the field of RF engineering the typical description of PDUN impedance is limited to higher frequency components only, in general above 9 kHz. Both descriptions are put into perspective thereby referring to the basics of transmission line equations. It provides the fundamentals for a broader description of PDUN impedance.

In PQ literature the discussion of transients in PDUN is limited as they usually do not have a widespread effect in contrast to voltage interruptions and dips. Chapter 6 gives an analysis of the occurrence and propagation of transients in PDUN. Parameters for propagation and reflection are provided before in Chapter 5 as part of the discussion of transmission line equations. In Chapter 6 a brief overview of the history of research on transients in PDUN is given. The findings resulted in the implementation of protection against electrical fast transients and bursts as well as surges in electronic equipment. Then, the limitations of PQ measurement equipment to capture transients on cables in PDUN is discussed. Furthermore, the design of an alternative for PQ analyzers to capture fast transients is proposed. The design has not been implemented yet and a laboratory setup using a standard fast oscilloscope is used to measure the propagation of transients. The measurement results are compared to reported findings in literature on ultra wideband voltage transients.

The equipment connected to the PDUN need also be modeled in order to simulate the entire PDUN. Chapter 7 describes the development of models for two kinds of nonlinear loads commonly found, one with a rectifier bridge without Power Factor Correction (PFC) and one with a rectifier bridge with active PFC. An overview of the Device Under Modelings (DUMs) and the requirements on the model are given before presenting the models. For the models not all specific details of the DUM needs to be known, but only the details common for similar devices. The parameterization of the models is based on measurements. The simulation results are compared to measurement results and also figures on the computational load of the models are taken into account.

The thesis provides findings from the field, theory and models. As such it serves as a gateway in predicting the interaction between equipment connected to the PDUN via conducted interference in the PDUN. Ultimately it should lead to directions and rules for designing PDUNs as well equipment connected to it. Still this is future work and the thesis ends with conclusions and recommendations in Chapter 8 which can be used for making a move in defining a new system engineering methodology.

Chapter 2

Characterization of power quality

PQ has a wide interest with the modernization of power distribution systems to include renewable energy sources and information technologies to establish efficient and environment friendly use of electricity. Focusing on modern power distribution systems, the conceivable keyword in this connection is not PQ but Smart Grids, which includes also the control of and interfacing between power distribution systems. As pointed out in [5] these Smart Grids will lead to more electronic equipment in power distribution systems. It therefore stresses the need of EMC for Smart Grids and the importance of PQ to achieve EMC between the Smart Grids and connected equipment, where the Smart Grid in turn is considered as a large installation.

The work described in this thesis does not focus on Smart Grids, but the work can be applied in Smart Grids. The main focus is on conducted EMI inside large PDUNs, like large installations inside buildings and large high-tech systems. In terms of physical dimensions, the range goes up to approximately 100 meters. The source and the victim of the conducted emissions are the electronic equipment connected to the power distribution system of the end user which in turn acts as a propagation path.

This chapter gives an overview of the basics of power distribution systems in large installations and conducted interference phenomena resulting from connected equipment. Section 2.1 describes the parties involved in supply and consumption of electrical power. Section 2.2 gives an overview of standards related to supply and consumption of electrical power on land. Section 2.3 describes the differences in focus between supply standards for land and naval vessel.

2.1 Supply and consumption of electrical power

The connection between the user and the power grid, the POI, is the interface between the grid operator and user of electrical power. It can be seen as a boundary between two fields as shown in Figure 2.1.

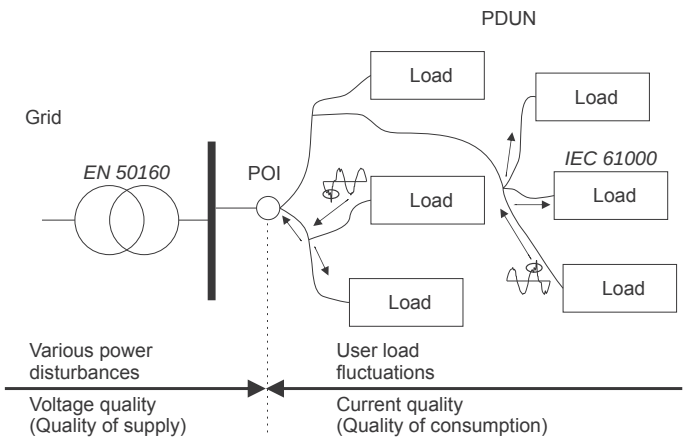

Figure 2.1: The POI interconnects the PDUN and the grid.

Starting from the grid, the grid operator is responsible for the quality of supply voltage or voltage quality [6]. The standards considering supply of voltage are effective up to the POI. In Europe the characteristics of a mains supply are defined in EN 50160 'Voltage characteristics of electricity supplied by public distribution systems' [4] to guarantee a minimum level of quality. In the Netherlands, the Netcode defines the minimum level of quality thereby referring to Nederlandse Norm (NEN) EN 50160 'Spanningskarakteristieken in openbare elektriciteitsnetten' [7]. EN 50160 standard is used as base for the NEN EN 50160 standard which has slightly more demanding requirements.

When determining voltage quality one can distinguish four categories related to voltage characteristics:

- voltage magnitude,
- voltage waveform,
- fundamental frequency of voltage or power frequency, and
- symmetry of voltage.

Any deviation in one or more of these characteristics affects the voltage quality. Examples of deviations are disturbances like:

- voltage dips or sags and interruptions,
- voltage surges or swells,

- voltage inter-harmonics, sub-harmonics, even harmonics, odd harmonics and DC components,
- temporary over voltages and voltage transients,
- (slow) voltage fluctuations,
- voltage unbalance,
- power frequency fluctuations, and
- voltage signalling disturbances.

These disturbances can originate from malfunctioning or failures like lightning and short-circuits to switching operations for operating and controlling the power distribution networks to operation of loads like switch mode power supplies injecting harmonics into the distribution networks. Some examples of disturbed voltage waveforms are shown in Figure 2.2.

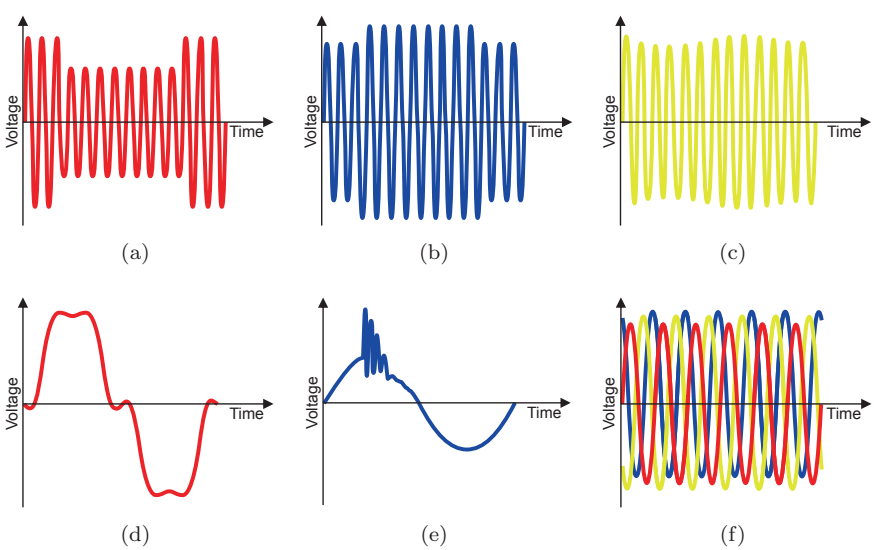

Figure 2.2: Disturbed voltage waveforms: (a) voltage dip; (b) voltage surge; (c) voltage fluctuations; (d) harmonic voltage distortion; (e) transient voltage; and, (f) voltage unbalance (three phase voltages).

The loads can influence to a large extent the voltage quality while being dependent on the voltage quality for functioning. The user is responsible for the current quality [6]. Its network, PDUN, has to be compliant to the standards covering emission and immunity of installations and equipment. Within the European Union all equipment and fixed installations put on the market shall fulfill the essential requirements of the European Directive on EMC [1]. As long

as equipment is compliant to the applicable standards in the EN 61000 series it is considered to fulfill the essential requirements and thus it can be connected to the PDUN and with it to the grid. The EN 61000-3 series consider the current emission, while the EN 61000-4 series consider the immunity to voltage variations. These voltage variations for apparatus level should be related to the PQ figures as listed in the EN 50160.

2.2 Standards for supply and consumption of electrical power

In the previous section, references to standards related to EMC and electrical power supply and consumption were made. This section discusses these standards in more detail. First an overview of IEC Basic EMC publications is given followed by the aspects focusing on electrical power supply and consumption. An evaluation showing confined conformity between standards for electrical power supply and consumption concludes this section.

IEC publications are not required to be implemented, but are used as base for legislation. An IEC standard can be adopted by Comité Européen de Normalisation Electrotechnique (CENELEC), with or without small modifications, and then the prefix IEC is replaced by EN. The reverse is also possible. A standard can be used in legal terms when it has been published in the Official Journal of the European Union, and then it is called a Harmonized Standard. The same applies to the Dutch NEN, which is used as NEN IEC or NEN EN.

The IEC Basic EMC publications are referred to as IEC 61000 series [8]. They can be considered as the starting point to achieve EMC since they define the general conditions or rules which are essential for it. As such, they make up the framework for the IEC technical committees to develop EMC Product standards. Two types of Basic EMC publications can be distinguished. Guidelines are given in non-normative Technical Reports and strict regulations are given in normative International Standards. The main goal is to set maximum levels for emission and minimum levels for immunity based on probability density functions. For setting limits use is made of compatibility levels which is defined by the IEC as: 'the specified electromagnetic disturbance level used as a reference level for co-ordination in the setting of emission and immunity limits.' This reference level for disturbance will be exceeded by a small probability for example 5% or 0.5%.

The IEC 61000 series is listed as follows:

Part 1: General

Safety function requirements

Safety integrity requirements

Part 2: Environment

Description of the environment

Classification of the environment

Compatibility levels

Part 3: Limits

Emission limits

Immunity limits

Part 4: Testing and measurement techniques

Measurement techniques

Testing techniques

Part 5: Installation and mitigation guidelines

Installation guidelines

Mitigation methods and devices

Part 6: Generic standards

Part 9: Miscellaneous

Formally Part 3 is not a Basic EMC publication but it is part of the IEC 61000 series. Parts 7 and 8 are left open for future use.

Part 2 of the IEC 61000-2 includes publications covering the grid. Examples are listed in Table 2.1. The main focus of these Technical Reports is on describing voltage characteristics and guidelines for further development of standardization.

Table 2.1: IEC 61000 publications covering grid

IEC 61000-2-2: Environment - Compatibility levels for low-frequency conducted disturbances and signalling in public low-voltage power supply systems
IEC 61000-2-8: Environment - Voltage dips and short interruptions on public electric power supply systems with statistical measurement results
IEC 61000-2-12: Environment - Compatibility levels for low-frequency conducted disturbances and signalling in public medium-voltage power supply systems

Also some Technical Reports have been published for connection of large installations, or installations injecting or drawing large currents, giving rise to undesirable deviations in grid voltage characteristics. Examples are listed in Table 2.2, describing characteristics and guidelines for further development of standardization.

The IEC 61000 series includes publications for characterizing the voltage supply but it does not set the limits. As described in the IEC 61000-4-30 'Power quality measurement methods' [9], IEC 61000 standards are strongly related to

Table 2.2: IEC 61000 publications covering connection of installations having the potential of disturbing the grid

IEC 61000-3-6: Limits - Assessment of emission limits for the connection of distorting installations to MV, HV and EHV power systems
IEC 61000-3-7: Limits - Assessment of emission limits for the connection of fluctuating installations to MV, HV and EHV power systems
IEC 61000-3-14: Assessment of emission limits for harmonics, interharmonics, voltage fluctuations and unbalance for the connection of disturbing installations to LV power systems
IEC 61000-3-15: Limits - Assessment of low frequency electromagnetic immunity and emission requirements for dispersed generation systems in LV network

the EN 50160 standard. The EN 50160 defines for public supply networks the main characteristics of the voltage delivered to a customer's PDUN, the POI, under normal operation conditions. In the scope of the standard it is emphasized that the standard is not intended to provide any levels for EMI. Nominal values and allowed deviations of voltage quality related quantities are specified in a statistical way. For example, every 10 minutes an average Root Mean Square (RMS) voltage is calculated and every week 95% and 100% probability ranges are calculated. The values corresponding to those probability ranges should be within the limits given in the EN 50160. 95% of the 10 minutes average RMS voltage intervals should be within ± 10% of the nominal voltage and 100% of the intervals should be within +10% and -15% of the nominal voltage. Additional background information and explanation on the application of the EN 50160 standard can be found in 'Guide for the application of the European Standard EN 50160' [10].

Five different categories are covered in the standards for supply and consumption:

- definitions and indices,
- tests, measurement, and monitoring techniques,
- limits for the voltage supply,
- emission limits, and
- immunity limits.

Tables 2.1 and 2.2 show that developments in standardization are ongoing. In general, developments are ongoing in all of the five above listed categories. New developments in electronics result in more EMI conducted phenomena in power supply systems and installations. To get more insight it is necessary to focus on the end user level or the PDUN and its connection to the grid, which is the main focus of this thesis.

From the end user side, or PDUN, the IEC 61000 series provides limits for emission at equipment level and testing and measurement techniques for immunity at equipment level. However, the aggregation of equipment is not taken into account in the sense that there are no limits defined. On the other side, EN 50160 gives a specification of the voltage characteristics at POI level, but by its nature it is not intended to give any limits for emission or immunity. The standards in the IEC 61000 series are prepared and worked out by Technical Committee (TC) 77 'Electromagnetic Compatibility'. TC 8 'Systems Aspects for Electrical Energy Supply' carries out the work on EN 50160. Evaluation at end user level of standards for supply and consumption results in the overview as listed in Table 2.3.

Table 2.3: EN 50160 and IEC 61000 listed by topic

EN 50160 (quality of supply)	IEC 61000 (quality of consumption)
Power frequency	IEC 61000-4-28: Testing and measurement techniques - Variation of power frequency, immunity test
Magnitude of the supply voltage	IEC 61000-4-14: Testing and measurement techniques - Voltage fluctuation immunity test
Supply voltage variations	IEC 61000-3-3: Limits - Limitation of voltage changes, voltage fluctuations and flicker in public low-voltage supply systems, for equipment with rated current $\leq$ 16 A per phase and not subject to conditional connection
	IEC 61000-3-11: Limits - Limitation of voltage changes, voltage fluctuations and flicker in public low-voltage supply systems. Equipment with rated current $\geq$ 75 A and subject to conditional connection
	IEC 61000-4-15: Testing and measurement techniques - Flickermeter. Functional and design specifications
Rapid voltage changes	IEC 61000-4-11: Testing and measurement techniques - Voltage dips, short interruptions and voltage variations immunity tests

Continued on next page

Table 2.3: EN 50160 and IEC 61000 listed by topic (cont'd)

EN 50160 (quality of supply)	IEC 61000 (quality of consumption)
Supply voltage dips	IEC 61000-4-11: Testing and measurement techniques - Voltage dips, short interruptions and voltage variations immunity tests
Short interruptions of the supply voltage	IEC 61000-4-11: Testing and measurement techniques - Voltage dips, short interruptions and voltage variations immunity tests
Long interruptions of the supply voltage	**Not covered**
Temporary power frequency overvoltages between live conductors and earth	IEC 61000-4-14: Testing and measurement techniques - Voltage fluctuation immunity test
Transient overvoltages between live conductors and earth	IEC 61000-4-4: Testing and measurement techniques - Electrical fast transient/burst immunity test
	IEC 61000-4-5: Testing and measurement techniques - Surge immunity test
Supply voltage unbalance	IEC 61000-4-27: Testing and measurement techniques - Unbalance, immunity test
Harmonic voltage	IEC 61000-4-13: Testing and measurement techniques - Harmonics and interharmonics including mains signalling at A.C. power port, low frequency immunity tests
Interharmonic voltage	IEC 61000-4-13: Testing and measurement techniques - Harmonics and interharmonics including mains signalling at A.C. power port, low frequency immunity tests
Mains signalling voltage on the supply voltage	IEC 61000-2-1: Guide to electromagnetic environment for low-frequency conducted disturbances and signalling in public power supply systems
Not covered	IEC 61000-3-2: Limits - Limits for harmonic current emissions (equipment input current $\leq$ 16 A per phase)

Continued on next page

Table 2.3: EN 50160 and IEC 61000 listed by topic (cont'd)

EN 50160 (quality of supply)	IEC 61000 (quality of consumption)
	IEC 61000-3-4: Limits - Limitation of emission of harmonic currents in low-voltage power supply systems for equipment with rated current greater than 16 A
	IEC 61000-4-16: Testing and measurement techniques - Test for immunity to conducted, common mode disturbances in the frequency range 0 Hz to 150 kHz
	IEC 61000-4-17: Testing and measurement techniques - Ripple on d.c. input power port immunity test
	IEC 61000-4-29: Testing and measurement techniques - Voltage dips, short interruptions and voltage variations on d.c. input power port immunity tests
	IEC 61000-4-30: Testing and measurement techniques - Power quality measurement methods

The developments in power electronics and electronics in general result in various types of nonlinear electronic equipment being connected close together in the PDUN. This equipment interacts via the PDUN with the risk of EMI. The PDUN is becoming more dense and complex while the standards for supply and consumption are mutually incompatible. As a result, the potential of EMI problems inside the PDUN is increasing. A single device having small rated power and emission will not disturb the supplied voltage. But, connecting lots of such devices may impact the PDUN's voltage waveform due to the inherently synchronous switching of current. Basic power electronics consisting of a rectifier bridge and bulk capacitor draw current in the peak of the supplied voltage only. An example of a heavily polluted voltage waveform measured at the terminals of a socket in office room CR 2528 in the Carré building at the University Twente is shown in Figure 2.3(a).

Furthermore, with the introduction of renewable energy in the PDUN the user becomes supplier of electrical power, injecting current in the PDUN and grid. A snapshot of the rise in voltage level at the terminals of a socket in a room of a farm is shown in Figure 2.3(b). During sunny periods some old equipment designed for a nominal RMS voltage of 220 V starts malfunctioning and after long periods of sun it became defective. The 45 kW PV system

injects current in the PDUN which is several hundreds of meters apart from the nearest transformer resulting in voltage rises up to about 30 V, which is up to about 13.6% of 220 V.

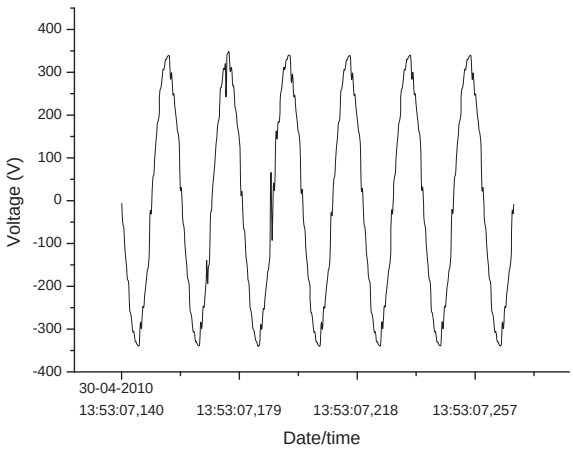

(a)

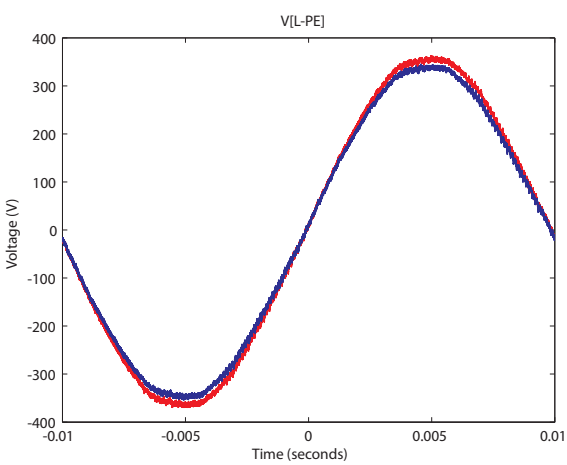

(b)

Figure 2.3: Voltage waveforms: (a) at terminals of a socket in office room CR 2528 in the Carré building at the University Twente (distribution board 2E3E group W22); and, (b) at terminals of a socket in an room of a farm with (red: 242 V) and without (blue: 228 V) current injection by PV-inverters.

The mismatch between the standards in Table 2.3 resulting in EMI, as for

example a high level of harmonic voltage distortion as in Figure 2.3(a) and an equipment malfunction caused by voltage rises due to a PV system, is not something separate. In the United States of America Institute of Electrical and Electronics Engineers (IEEE) standards are used and in particular for harmonic distortion the IEEE 519 standard [11]. It is a guide for the design of power distribution systems that include both linear and nonlinear loads. Recommended limits for voltage and current are given for conducted disturbances to the power distribution system in steady state or normal conditions. Its main focus is on the PQ at the POI. The same developments in power electronics and electronics in general are ongoing as in Europe. Also there the PDUN is becoming more dense and complex resulting in an increasing potential of EMI problems as there are nearly no legal requirements and the interest in PDUN related EMI standards is less compared to Europe.

2.3 Non public and offshore platforms

For the greater part the previous section is concentrated on civil power distribution networks on land. Among others, another application of power distribution networks is the power supply system on naval vessels, which has its own power generators and has no connection to a central power generator or distribution system. It is an instance of a decentralized or micro grid. As a naval vessel is a military off shore platform, other standards than those discussed in the previous section apply. This section focuses on these differences in standards by comparing the way limits are defined.

The PDUNs and equipment onboard of North Atlantic Treaty Organization (NATO) naval ships are required to meet the Standardization Agreement (STANAG) 1008 military standard 'Characteristics of Shipboard Electrical Power Systems in Warships of the Nato Navies [12]. The scope of STANAG 1008 standard is the quality of voltage at the terminals of the equipment. Thus it includes also the PDUN. A brief overview of limits is listed in Table 2.4. Limits for variations in RMS voltage or frequency lasting shorter than 2 seconds are less severe than the limits for variations in RMS voltage or frequency lasting 2 seconds and longer.

As already discussed in Section 2.2 the scope of EN 50160 is confined to the electricity supplied at the supply terminals or the POI. It does not deal with PDUN and equipment and the EN 50160 standard does not provide any levels for EMI. Nominal values and allowed deviations of voltage quality related quantities are specified in a statistical way. A brief overview of limits are listed in Table 2.5. The percentages between brackets are the ranges of the time period, one week or one year, for the 10 minutes mean values. A subset of the limits for each individual harmonic component up to the 13^{th} order is listed in Table 2.6.

The values for transient voltages listed in Tables 2.4 and 2.5 are indicative values. Both standards STANAG 1008 and EN 50160 mention that the given values may be exceeded occasionally. Then apart from the transient voltages,

Table 2.4: Overview STANAG 1008 limits [12]

Voltage		
Nominal voltage	115 V	440 V
Over- / under-voltage	±20% (<2 s) ±5%	
Voltage transient	1 kV	2.5 kV
Total harmonic distortion	5%	
Individual harmonic distortion	3%	
Frequency		
Nominal frequency	60 Hz	400 Hz
Over- / under-frequency	±5.5% (<2 s) ±3%	

Table 2.5: Overview EN 50160 limits [4]

Voltage	
Nominal voltage	230 V
Over- / under-voltage	±10% (95%)* +10/-15% (100%)*
Voltage transient	6 kV
Total harmonic distortion	8% (95%)*
Individual harmonic distortion	see Table 2.6 (95%)*
Frequency	
Nominal frequency	50 Hz
Over- / under-frequency	±1% (99.5%)** +4/-6% (100%)**

* range of 10 minutes mean values for 1 week

** range of 10 minutes mean values for 1 year

Table 2.6: EN 50160 harmonic voltage limits up to the 13$^{\text{th}}$ order

Harmonic order n	Limit mean RMS values (%)	Harmonic order n	Limit mean RMS values (%)
2	2	8	0.5
3	5	9	1.5
4	1	10	0.5
5	6	11	3.5
6	0.5	12	0.5
7	5	13	3

comparing STANAG 1008 and EN 50160 standards two significant differences are observed:

- STANAG 1008 limits are rigid in the sense that they hold at all times and are defined at the terminals of connected equipment, and
- STANAG 1008 limits can be used for naval equipment voltage susceptibility curves.

However, as in civil application, the connection between the voltage quality requirements and the equipment EMI is weak. The main reason is the coverage of the standards by different committees. The NATO working group on STANAG Allied Environmental Conditions and Test Publication (AECTP) is looking at a better and more coherent framework between AECTP 259 and STANAG 1008 [13]. AECTP 259 is entitled 'Electrical Power Quality and Intra-System Electromagnetic Environment' and describes the conducted emissions from Alternating Current (AC) to DC power converters impinging on equipment installed in weapon system platforms or land based communication-electronic facilities and shelters.

2.4 Summary

In a modern PDUN the risk of conducted EMI is increasing. With the introduction of nonlinear electronic equipment more interaction will occur via the PDUN. The current standards for supply and consumption of electrical power do not anticipate on these developments. Moreover, the standards for supply and consumption do not match. However, those standards are supposed to reflect the responsibilities of the grid operator and electrical power consumers. In principle, the grid operator is responsible for the voltage quality and the consumer of electrical power should be responsible for the current quality.

An improvement in standardization can be made by aligning the point of interest of the TCs to include the uncovered area between the POI and the terminals of the equipment, the PDUN. This means that requirements on the voltage quality and current quality inside the PDUN has to be defined. These requirements have to reflect the interaction between voltage and current in the PDUN and therefore the interaction between equipment via conducted interference in the PDUN. The following chapter describes the fundamentals of steady state conducted EMI resulting from modern electronic equipment.

Chapter 3

Conducted EMI due to modern electronic equipment

The degrading of PQ in PDUNs due to electronic equipment is occurring in almost all case studies discussed in next chapter. Most of the issues in those cases is about harmonic distortion. While the basics of harmonic distortion and recommended practices for mitigation of distortion as for example in [14] are known, the deployment on a large scale of electronic equipment results in new challenges. Conventional approaches need to be revised. This chapter will discuss the critical fundamentals when dealing with harmonic distortion in the PDUN. Section 3.1 discusses the basics of describing voltage, current and power in the sinusoidal steady state. Subsequently, Section 3.2 focuses on non sinusoidal periodic steady state. Section 3.3 discusses the implementation of the concepts regarding harmonic distortion in standards for supply and consumption of electrical power. The consequences of harmonic distortion on the PDUN is discussed in Section 3.4.

3.1 Sinusoidal steady state

Consider a sinusoidal signal $x(t)$ described by

$$x(t) = X_s \cos(\omega_0 t + \alpha) \tag{3.1}$$

in which the amplitude of $x(t)$ is X_s, its angular frequency is ω_0 and its phase is α. The RMS value of the signal is calculated using the following equation

$$X_{\mathrm{RMS}} = \widehat{X} = \sqrt{\frac{1}{T}\int_0^T x^2(t)\,\mathrm{d}t} = \sqrt{\frac{1}{T}\int_0^T X_s^2\cos^2(\omega_0 t+\alpha)\,\mathrm{d}t} \tag{3.2}$$
$$= \sqrt{\frac{1}{T}\int_0^T X_s^2\left[\frac{1}{2}+\frac{1}{2}\cos(2\omega_0 t+2\alpha)\right]\mathrm{d}t}$$
$$= \frac{X_s}{\sqrt{2}}$$

Using Euler's identity the signal $x(t)$ is expressed in another way as

$$x(t) = X_s\frac{\mathrm{e}^{\mathrm{j}(\omega_0 t+\alpha)}+\mathrm{e}^{-\mathrm{j}(\omega_0 t+\alpha)}}{2} \tag{3.3}$$
$$= \mathrm{Re}\left\{X_s\mathrm{e}^{\mathrm{j}(\omega_0 t+\alpha)}\right\}$$

Then using Equations 3.2 and 3.3 gives the phasor notation for describing the sinusoidal signal as

$$X = \widehat{X}\mathrm{e}^{\mathrm{j}\alpha} = \frac{X_s}{\sqrt{2}}\mathrm{e}^{\mathrm{j}\alpha} \tag{3.4}$$

Now consider a sinusoidal voltage $v(t)$ expressed in Volt (V) and current $i(t)$ expressed in Ampere (A) respectively given by

$$v(t) = \sqrt{2}\widehat{V}\cos(\omega_0 t+\alpha) \tag{3.5a}$$
$$i(t) = \sqrt{2}\widehat{I}\cos(\omega_0 t+\beta) \tag{3.5b}$$

The real power P expressed in Watt (W) is obtained by integration of the instantaneous power $p(t)$, the product of $v(t)$ and $i(t)$, over one period

$$P = \frac{1}{T}\int_0^T p(t)\,\mathrm{d}t = \frac{1}{T}\int_0^T 2\widehat{V}\widehat{I}\cos(\omega_0 t+\alpha)\cos(\omega_0 t+\beta)\,\mathrm{d}t \tag{3.6}$$
$$= \frac{1}{T}\int_0^T \widehat{V}\widehat{I}\cos(\alpha-\beta)+\widehat{V}\widehat{I}\cos(2\omega_0 t+\alpha+\beta)\,\mathrm{d}t$$
$$= \widehat{V}\widehat{I}\cos(\alpha-\beta) = \widehat{V}\widehat{I}\cos(\theta)$$

The phase difference between the voltage and current is denoted by θ. The real power P is also called active power. Using the phasor representation of the voltage and current

$$V = \widehat{V}\mathrm{e}^{\mathrm{j}\alpha} \tag{3.7a}$$
$$I = \widehat{I}\mathrm{e}^{\mathrm{j}\beta} \tag{3.7b}$$

the real power P is expressed in phaser representation as

$$\begin{aligned} P &= \mathrm{Re}\left\{\widehat{V}\widehat{I}\mathrm{e}^{\mathrm{j}\theta}\right\} \\ &= \mathrm{Re}\left\{\widehat{V}\mathrm{e}^{\mathrm{j}\alpha}\widehat{I}\mathrm{e}^{-\mathrm{j}\beta}\right\} \\ &= \mathrm{Re}\left\{VI^*\right\} \end{aligned} \tag{3.8}$$

P is the real part of the complex power S. The complex power S is expressed as

$$\begin{aligned} S = VI^* &= \widehat{V}\widehat{I}\mathrm{e}^{\mathrm{j}\theta} \\ &= \widehat{V}\widehat{I}\cos\theta + \mathrm{j}\widehat{V}\widehat{I}\sin\theta \\ &= P + \mathrm{j}Q \end{aligned} \tag{3.9}$$

where

$$P = \widehat{V}\widehat{I}\cos\theta \tag{3.10a}$$

$$Q = \widehat{V}\widehat{I}\sin\theta \tag{3.10b}$$

$$|S| = \widehat{V}\widehat{I} \tag{3.10c}$$

The imaginary part of the complex power is called reactive power and expressed in the units VAr (volt-ampere reactive). The magnitude of the complex power, $|S|$, is the apparent power and is the product of RMS values of the voltage and current. The units of complex power and apparent power is VA (volt-ampere).

The real power is the power consumed, which is needed, and the reactive power is the power flowing back and forth. The apparent power is the power which has to be delivered. This might also become clear from rewriting the instantaneous power $p(t)$ as

$$\begin{aligned} p(t) &= 2\widehat{V}\widehat{I}\cos(\omega_0 t + \alpha)\cos(\omega_0 t + \alpha - \alpha + \beta) \\ &= 2\widehat{V}\widehat{I}\cos(\omega_0 t + \alpha)\cos(\omega_0 t + \alpha + \theta) \\ &= 2\widehat{V}\widehat{I}\cos(\omega_0 t + \alpha)[\underbrace{\cos(\omega_0 t + \alpha)\cos(\theta)}_{\text{in phase}} - \underbrace{\sin(\omega_0 t + \alpha)\sin(\theta)}_{\text{quadrature}}] \end{aligned} \tag{3.11}$$

and distinguish the orthogonal components. The in phase component contributes to active power and the quadrature component to reactive power.

The power factor PF is defined as ratio of real power to apparent power

$$PF = \frac{P}{|S|} = \frac{P}{\widehat{V}\widehat{I}} = \cos\theta \tag{3.12}$$

When the PDUN is fed by a sinusoidal voltage waveform and the equipment connected to the PDUN are (or behave) linear the ratio between the apparent

power $|S|$ and real power P is only a phase shift (θ) between current and voltage. In this case the Power Factor (PF) is just a displacement power factor. Therefore, inductive loads consuming a high reactive power Q could be compensated by adding capacitors and vice versa such that the PF is 1, resulting in the same real power P as complex power S.

3.2 Periodic steady state

Any function with a form repeating itself in uniform time intervals of time T is periodic, which is expressed as

$$x(t \pm nT) = x(t) \quad \text{for } t > 0 \tag{3.13}$$

When this function describes a physical signal, it can be represented by an infinite series of trigonometric functions, a Fourier series, as follows

$$\begin{aligned} x(t) &= a_0 + a_1 \cos \omega_0 t + a_2 \cos 2\omega_0 t + \ldots + a_n \cos n\omega_0 t + \ldots \\ &\quad + b_1 \sin \omega_0 t + b_2 \sin 2\omega_0 t + \ldots + b_n \sin n\omega_0 t + \ldots \\ &= a_0 + \sum_{n=1}^{\infty} (a_n \cos n\omega_0 t + b_n \sin n\omega_0 t) \end{aligned} \tag{3.14}$$

The angular frequency of the periodic function, $\omega_0 = \frac{2\pi}{T}$, is the fundamental frequency. The integer multiples of the fundamental frequency are the harmonics. The coefficients a_n and b_n are found using the following formulas

$$a_0 = \frac{1}{T} \int_0^T x(t)\ \mathrm{d}t = \frac{1}{2\pi} \int_0^{2\pi} x(t)\ \mathrm{d}(\omega_0 t) \tag{3.15a}$$

$$a_n = \frac{2}{T} \int_0^T x(t) \cos n\omega_0 t\ \mathrm{d}t = \frac{1}{\pi} \int_0^{2\pi} x(t) \cos n\omega_0 t\ \mathrm{d}(\omega_0 t) \tag{3.15b}$$

$$b_n = \frac{2}{T} \int_0^T x(t) \sin n\omega_0 t\ \mathrm{d}t = \frac{1}{\pi} \int_0^{2\pi} x(t) \sin n\omega_0 t\ \mathrm{d}(\omega_0 t) \tag{3.15c}$$

The RMS value of the signal $x(t)$ is calculated using orthogonality as

$$\begin{aligned}\widehat{X} &= \sqrt{\frac{1}{T}\int_0^T x^2(t)\,\mathrm{d}t} \\ &= \sqrt{\frac{1}{T}\int_0^T \left(a_0 + \sum_{n=1}^{\infty}(a_n\cos n\omega_0 t + b_n \sin n\omega_0 t)\right)^2 \mathrm{d}t} \\ &= \sqrt{a_0^2 + \frac{1}{2}\left(\sum_{n=1}^{\infty} a_n^2 + \sum_{n=1}^{\infty} b_n^2\right)}\end{aligned} \tag{3.16}$$

It is the root of the sum of squared coefficients. Expressing the signal $x(t)$ using Euler's identity results in summation of exponentials

$$\begin{aligned}x(t) &= a_0 + \sum_{n=1}^{\infty} a_n \frac{\mathrm{e}^{\mathrm{j}(n\omega_0 t+\alpha_n)} + \mathrm{e}^{-\mathrm{j}(n\omega_0 t+\alpha_n)}}{2} \\ &\quad + \sum_{n=1}^{\infty} b_n \frac{\mathrm{e}^{\mathrm{j}(n\omega_0 t+\beta_n)} - \mathrm{e}^{-\mathrm{j}(n\omega_0 t+\beta_n)}}{\mathrm{j}2} \\ &= a_0 + \sum_{n=1}^{\infty} \mathrm{Re}\left\{a_n \mathrm{e}^{\mathrm{j}(n\omega_0 t+\alpha_n)}\right\} + \sum_{n=1}^{\infty} \mathrm{Im}\left\{b_n \mathrm{e}^{\mathrm{j}(n\omega_0 t+\beta_n)}\right\}\end{aligned} \tag{3.17}$$

Consider a non-sinusoidal voltage $v(t)$ expressed in Volt (V) and current $i(t)$ expressed in Ampere (A) respectively given by

$$v(t) = V_0 + V_1\cos(\omega_0 t + \alpha_1) + V_2\cos(2\omega_0 t + \alpha_2) + \ldots \tag{3.18a}$$

$$i(t) = I_0 + I_1\cos(\omega_0 t + \beta_1) + I_2\cos(2\omega_0 t + \beta_2) + \ldots \tag{3.18b}$$

where

$$V_i = \sqrt{2}\widehat{V}_i \quad \text{for } i \geq 1 \tag{3.19a}$$

$$I_j = \sqrt{2}\widehat{I}_j \quad \text{for } j \geq 1 \tag{3.19b}$$

In this Fourier series expansion V_0 and I_0 represents the DC components and V_k and I_k represent the amplitudes of the k^{th} harmonics. Since the voltage $v(t)$ and current $i(t)$ do not contain sine terms, the voltage and current can be respectively represented in phasors as

$$V = V_0 + \sum_{n=1}^{\infty} \widehat{V}_n \mathrm{e}^{\mathrm{j}\alpha_n} \tag{3.20a}$$

$$I = I_0 + \sum_{n=1}^{\infty} \widehat{I}_n \mathrm{e}^{\mathrm{j}\beta_n} \tag{3.20b}$$

The active power P is obtained by integration of $p(t)$, the product of $v(t)$ and $i(t)$, over one period. However, this integration will result in a rather extensive expression. First examine the instantaneous power $p(t)$. It consists of a product of two DC components, products of a harmonic frequency and a DC component, products of the same harmonic frequency as well as products of two different harmonic frequencies

$$\begin{aligned} p(t) &= V_0 I_0 + \sqrt{2} V_0 \sum_{s=1}^{\infty} \widehat{I}_s \cos(s\omega_0 t + \beta_s) \\ &\quad + \sqrt{2} I_0 \sum_{r=1}^{\infty} \widehat{V}_r \cos(r\omega_0 t + \alpha_r) \\ &\quad + 2 \sum_{\substack{r=1 \\ r\neq s}}^{\infty} \sum_{\substack{s=1 \\ s\neq r}}^{\infty} \widehat{V}_r \widehat{I}_s \big\{ \cos(r\omega_0 t + \alpha_r) \cos(s\omega_0 t + \beta_s) \big\} \\ &\quad + 2 \sum_{u=1}^{\infty} \widehat{V}_u \widehat{I}_u \big\{ \cos(u\omega_0 t + \alpha_u) \cos(u\omega_0 t + \beta_u) \big\} \end{aligned} \tag{3.21}$$

Then consider that only the product of the two DC components and the products of the same frequency will contribute to the active power P, resulting in

$$\begin{aligned} P &= \frac{1}{T} \int_0^T p(t)\, \mathrm{d}t \\ &= V_0 I_0 + \sum_{k=1}^{\infty} \frac{1}{T} \int_0^T V_k I_k \cos[(k\omega_0 t + \beta_k) + \theta_k] \cos(k\omega_0 t + \beta_k)\, \mathrm{d}t \\ &= V_0 I_0 + \sum_{k=1}^{\infty} \frac{V_k I_k}{2} \cos\theta_k \\ &= P_0 + \sum_{k=1}^{\infty} \widehat{V}_k \widehat{I}_k \cos\theta_k \end{aligned} \tag{3.22}$$

The complex power S can be expressed with terms voltage and current phasors as

$$\begin{aligned} S = VI^* &= \left(V_0 + \sum_{r=1}^{\infty} \widehat{V}_r \mathrm{e}^{\mathrm{j}\alpha_r} \right) \left(I_0 + \sum_{s=1}^{\infty} \widehat{I}_s \mathrm{e}^{-\mathrm{j}\beta_s} \right) \\ &= V_0 I_0 + V_0 \left(\sum_{s=1}^{\infty} \widehat{I}_s \mathrm{e}^{-\mathrm{j}\beta_s} \right) + I_0 \left(\sum_{r=1}^{\infty} \widehat{V}_r \mathrm{e}^{\mathrm{j}\alpha_r} \right) \\ &\quad + \sum_{u=1}^{\infty} \widehat{V}_u \widehat{I}_u \mathrm{e}^{\mathrm{j}\alpha_u} \mathrm{e}^{-\mathrm{j}\beta_u} + \sum_{\substack{r=1 \\ r\neq s}}^{\infty} \sum_{\substack{s=1 \\ s\neq r}}^{\infty} \widehat{V}_r \widehat{I}_s \mathrm{e}^{\mathrm{j}\alpha_r} \mathrm{e}^{-\mathrm{j}\beta_s} \end{aligned} \tag{3.23}$$

Again a product of two DC components, products of a harmonic frequency and a DC component, products of the same harmonic frequency as well as products of two different harmonic frequencies show up. Considering Equations 3.23 and 3.21 it is clear that simply adding a term $\mathrm{j}\sum_{k=1}^{\infty}\widehat{V}_k\widehat{I}_k\sin\theta_k$ to P in Equation 3.22 does not give the complex power S. However, for obtaining the apparent power $|S|$ it is not necessary to take the absolute value of Equation 3.23 as the apparent power $|S|$ can also be expressed as

$$\begin{aligned} |S| &= \widehat{V}\widehat{I} \\ &= \sqrt{{V_0}^2 + \frac{1}{2}\sum_{i=1}^{\infty} V_i^2}\sqrt{I_0^2 + \frac{1}{2}\sum_{j=1}^{\infty} I_j^2} \\ &= \sqrt{{V_0}^2 + \sum_{i=1}^{\infty} \widehat{V}_i^2}\sqrt{{I_0}^2 + \sum_{j=1}^{\infty} \widehat{I}_j^2} \end{aligned} \tag{3.24}$$

The power factor PF, ratio of real power to apparent power, is expressed as

$$PF = \frac{P}{|S|} = \frac{P_0 + \sum_{k=1}^{\infty}\widehat{V}_k\widehat{I}_k\cos\theta_k}{\sqrt{{V_0}^2 + \sum_{i=1}^{\infty}\widehat{V}_i^2}\sqrt{{I_0}^2 + \sum_{j=1}^{\infty}\widehat{I}_j^2}} \tag{3.25}$$

As long as the harmonic components, including DC, present in the voltage are also present in the current and every k^{th} harmonic current is in phase with corresponding k^{th} harmonic voltage then and only then $PF = 1$. This means that all power delivered, that is the apparent power $|S|$, is consumed and therefore is real or active power P. This will be the case for a resistive load fed by a distorted voltage waveform. Consider a perfect sinusoidal voltage waveform feeding loads drawing harmonic currents. In this case, only the part of the current component at fundamental frequency being in phase with the voltage will contribute to the active power P. The remaining part of the current, consisting of the harmonic components and the quadrature current component at fundamental frequency, is flowing back and forth contributing to the apparent power $|S|$. If the fundamental frequency component is only present in both voltage and current, Equation 3.25 for the PF reduces to Equation 3.12.

Equation 3.25 for PF is very important since it has great consequences for PDUNs and power distribution networks in general. It should be realized that:

- All harmonic components, including DC, in voltage as well as in current should be taken into account when evaluating active power, complex power, apparent power and the PF, and
- $PF = 1$ if and only if all harmonic components, including DC, present in the voltage are also present in the current and every k^{th} harmonic current is in phase with corresponding k^{th} harmonic voltage.

Furthermore it is important to note that:

- Equation 3.12 for the PF is an instance of Equation 3.25 when sinusoidal voltage and current waveforms are involved, and
- The concept of Displacement Power Factor (DPF) $\cos\theta$ as well as all related measures based on it cannot be used when non-sinusoidal waveforms are involved.

For evaluating the PQ, the PF is not enough. The PF can be high while having significant harmonic distortion in the PDUN. A measure of harmonic distortion for respectively voltage and current can be expressed as

$$V_{\text{THD 1}} = \sqrt{\sum_{i=2}^{\infty} \left(\frac{\widehat{V}_i}{\widehat{V}_1} \right)^2} \tag{3.26a}$$

$$I_{\text{THD 1}} = \sqrt{\sum_{i=2}^{\infty} \left(\frac{\widehat{I}_i}{\widehat{I}_1} \right)^2} \tag{3.26b}$$

or

$$V_{\text{THD RMS}} = \sqrt{\sum_{i=2}^{\infty} \left(\frac{\widehat{V}_i}{\widehat{V}} \right)^2} \tag{3.26c}$$

$$I_{\text{THD RMS}} = \sqrt{\sum_{i=2}^{\infty} \left(\frac{\widehat{I}_i}{\widehat{I}} \right)^2} \tag{3.26d}$$

where the fundamental component or the total RMS value can be used for normalization. However, the equations for Voltage Total Harmonic Distortion (V-THD) and Current Total Harmonic Distortion (I-THD) in Equation 3.26 do not describe the shape of the waveforms. The Crest Factor (CF) describes the shape of the waveform by expressing its peak value in terms of its RMS value.

$$CF = \frac{|x|_{\text{peak}}}{\widehat{X}} \tag{3.27}$$

The CF for 6 signals are listed in Table 3.1. A small deviation in the waveform from a pure sinusoidal will result in a CF value diverging from $\sqrt{2}$. However, it does not completely describe the difference to a perfect sinusoidal. Furthermore, it does not take into account non symmetry in the zero line. The results for a full-rectified sine wave is the same as for a sine wave.

When evaluating the PQ in terms of voltage and current waveforms, a combination of measures will be needed when the PQ is expressed in numbers. A subsystem in a PDUN drawing small currents might have a low PF, high I-THD and a CF significantly different from $\sqrt{2}$ while not affecting the voltage waveform and PDUN. On the other hand in a PDUN feeding resistive loads only both voltage and current waveforms might be heavily distorted and have a CF significantly different from $\sqrt{2}$ while the PF equals 1.

Table 3.1: CF for 6 typical signals

Signal	Peak	RMS	CF
DC	1	1	1
Sine wave	1	$\frac{1}{\sqrt{2}}$	$\sqrt{2}$
Full-wave rectified sine	1	$\frac{1}{\sqrt{2}}$	$\sqrt{2}$
Half-wave rectified sine	1	$\frac{1}{2}$	2
Triangle	1	$\frac{1}{\sqrt{3}}$	$\sqrt{3}$
Square wave	1	1	1

3.3 Implementation of concepts in standards

EN 50160 'Voltage characteristics of electricity supplied by public distribution systems' uses the nominal voltage as reference for voltage characteristics [4], but IEC 61000-4-30 'Power quality measurement methods' references harmonic measurements to the value of the fundamental component at the time of measurement [9]. CLC/TR 50422 the 'Guide for the application of the European Standard EN 50160' states that it is typical for measuring instruments to reference harmonic measurements to the RMS voltage [10]. It also states that many measuring instruments, especially those indicating Total Harmonic Distortion (THD), reference harmonic measurements to the fundamental component. When the THD is low the difference will be negligible. For rather clean waveforms the difference will be insignificant, but for distorted waveforms it will be significant.

The level of harmonic voltage distortion is a function of both harmonic currents of electronic equipment and impedance of the PDUN and the network of the grid operator. Emission limits of equipment as described in IEC 61000-3-2 'Limits for harmonic current emissions (equipment input current $\leq$ 16 A per phase)' [15], and IEC 61000-3-12 'Limits for harmonic currents produced by equipment connected to public low-voltage systems with input current $>$ 16 A and $\leq$ 75 A per phase' [16] for Europe and IEEE 519 'IEEE Recommended Practices and Requirements for Harmonic Control in Electrical Power Systems' [11] for USA are established on the basis of the reference network impedance as defined in IEC 60725 'Consideration of reference impedances and public supply network impedances for use in determining disturbance characteristics of electrical equipment having a rated current $\leq$ 75 A per phase' [17]. As illustrated in Figure 3.1 the generic network impedance is defined for the fundamental frequency only as 0.24 + j0.15 Ω for phase and 0.16 + j0.1 Ω for neutral.

Within the European Union all equipment on the market shall fulfill the essential requirements of the European Directive on EMC [1]. Emission standards are IEC 61000-3-2 and IEC 61000-3-12 are considered to be part of harmonized standards. As equipment is compliant with the applicable standard then the

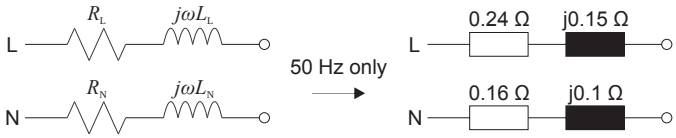

Figure 3.1: The generic network impedance is defined for the fundamental frequency.

equipment is presumed to be in conformity with the European Directive on EMC. The limits in these harmonized standards are set in such a way that voltage distortion limits can be met, assuming certain load diversity. The limits should assure that the transformer connecting customers to the grid does not transport harmonic currents in excess of 5% of its rated current. However, since virtually all electrical equipment has an power electronic interface the assumption of load diversity is not valid anymore. Nowadays it is just the opposite, only a very limited number (or no) conventional linear loads are present.

IEC 61000-3-2 defines for equipment with a rated current up to 16 A four classes. The classification is based on device type and usage, with separate emission limits for every class.

Class A: Normal usage
Balanced three-phase equipment
Household appliances
Tools
Dimmers for incandescent lamps
Audio equipment

Class B: Very short usage
Portable tools
Arc welding equipment

Class C: Continuous usage
Lighting equipment

Class D: Normal usage but special current wave shape
Personal Computers (PCs)
PC monitors
TV-sets

Depending on the rated power of the equipment, limits are specified as absolute current, as a percentage of the fundamental current or ratio of active power times a constant. As example the limits for Class C equipment are listed in

Table 3.2. The circuit power factor λ is defined as the ratio of measured active input power to the product of the supply RMS voltage and RMS current.

Table 3.2: Current limits for Class C equipment in IEC 61000-3-2

Harmonic order n	Maximum permissible harmonic current in terms of input current at fundamental frequency (%)
2	2
3	30×λ (λ = circuit power factor)
5	10
7	7
9	5
11≤ n ≤39	3

IEC 61000-3-12 defines the categories balanced three-phase devices, balanced three-phase devices under specified conditions, and other devices. All limits from this standard are specified as percentage of the fundamental current. The limits are dependent on the short circuit ratio. The short circuit ratio is defined as the ratio of the short circuit power of the supply system at the point of intended connection and the equivalent apparent power of the device. The equivalent apparent power is defined as the maximum phase apparent power of the device multiplied by three. For single-phase equipment it is three times the apparent power of the device. For devices with two or three phases, it is the highest of its phase values multiplied by three. In case of balanced three-phase equipment it is equal to the rated apparent power of the device. A higher ratio allows an higher emission of the device in percents.

The IEC 61000-3-2 and IEC 61000-3-12 are applicable to most equipment, but there are several exceptions. There are no emission limits or emission limits are relaxed for:

Equipment (not lighting) < 75 W

Professional equipment > 1000 W

Symmetrical heating control < 200 W

Independent dimmers for incandescent lamps < 1000 W

The standards do not anticipate on the effect of connecting a large number of nonlinear low power equipment to a PDUN as only a single piece of equipment is considered. Furthermore, equipment other than lighting equipment with a rated active power below 75 W is not considered at all.

3.4 Synchronous switching

In the previous section about standards, four weak points showed up. First, when evaluating the V-THD or I-THD care should be taken about normalization since significant differences will result for distorted waveforms. The differences between the RMS magnitude of the fundamental component or the RMS magnitude of the whole signal increases for increasing distortion. Second, the emission limits are based on a fundamental frequency reference impedance while the limits are defined for higher harmonics. The impedance faced by the equipment connected to the PDUN is not considered. Third, the presumption of load diversity is not valid anymore in case of similar equipment with power electronic interfaces. Examples are large office buildings where lots of identical devices are used in every office room and hallway. Fourth, no or relaxed emission limits are defined for low power equipment. The standards do not take into account the aggregation of equipment.

Low power equipment is nonlinear and dynamic. This leads to current peaks occurring twice every period. Current is drawn around the top of the voltage waveform. The voltage drop in the PDUN is a function of impedance and current. The current peaks lead to deviations in the voltage waveform, temporary flattening or decrease as function of the current. Since the current drawn by the equipment is dependent on the voltage an interaction between voltage and current waveforms takes place resulting in synchronization of current.

A large number of equipment drawing a highly distorted current will unavoidably have an impact on the voltage waveform. It is important to take into account the apparent power as well as the peak currents needed to operate the equipment. Despite the RMS value of the current being low, its peak current can be high. The voltage distortion is therefore higher than what might be expected on base of the RMS value.

3.5 Summary

In case of sinusoidal waveforms the RMS voltage and current respectively are $\frac{1}{\sqrt{2}}$ times the amplitude of the voltage and current. The voltage and current can be easily described using the phasor representation. The complex power (S) is the vectorial sum of active power (P) and imaginary reactive power (Q). The active power can be considered as the in phase component and the reactive power as the quadrature component of complex power. The PF (PF) is the ratio real power over apparent power $|S|$ and is equal to $\cos\theta$, where θ is the angle between sinusoidal current and sinusoidal voltage. The apparent power is needed while only the active power is consumed. The reactive power is flowing back and forth.

Distorted voltage and current waveforms can be described by Fourier series. Each harmonic component and DC component should be included in the expressions for RMS voltage and current as well as for power. Only the DC components and the in phase components of voltage and current harmonics of

the same order will contribute to the active power. Also in the expression for apparent power, being equal to the product of RMS voltage and current, all harmonic and DC components show up. To describe the integrity of waveforms combination of measures will be needed when being expressed in numbers. At least harmonic distortion, V-THD and I-THD, and the deviation of the peak value from the RMS value, crest factor (CF), have to be taken into account.

Standardization is based on dominant linear behavior and underestimates the impact of low power equipment on PQ. It does not take into account that virtually all equipment has power electronic interfaces resulting in nonlinear and dynamic behavior. The interaction between current and voltage result in synchronization effects of low power electronic equipment. The deviations in the voltage waveform are a function of impedance of PDUN and current. Not only apparent power, but also the peak currents needed to operate the equipment has to be taken into account. In the following chapter case studies are presented showing the interactions between current and voltage waveforms. Then not only steady state effects, but also intermittent events as cold start effects are discussed.

Chapter 4

Case studies

Developments in electronics produced a shift in society. The amount of as well as the range of application of electronic equipment is growing. Whereas several decades ago mainly linear loads were connected to the PDUN, nowadays linear loads in the PDUN are becoming very exceptional. Power electronics are used to control all kind of equipment from large electrical motors to small electronic equipment for entertainment and comfort. Beneficial properties of power electronics are low weight, small size and ease of mass production. Moreover, power electronics are very efficient in power conversion, thereby reducing the overall active power consumption.

Studies as in [18–20] show different results on emissions from large number of low power equipment. Depending on the type of equipment, type of PFC (if any), electrical components inside equipment, and considered frequency, the emissions may add constructively to a certain level. Load diversity can result in mitigation of the emission in terms of current distortion. However, in the conclusion of the studies [18–20] the demand for intensification of research is emphasized. Studies [21, 22] show an increasing level of harmonic distortion in PDUN, while there was no significant effect of low power equipment on the grid.

In this chapter the consequences of modern electronic equipment on the PDUN are discussed using a pragmatic approach. Case studies are used to illustrate the challenges which will be encountered in the future, near future or even nowadays. Before the discussion of insitu measurements in Sections 4.4–4.6 the evaluation of PQ is discussed in Section 4.1. Section 4.2 discusses the basic input circuit of low power equipment. The effect of aggregation of low power equipment on the power supply is discussed in Section 4.3. Finally, in Sections 4.4–4.6 observations are discussed made in a recently constructed modern office building, at farms with recently installed PV systems and at a recently constructed modern naval vessel.

4.1 PQ in terms of continuous and intermittent events

There are many electrical power related quantities. In many ways quality parameters can be defined to describe the quality of those quantities, including but not limited to:

- V-THD,
- I-THD,
- number of voltage dips,
- amplitude of voltage dips,
- number of voltage surges,
- amplitude of voltage surges,
- number of transients, and
- amplitude of transients.

More quality parameters for electrical power related quantities can be found in Table 2.3 of Chapter 2. Using these parameters many measurement data has been published giving a general picture of PQ variations in power grids worldwide. Real-time data on selected locations can be found on and downloaded from the website of Power Standards Lab [23]. Depending on the purpose, a different approach for data processing can be used for evaluating the PQ parameters.

Measurements have been performed at 9 places in urban and rural areas to evaluate the PQ inside PDUN and these have been published in [24]. As these 9 places are different from each other, diversity in results is obtained which is used to show the significance of taking into account short term variations. Many phenomena have been measured, such as voltage dips and surges, and frequency variations, but the V-THD is used as the first parameter for comparison with a focus on EMI. An overview of the locations is given in the following list:

1. Cartagena, Colombia, hotel room
2. Ko Samui island, Thailand, cottage on holiday park
3. Shanghai, China, hotel room
4. Enschede, Netherlands, flat in city center
5. Enschede, Netherlands, office in new campus building
6. Long Beach, USA, hotel room
7. Enschede, Netherlands, laboratory in old campus building

8. Rural area A near Enschede, Netherlands, farm with PV system
9. Rural area B near Groningen, Netherlands, converted farmhouse

Locations 1, 3, 4, 5, 6 and 7 are situated in an urban area. The other locations are several hundred meters or more away from the last transformer. The voltage is monitored at an outlet on all locations, except for location 8. On location 8, the voltage at the line from PV to the branch feeding conventional machines is monitored. The monitoring period of the different locations is between one and several weeks.

The results of the measurements are listed in Table 4.1. Three ways of expressing the V-THD has been used. The maximum value of V_{THD} during normal operation, without any special events like interruption or inrush effects, is listed in the second column. The maximum value of V_{THD} during a special event is listed in the third column. This transient peak value is actually not a harmonic distortion phenomenon despite the voltage waveform is deviating, but an indication of a failure. The time of duration of these events can be very short, up to a few periods, but those can cause EMI effects. The last measure for expressing V-THD is the upper bound of the 95% cumulative probability range of V_{THD}. This long term trend measure for V-THD is listed in the last column.

Table 4.1: Overview measured V_{THD} at 9 different locations

Location	V_{THD} max	V_{THD} transient peak	V_{THD} upper bound 95% ranges*
Cartagena, hotel	**	52.2%	2.9%
Thailand, cottage on island	5.5%	52.1%	1.5%
Shanghai, hotel	5.8%	45.5%	2.0%
Enschede, flat	6.9%	39.4%	2.8%
Enschede, new office building	8.3%	-	7.0%
Long Beach, hotel	2.2%	8.1%	2.0%
Enschede, old office building	5.6%	-	2.8%
NL, rural area A, PV	4.6%	5.1%	2.0%
NL, rural area B	2.4%	-	2.2%

* range of 10 minutes mean values for measurement period

** overwhelmed by voltage dips

The number of events with a transient peak value of V_{THD} can be different for each location. During one week of monitoring several dips and several tens of dips respectively occurred on the island in Thailand and in the hotel in Colombia. In Thailand, one day the power system became instable for more than 1 hour. The power frequency varied by 2 Hz, the level of V-THD increased by about 10% and the RMS line voltage was 15 V lower between several interruptions as shown in Figure 4.1 In Colombia there were so many

dips, that determining a maximum V_{THD} was not feasible. On the other hand, during 5 weeks of monitoring only one dip occurred in the flat in city center of Enschede.

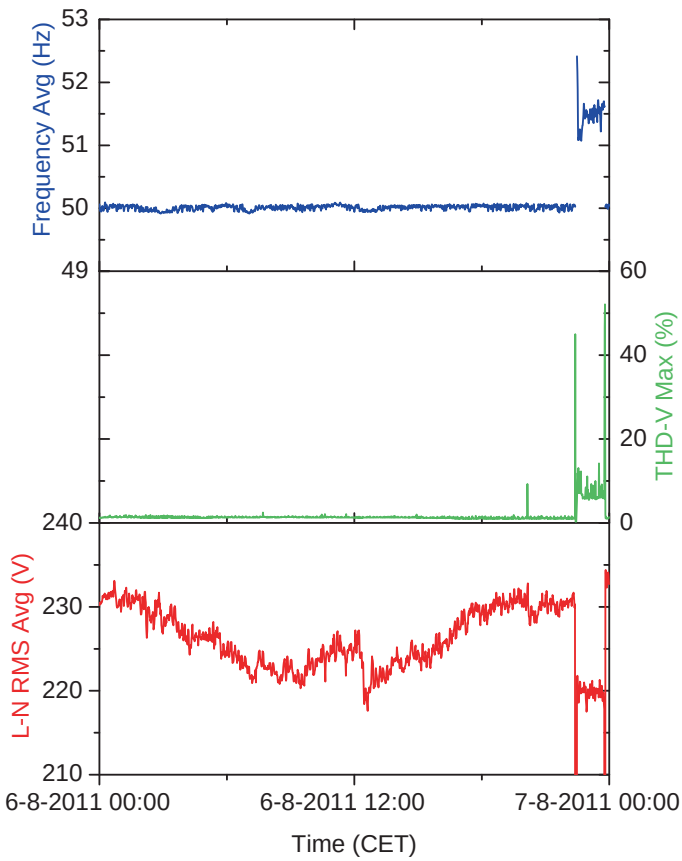

Figure 4.1: Unstable power system, as on location 2, is a potential source for EMI: (top) large power frequency variation, (middle) high V-THD, and (bottom) lower line voltage and several interruptions.

For determining the risk of EMI not only the long term conditions, but also the short term variations need to be considered. A single event causing a temporary but significant deviation of at least one PQ parameter may result in malfunctioning or disturbance of connected equipment. Therefore, in terms of measured highest V-THD, the order of presenting the list of locations is in increasing order of PQ.

4.2 Basic power electronic circuit

Rectifier bridges in single phase and three phase equipment convert AC power to DC power. Energy is stored by capacitors connected to the bridges. The charging of capacitors results in non-sinusoidal current waveforms. To compensate for this nonlinear behavior PFC can be employed using passive and active components. Furthermore, three phase equipment can be equipped with double (12 pulse) or triple (18 pulse) rectifier bridges, such that the current waveform becomes smoother as a result of extra pulses.

The basic input circuit of single phase electronic equipment consist of a rectifier diode bridge and a capacitor for energy storage feeding the DC bus. A typical example of this circuit is shown in Figure 4.2 together with the terminal voltages. The current waveform is not sinusoidal and only in the top of the voltage waveform a current pulse is drawn to charge the capacitor. By drawing non-sinusoidal current waveforms, or portions of sinusoidal current waveforms, energy saving is established.

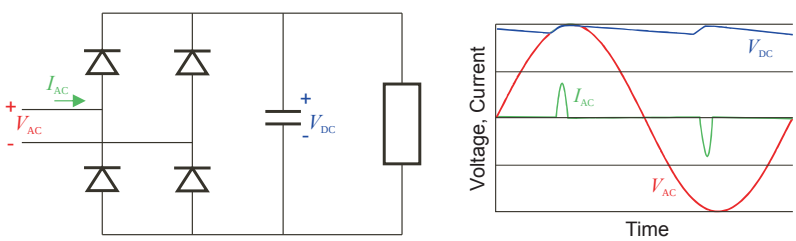

(a) (b)

Figure 4.2: Conventional rectifier: (a) circuit diagram; and, (b) terminal voltages and currents.

As an example, voltage and current waveforms are measured for an 11 W Compact Fluorescent Light (CFL) and an 1.2 W Light Emitting Diode (LED) lamp used in an office environment, in this case in the Carré building of University of Twente, and the results are respectively shown in Figures 4.3(a) and 4.3(b). The CFL, producing an equivalent number of lumen (amount of visible light) as a 60 W incandescent light bulb, needs an apparent power of 19 VA and draws a peak-to-peak current of 0.58 A. As a result of flat parts in the voltage waveform the charging current declines temporarily resulting in multiple current peaks when the DC capacitor is charged. The 1.2 W LED, producing an equivalent number of lumen as a 10 W incandescent light bulb, needs an apparent power of 4.5 VA and draws a peak-to-peak current of 0.10 A. Also in this case a declining charging current arises due to the flat parts in the voltage waveform resulting in multiple peaks in the current waveform.

Nowadays, one can find different types of electronic equipment in residential and office environments among other but not limited to:

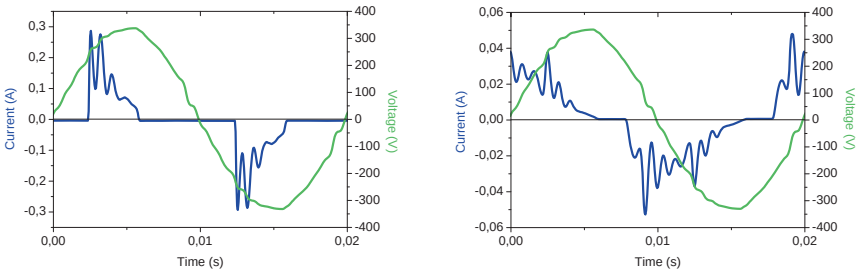

(a) (b)

Figure 4.3: Measured waveforms low power equipment: (a) Philips Genie 11 W CF light; and, (b) XQ-lite 1.2 W LED.

- TFT-screens,
- PCs,
- laptops including docking stations,
- mobile phone chargers,
- DECT-phone base stations,
- wireless-LAN routers,
- controlled lighting systems including control of sun screens,
- audio sets, and
- reading lamps.

The active power consumption of these equipment is in the order of 1–100 W. However, their apparent power can be 1.5 to 10 times higher and is therefore relative high. Especially in the no load or low load conditions, the apparent power is much higher than the real power [22]. Only the laptop charger has an active PFC circuit, which tries to make the current waveform follow the voltage waveform. In Table 4.2 the measured active power and apparent power of different types of equipment with their load condition is listed. For determining the power consumption of the equipment under test a programmable power source is used for providing a sinusoidal voltage waveform. The PF and DPF ($\cos\theta$) is listed in Table 4.3. As defined in sections 3.2 and 3.1 the PF is the ratio of active power over apparent power and the DPF is a measure for the phase shift between the fundamental components of voltage and current. When harmonic current distortion is present the PF is smaller than the DPF. This means that in most cases, the tested equipment does not behave as a linear

Table 4.2: Tested devices and measured powers

Device	Load condition	Active power (W)	Apparent power (VA)
Philips LED Warm White 2 W	on	1.4	2.9
Philips Genie 11 W	on	11.7	19.0
Philips Softone 12 W	on	11.9	19.9
XQ-lite LED strip XQ0945	on	7	16.4
Dimmer 60 W incandescent lamp	threshold	4	24.1
Dimmer 60 W incandescent lamp	±50%	37.8	51.0
HTC mobile phone charger TC-P300	no load	0.1	1.1
HTC mobile phone charger TC-P300	HTC P3700 standby	6	14.7
Dell 1504FP TFT screen	off	1.2	6.3
Dell 1504FP TFT screen	on	27.1	59.3
Delta Electronics Inc. ADP-90SB BB laptop charger	no load	0.1	18.2
Delta Electronics Inc. ADP-90SB BB laptop charger	Acer TravelMate 6593 critical battery, on	68	79.5
Dell 1504FP TFT screen + Delta Electronics Inc. ADP-90SB BB laptop charger	on Acer TravelMate 6593 on (charging)	94.3	124.5

load and the reactive power cannot be compensated by adding capacitor banks.

Current waveforms reveal more details on harmonic distortion. Waveforms of some of the equipment listed in Tables 4.2 and 4.3 measured in the Carré building of University of Twente are shown in Figures 4.4 and 4.5. An Iiyama Prolite E481S TFT screen is replacing the Dell 1504FP TFT screen showing similar shape of current waveforms for the different load conditions. In all cases switching of current is observable in the current waveform, indicating nonlinear behavior. The nonlinear behavior of the laptop charger without load is now observable. The current waveform of the AC powered laptop closest resembles the voltage waveform. In the current waveform of the system consisting of the AC-powered laptop and monitor, the sharp peak of the monitor is still recognizable. If the equipment was resistive the current waveform would have the same shape as the voltage waveform, since the current waveform of a resistor would follow the voltage waveform.

Table 4.3: Tested devices and measured power quality related parameters

Device	Load condition	PF (W/VA)	DPF ($\cos\theta$)
Philips LED Warm White 2 W	on	0.47	0.96
Philips Genie 11 W	on	0.61	0.89
Philips Softone 12 W	on	0.60	0.89
XQ-lite LED strip XQ0945	on	0.43	0.95
Dimmer 60 W incandescent lamp	threshold	0.17	0.35
Dimmer 60 W incandescent lamp	±50%	0.74	0.87
HTC mobile phone charger TC-P300	no load	0.12	0.85
HTC mobile phone charger TC-P300	HTC P3700 standby	0.41	0.98
Dell 1504FP TFT screen	off	0.19	0.22
Dell 1504FP TFT screen	on	0.46	0.97
Delta Electronics Inc. ADP-90SB BB laptop charger	no load	<0.02	<0.02
Delta Electronics Inc. ADP-90SB BB laptop charger	Acer TravelMate 6593 critical battery, on	0.86	0.95
Dell 1504FP TFT screen + Delta Electronics Inc. ADP-90SB BB laptop charger	on Acer TravelMate 6593 on (charging)	0.76	0.96

Due to the storage capacity of capacitors in the DC bus, modern electronics could withstand large frequency and voltage variation without any interference. But the capacity is not unlimited and often based on a standard dip as defined by the curve in [25]. It might be useful to allow for a large power supply variation, but at the same time this requires larger storage capacity of the DC bus. This consideration, or trade-off, is an issue to be discussed by several technical committees within the IEC. The drawback of larger DC bus energy storage with identical buffer capacitor value is the relative higher voltage in the DC bus and as a result a shorter charging time in the top of the AC voltage. Furthermore, the drawback of enlarging the buffer capacitor results in larger and heavier components as well as larger inrush currents. Higher inrush currents and shorter charging times can be solved using PFC circuits and again the trade-offs should be taken into account by the IEC. In this trade off the effect of active PFC circuits to follow the voltage waveform should be taken into account. The PFC circuit in the Delta Electronics Inc. ADP-90SB BB laptop charger tries to make the current waveform to resemble the voltage waveform

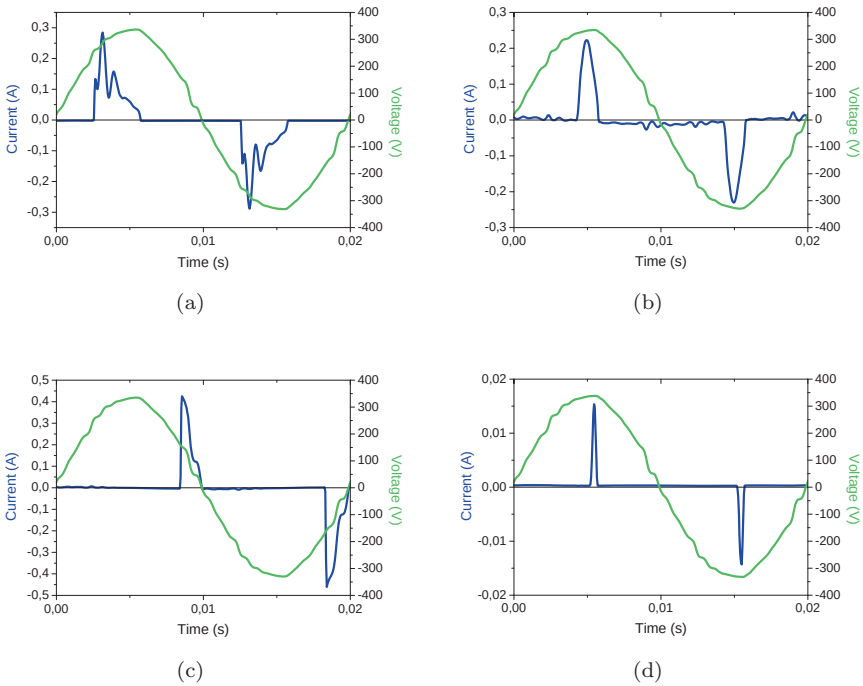

Figure 4.4: Waveforms low power equipment (1): (a) Philips Softone 12 W; (b) XQ-lite LED strip XQ0945; (c) Dimmer incandescent lamp 60 W (threshold); and, (d) HTC mobile phone charger TC-P300 (no load).

and therefore also reacts to the deviations in the voltage waveform.

The results in Tables 4.2 and 4.3 and Figures 4.4 and 4.5 show that effect of nonlinear behavior on the PF. As discussed in Section 3.2 the PF is always lower than the DPF. As most of the equipment are spared in the IEC 61000-3-2 standards, that is they are not required to meet emission limits or the emission limits they have to meet are relaxed, the nonlinear behavior is basically charging of a capacitor behind a rectifier bridge. This charging is a function of the voltage on the input of the rectifier, as a capacitor is only charged when the voltage put on it (V_{AC} in Figure 4.2) is higher than the (remaining) voltage available on the capacitor (V_{DC} in Figure 4.2). This results in the multiple peaks in the current waveforms in Figures 4.4 and 4.5. In case of PFC as implemented in the Delta Electronics Inc. ADP-90SB BB laptop charger, effort is taken to make the current waveform to resemble the voltage waveform including any deviations. The following sections in this chapter focus on the resulting synchronous switching previously discussed in Section 3.4.

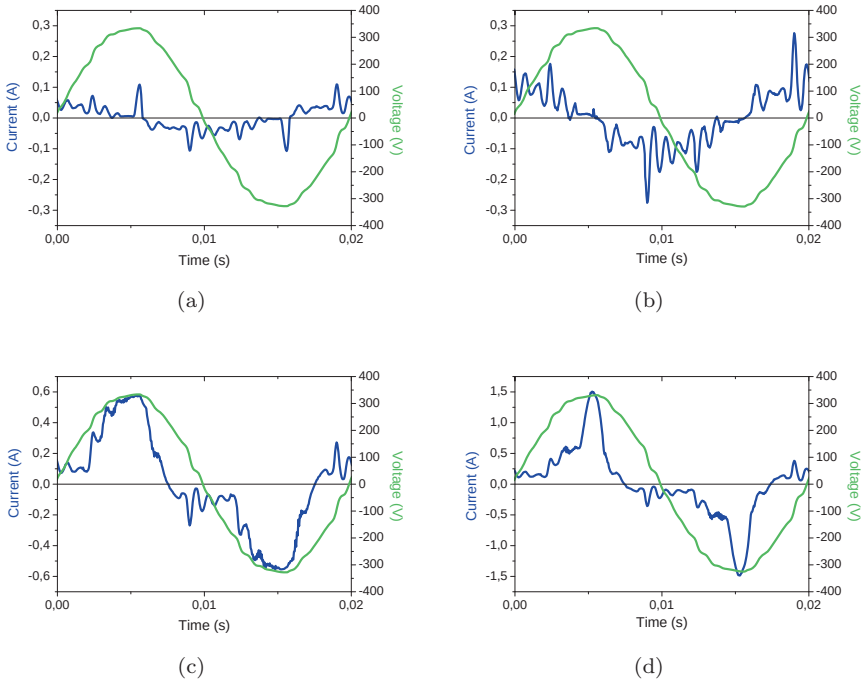

Figure 4.5: Waveforms low power equipment (2): (a) Iiyama Prolite E481S TFT screen (off); (b) Delta Electronics Inc. ADP-90SB BB laptop charger (no load); (c) Delta Electronics Inc. ADP-90SB BB (powering Acer TravelMate 6593); and, (d) Iiyama Prolite E481S TFT screen + Acer TravelMate 6593.

4.3 Strength of PDUN

In the previous section the focus was on the emission in terms of current of an individual piece of low power equipment. In this section the focus is on the effect of connecting a large number of low power equipment on the PDUN. The study is restricted two types of energy saving lamps, 11 W CFL and 2 W LED lamps, to show the influence of basic power electronics on the PDUN. First the emissions of an installation of many energy saving lights is discussed, where the installation is connected to a clean, strong PDUN [26]. Then, the strong PDUN is replaced by a weak one, simulated by a mobile power generator [27]. A schematic overview is shown in Figure 4.6. The clean, strong PDUN has an internal resistance R_G which is significant lower than the internal resistance of the mobile power generator. As a result, the voltage drop resulting from the current I_G flowing through the internal resistance R_G will be different. In the case of the strong PDUN the voltage U_M supplied to the lamps is about the

generator voltage U_G while in the case of the mobile generator the voltage U_M supplied to the energy saving lamps is significantly different from the generator voltage U_G for large current I_G.

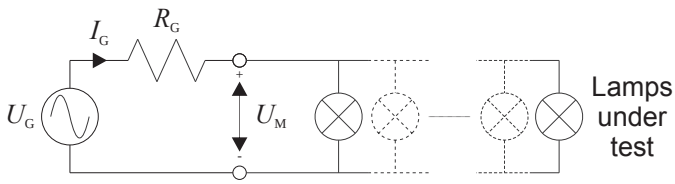

Figure 4.6: Simplified scheme for studying the influence of basic power electronics on the PDUN.

4.3.1 Strong PDUN feeding energy saving lights

An installation of energy saving lamps is constructed by connecting up to 48 CFL and LED lamps to a string, a flat cable with sockets connected in parallel. The string is fed by a programmable power source providing a clean voltage. The powers at feeding point are evaluated as function of number of lamps in Table 4.4. The PF slightly increases with increasing number of lamps. The PF of the combination of 48 LED and 48 CFL lamps is slightly better than the power factor of 48 CFL lamps.

Table 4.4: Measured power and power factor of CFL and LED lamps

Lamp type	# lamps	Active power (W)	Apparent power (VA)	Power factor (W/VA)
CFL	1	11.9	18.8	0.63
	2	22.0	35.5	0.62
	4	43.1	69.1	0.62
	8	87.5	138	0.63
	16	171	271	0.63
	32	352	553	0.64
	48	513	799	0.64
LED	1	2.06	5.76	0.36
	2	3.74	11.8	0.32
	4	8.77	23.9	0.37
	8	16.7	44.8	0.37
	16	32.9	88.3	0.37
	32	62.4	175	0.36
	48	102	270	0.38
CFL + LED	96 (48 + 48)	627	935	0.67

Increasing the number of CFL lamps result in smoothing of current. The high frequency content in the current waveform reduces with increasing number of CFL lamps as is shown in Figures 4.7(a) and 4.7(c). The effect of filtering is also observable for a single CFL lamp at the end of the string with other CFL lamps preceding it. If no other lamps are present the current waveform for a single CFL lamp at the end of the string is the same as in 4.7(a), but when 31 CFL precede it the current waveform of Figure 4.8(a) results. In contradiction to the CFL lamps there is no significant smoothing of current with increasing number of LED lamps. But a remarkable effect is the half-wave rectified current drawn by the LED lamps as shown in Figures 4.7(b) and 4.7(d). This type of LED lamps is therefore a special application of lamps. The current of LED lamps has DC as well as even harmonic components. Whether 31 LED lamps do or do not precede a single LED lamp at the end of the string, the current waveform does not significant differ from that of a single LED at the front of the string. Therefore there is no difference between Figures 4.7(b) and 4.8(a). Also in the combination of 48 LED and 48 CFL lamps the half-wave rectified current waveform of the LED lamps is significantly present as shown in Figure 4.8(c).

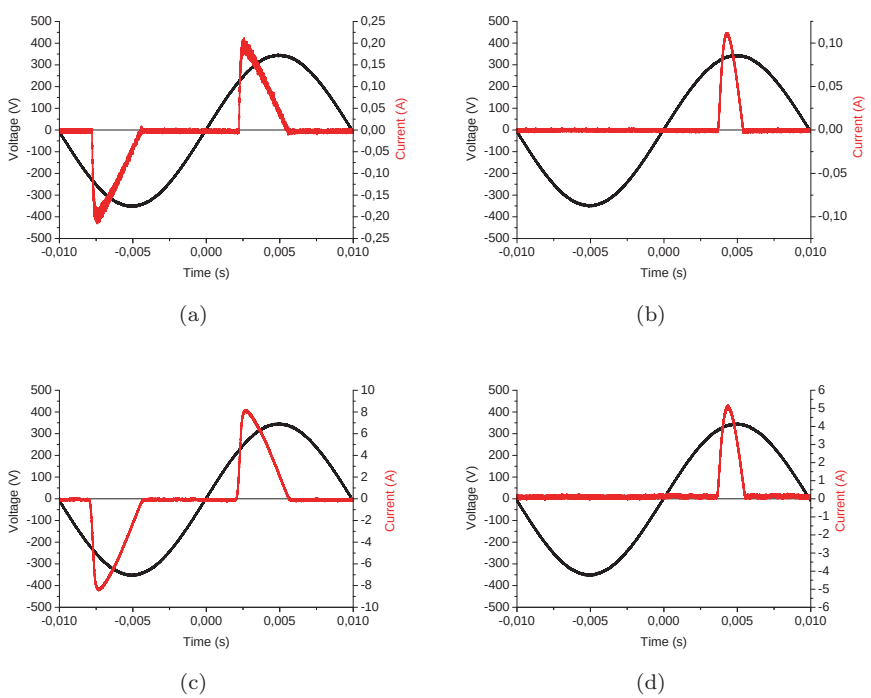

Figure 4.7: Waveforms energy saving lamps (1): (a) 1 CFL lamp; (b) 1 LED lamp; (c) 48 CFL lamps; and, (d) 48 LED lamps.

Depending on number of lamps mitigation of harmonic components arises

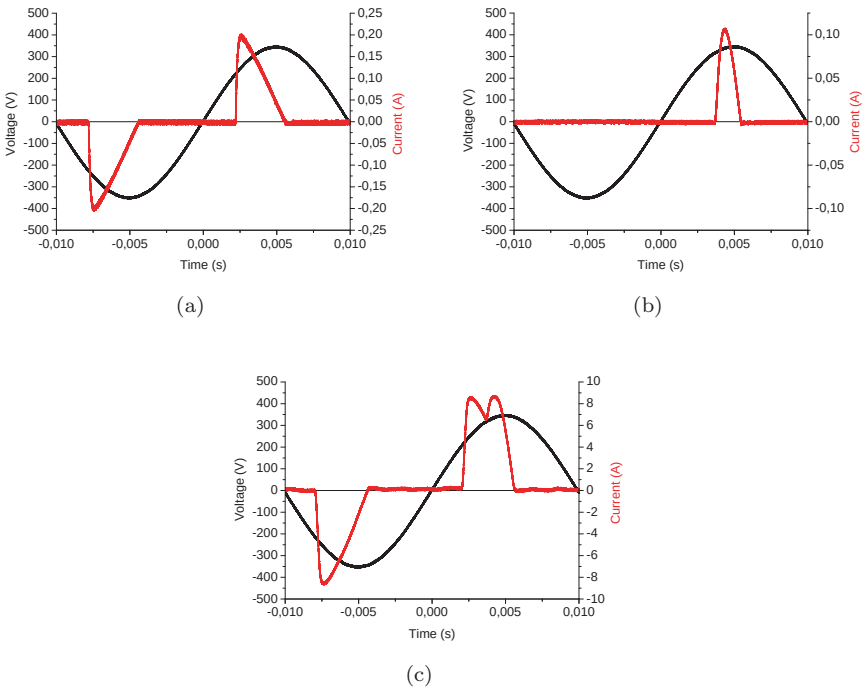

Figure 4.8: Waveforms energy saving lamps (2): (a) single CFL lamp at end of string with 31 CFL lamps preceding it; (b) single LED lamp at end of string with 31 LED lamps preceding it; and, (c) 48 LED and 48 CFL lamps.

for CFL lamps as is shown in Figure 4.9(a). For generating this spectrum plot, an EMI Test receiver is used where the 50 Hz harmonic components are evaluated in 20 Hz frequency windows. The mitigation of harmonic components corresponds to the filtering effect observed in the current waveforms as function of the number of lamps. The spectrum plot for the LED lamps is shown in Figure 4.9(b). As the shape of the current waveforms did not change significantly, the shape of the envelope of the LED lamps spectrum does also not change significantly. Because of the half-wave rectification of the LED lamp current, the even harmonic components are higher in the LED lamps current spectrum than in the CFL lamps current spectrum. In Figure 4.9(c), the spectrum of the combination of LED and CFL lamps, the harmonic components of LED and CFL lamps are distinguishable. The even harmonics due to LED lamps as well as mitigation of the harmonics resulting from the CFL lamps is clearly visible.

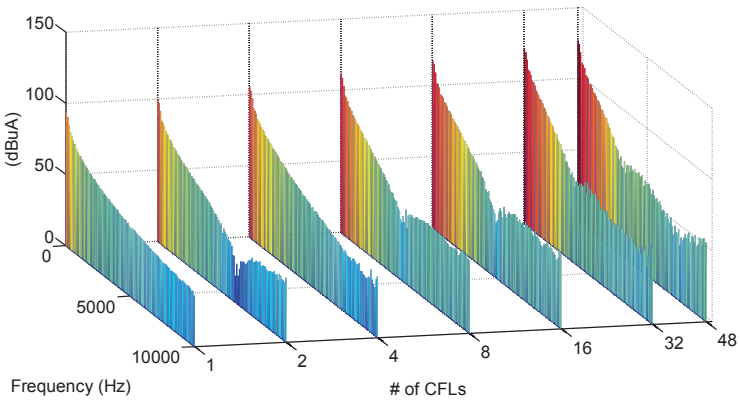

(a)

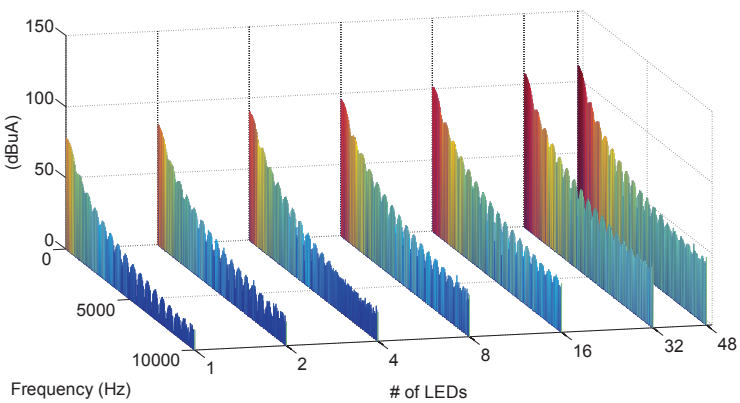

(b)

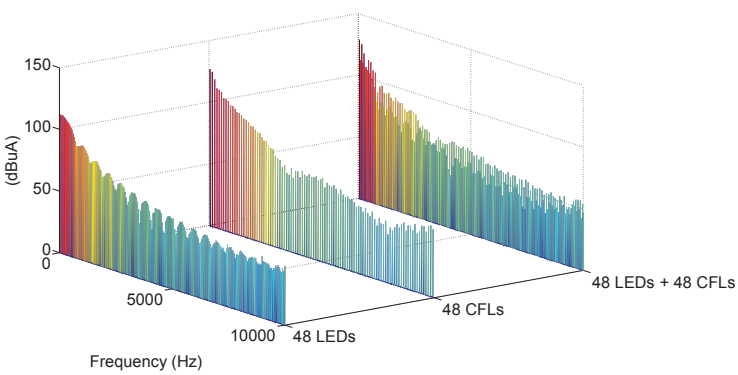

(c)

Figure 4.9: Spectrogram of total current feeding energy saving lamps: (a) up to 48 CFL lamps; (b) up to 48 LED lamps; and, (c) 48 CFL, 48 LED, and 48 CFL and 48 LED lamps.

Individual low power equipment having high levels of current distortion will not have significant effects on the power distribution network because its absolute current is small. This is reflected in the IEC 61000-3-2 standard by making exemptions on current emission limits for low power equipment as discussed in Section 3.3. A large load, such as large numbers of similar low power equipment, even having lower levels of current distortion can have a significant impact on PDUN. Despite tolerances of components of power electronics in identical loads which will give rise to spreading of current peaks or mitigation of harmonic current components. Even when this spreading is increased by mixing different kind of low power equipment equipment, the basic working principle of power electronics will result in an alignment of current peaks. The low power equipment will draw currents in or around the top of voltage waveform and as a result the current peaks are synchronized in time. The absolute current is significant and therefore a glitch in the waveform of this load can have adverse effects on the PDUN. Since, as discussed in Section 3.4, the IEC 61000-3-2 standard does not take into account the number of connected equipment to a PDUN, it does not anticipate on synchronous switching resulting from interaction between several instances of (low power) equipment.

4.3.2 Weak PDUN feeding energy saving lights

The programmable power supply is replaced by a mobile 2-stroke generator to simulate a weak PDUN. The mobile power generator has a specified rated nominal active power of 650 W and peak active power of 800 W. The zero load voltage waveform measured at the feeding point of the string is shown in Figure 4.10(a). As reference 60 W incandescent lamps are used beside the previous used 2 W LED and 11 W CFL lamps. The individual current waveforms of a single LED, CFL and incandescent lamp connected to the generator are shown in Figure 4.10(b). The current waveform of the incandescent lamp is a scaled copy of the voltage waveform. The charging of the bulk capacitor determine the current waveforms of the LED and CFL lamps.

To determine the effect of CFL lamps on the mobile generator, the waveforms feeding 32 CFL lamps and those feeding 6 incandescent lamps is plotted in Figure 4.11. The rated active power consumption is comparable: 32 x 11 W = 352 W and 6 x 60 W = 360 W respectively. As is typical for resistive loads, the waveforms at the generator ports feeding 6 incandescent lamps are scaled copies. The peak-to-peak current feeding the incandescent lamps is 4.5 A. While the rated active power is somewhat lower the peak-to-peak current feeding the 32 CFL lamps is higher, 5.3 A. Furthermore, the 32 CFL lamps give rise to voltage flattening due to the voltage drop over the internal resistance of the generator (R_G in Figure 4.6).

The resulting effects of the LED lamps on the mobile generator is even worse. The waveforms feeding 32 LED lamps are compared with 1 incandescent lamp in Figure 4.12, respectively corresponding to 64 W and 60 W active power.

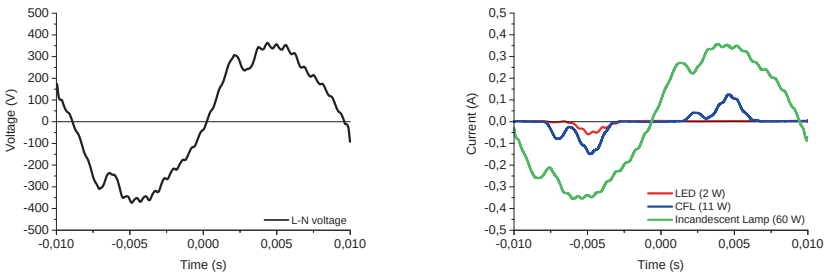

(a) (b)

Figure 4.10: Waveforms for reference mobile power generator: (a) zero load voltage waveform; and, (b) current waveforms 2 W LED, 11 W CFL and 60 W incandescent lamp.

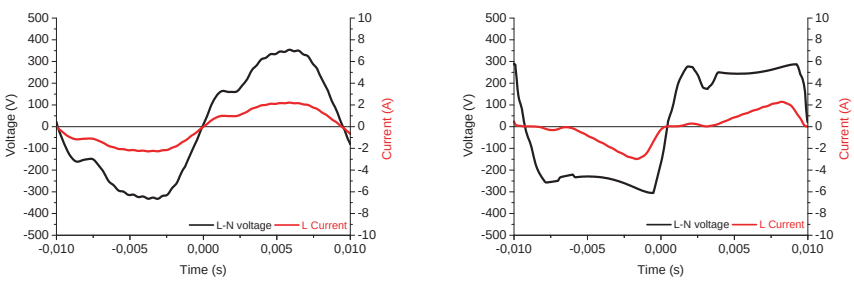

(a) (b)

Figure 4.11: Effect of CFL lamps on mobile power generator: (a) current and voltage waveforms 6 incandescent lamps; and, (b) current and voltage waveforms 32 CFL lamps.

The differences in minimum and maximum current for the LED (1.4 A) is twice the peak-to-peak current of the incandescent lamp (0.7 A). The LED lamps only draws current in the first half of the period such that the voltage is flattened only the first half of the period.

To study the aggregated effect of LED and CFL lamps, 50 of each were connected simultaneous to the generator. This corresponds to total rated power of 650 W: 100 W for LED and 550 W for CFL lamps. The resulting waveforms are shown in Figure 4.13. The voltage is flattened during the whole period. In the first half period both LED and CFL lamps are drawing current, but in the second half period only the CFL lamps are drawing current. The generator has a heavier load to supply in the first half of the period than in the second half. As a result both the generated voltage and current is lower in the first

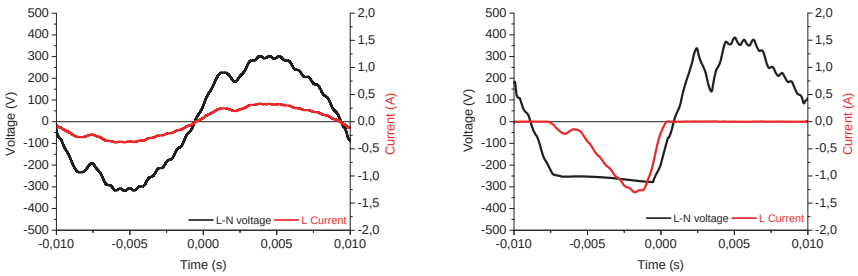

Figure 4.12: Effect of LED lamps on mobile power generator: (a) current and voltage waveforms 1 incandescent lamps; and, (b) current and voltage waveforms 32 LED lamps.

half of the period. The difference between the minimum and maximum current in the first half period is 4.9 A, in the second half period 6.4 A, resulting in a peak-to-peak current of 11.3 A.

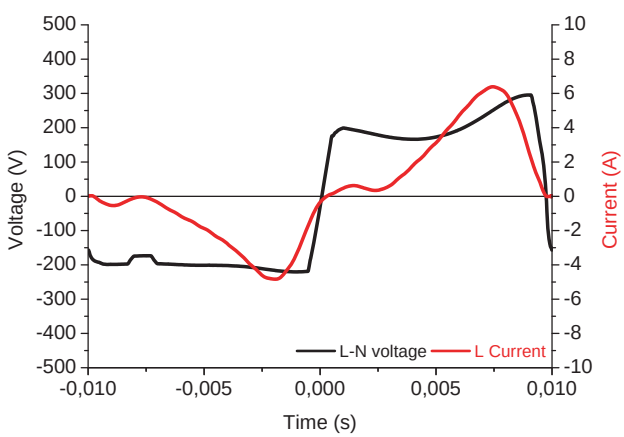

Figure 4.13: Current and voltage waveforms 50 CFL + 50 LED lamps

The mobile power generator is not able to maintain the shape of the voltage waveforms when feeding nonlinear loads. A comparison of a strong PDUN feeding resistive loads and a weak PDUN feeding nonlinear loads is shown in Figure 4.14. The current I_G in the strong PDUN is a linear function of the voltage U_G as the loads $R_{\mathrm{L}1} \cdots R_{\mathrm{L}n}$ are resistive. The weak PDUN, like the mobile generator, has higher internal resistance R'_G, $R'_G >> R_G$. The low power equipment $Z_{\mathrm{L}1} \cdots Z_{\mathrm{L}n}$ cannot be modeled by resistive components and

the current I'_G is not a linear function of the voltage U'_G. Current is consumed in the peak of the supplied voltage only to charge the bulk capacitor behind the rectifier bridge. In Chapter 5 models are presented representing this nonlinear behavior of electronic equipment. The voltage drop over the internal resistance R'_G is a linear function of I'_G resulting in a voltage U'_M with a distorted waveform. Furthermore, but not included in the Figure 4.14, the available power is limited.

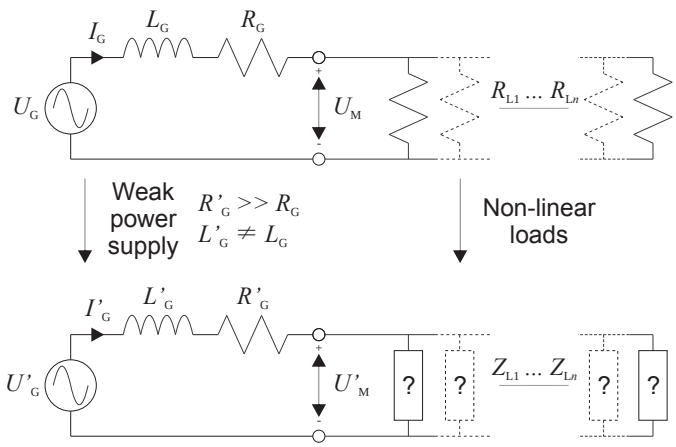

Figure 4.14: Schematic overview of change from strong PDUN feeding resistive loads to weak PDUN feeding nonlinear loads

Besides the waveforms, also the sound produced by the generator and the behavior of the lamps indicated the level of generator stressing. When connecting an increasing number CFL and to a lesser degree LED lamps, the generator produced much more noise and was becoming more and more an unstable and roughly running engine. When simultaneous connecting 50 LED and 50 CFL lamps, which corresponds to the rated nominal power of the generator of 650 W, the generator produced more noise, but it was running steadily. The noise production immediately reduced and the generator immediately ran faster at opening of the circuit. After reclosing the circuit, the generator became instable and noise production increased again. The basic power electronics give rise to high inrush currents during a cold start. It took some seconds for the fluctuations in intensity of light from the CFL lamps to fade away. The combination of cold start and power fluctuations made the CFL take longer to start, resulting in long flashing of CFL lamps. It was expected that the generator would trip, but the control circuit in the (low cost) generator is not 'smart' enough to switch off. A large generator set would actually switch off due to the high nonlinear load and high inrush currents.

The current waveform of low power equipment is dependent on the voltage waveform and the other way around. In a weak PDUN a significant voltage drop can arise over the impedance of the PDUN as a result of the peak current

drawn by the power electronics in low power equipment. This can result in a dramatic change in the waveform of the supplied voltage, especially when the available power is limited. Furthermore, the inrush currents during cold start of the low power equipment can result in stability problems.

4.4 Modern PDUN and harmonic distortion

In new buildings many small energy efficient equipment are being installed. In general, virtually all electrical equipment connected to the PDUN has an power electronic interface. As a result only a very limited number (or no) conventional linear loads remain. Direct connection to the PDUN of purely resistive loads and phase lagging loads like motors or transformers does not take place anymore in those new buildings.

This section discusses the resulting harmonic voltage distortion due to a multitude of electronic equipment in the new Carré building of University of Twente [21, 22]. The building has 5 levels and a total floor area of 36.000 m^2. It contains lecture, study, office, meeting and laboratory rooms. A picture of the Carré building is shown in Figure 4.15. One would expect to have a tidy voltage waveform in a recently constructed building, but the effect of nonlinear electronic equipment was underestimated in the design of the PDUN, due to the fact that the design was based on the conventional assumptions of $\cos\theta$ and linear loads. As a consequence transformers got overheated. The resulting voltage waveform distortion at socket level is shown Figure 4.16. Dual zero crossing are present which can interfere with equipment using zero crossing for synchronization purposes like timers in laundry machines and alarm clocks as occurred in Coburg, Germany [28].

Figure 4.15: The east side of Carré building

Overheating of transformers and tripping of equipment due to dual zero crossings are not the only effect of harmonic distortion in a PDUN. In three-phase 'Y' distribution networks nonlinear loads with an identical harmonic

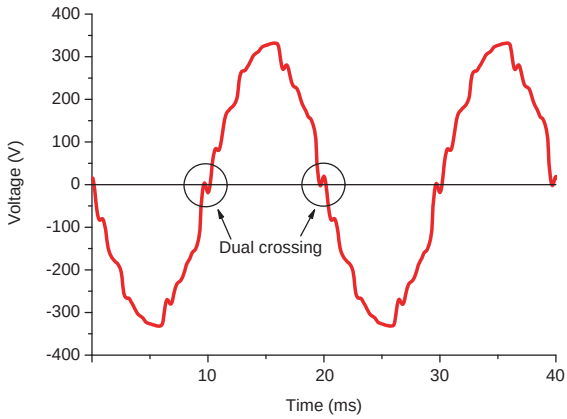

Figure 4.16: High level of voltage harmonic distortion at end of line of supply

current spectrum cause cumulation of 3rd harmonic and its uneven multiples in the neutral or Protective Earth Neutral (PEN) conductors. As the current in those conductors is normally not monitored, there is a risk that they will be overloaded. Just like transformers, overloaded conductors can get overheated and catch fire. Furthermore, the sensitivity of fuses are also affected by current harmonics [29].

Mains power supply filters have 'Y' capacitors. Feeding those filters with a distorted voltage will result in leakage currents. Large leakage currents will cause changes in the sensitivity of the Residual Current Device (RCD) [30] and degradation of lifetime of 'Y' capacitors.

The PDUN of the Carré building feeding point consists of 4 transformers each having an apparent power of 1000 kVA. A conventional approach, including aspects like DPF and simultaneity, was used for the design of the PDUN. Derating of the apparent power of the transformers to account for harmonic distortion of current was not done. From the main switchboard the power is distributed over the 5 levels. At each level a couple of distribution boards distribute the power over the rooms. A scheme of the PDUN is shown in Figure 4.17. The 4 transformers of the Carré building supply also feed a redeveloped lecture and conference hall.

At the main switchboard, the low voltage side of Transformer 4 is directly measured. By temporarily connecting the load of Transformer 4 to Transformer 3 the voltage of Transformer 4 under no load condition can be measured. This gives the opportunity to evaluate the voltage quality supplied by the grid. The measured RMS voltage in no load condition is about 5 V higher than in load condition. Figures 4.18(a) and 4.18(b) respectively show the voltage waveforms at Transformer 4 just before and after switching the load from Transformer 4

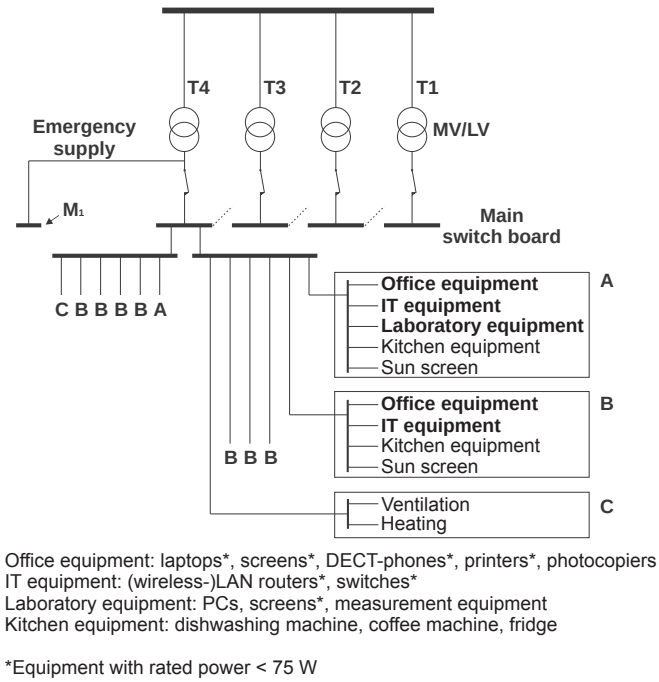

Figure 4.17: Scheme of PDUN Carré building: waveforms are captured at location M_1

to 3. The measured levels of V-THD are listed in Table 4.5. Since the voltage level does not significantly change and the V-THD is about 1% when there is no load connected to Transformer 4, the voltage quality delivered by the grid can be considered to be of a decent level.

Table 4.5: Measured contribution of loads to voltage distortion

Location	V_{THD} (% FUND)					
	Transformer 4 with load			Transformer 4 without load		
	V_A	V_B	V_C	V_A	V_B	V_C
Main switchboard M_1	5.4	5.4	5.7	1.2	0.9	1.0

Furthermore, the level of V-THD is measured along the path from main switchboard to office. The scheme of this path with three measurement locations (M_1, M_2 and M_3) is shown in Figure 4.19. One measurement device for analyzing the voltage is moved along the path and another device is placed stationary at the last measurement location (M_3) for reference. By comparing the voltage waveform of Figure 4.16 taken at terminals of a socket in office

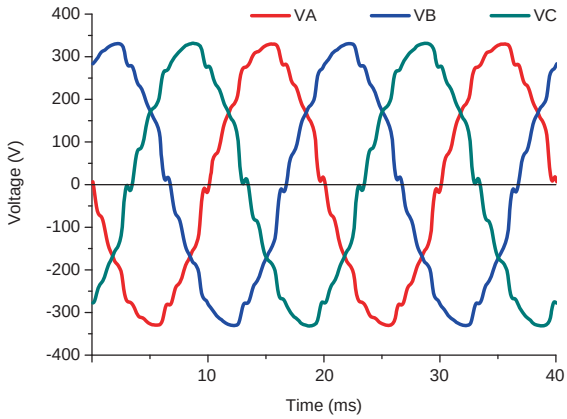

(a)

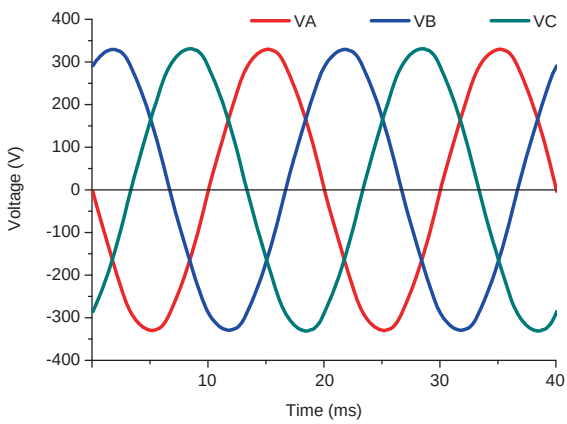

(b)

Figure 4.18: Measured voltage waveforms Transformer 4: (a) with load; and, (b) without load.

CR 2116 (distribution board E2E7 group W18) to the voltage waveforms in Figure 4.18(a), it can be seen that the harmonic distortion at the end of the line is higher than at transformer level.

The 95% values of levels of the V-THD and the harmonics up to the 25^{th} component at transformer level are collected and listed in Table 4.6. The last column lists the maximum level given in the EN 50160 standard. The 15^{th}, 19^{th}, 21^{st}, 23^{rd} and 25^{th} voltage harmonic components do not comply the EN

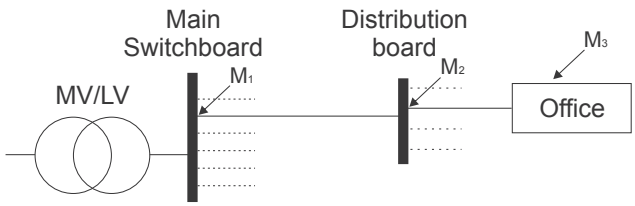

Figure 4.19: Scheme of distribution of power supply in Carré: M_1, M_2 and M_3 designate the measurement locations

50160 requirements; the values exceeding the limit are in bold.

Table 4.6: Voltage harmonics at Transformer 4

Harmonic component	95% limit			
	V_A	V_B	V_C	EN 50160
V_{THD}	5.31	5.38	5.69	<8.00
2	0.04	0.04	0.04	<2.00
3	0.63	0.80	0.68	<5.00
4	0.02	0.02	0.02	<1.00
5	2.27	2.46	2.54	<6.00
6	0.02	0.03	0.02	<0.50
7	2.24	2.15	2.20	<5.00
8	0.02	0.03	0.03	<0.50
9	0.48	0.74	0.57	<1.50
10	0.04	0.04	0.03	<0.50
11	1.72	1.78	1.61	<3.50
12	0.04	0.04	0.04	<0.50
13	1.49	1.50	1.65	<3.00
14	0.03	0.03	0.03	<0.50
15	**0.55**	**0.72**	**0.60**	<0.50
16	0.02	0.02	0.02	<0.50
17	1.96	1.83	1.81	<2.00
18	0.03	0.03	0.03	<0.50
19	**2.05**	**2.02**	**2.95**	<1.50
20	0.04	0.03	0.04	<0.50
21	**0.87**	**1.12**	**0.94**	<0.50
22	0.04	0.04	0.04	<0.50
23	**1.85**	**1.84**	1.31	<1.50
24	0.04	0.04	0.04	<0.50
25	**1.73**	**1.65**	**1.82**	<1.50

To reduce the distortion of the voltage waveform, two extra 1600 kVA transformers were installed, an unforeseen and very costly operation. These two transformers are used to feed the redeveloped lecture and conference hall. In other words the redeveloped lecture and conference hall got its own supply and has been disconnected from the Carré building supply. The results of the measurements at the three different locations before and after splitting up the original load of the Carré building supply are listed in Table 4.7. After removing the redeveloped lecture and conference hall V-THD dropped by a factor 2. Now the total supply apparent power is 7.2 MVA, while on completion of the building it was 4.0 MVA. The real power consumption is still about 3.0 MW.

Table 4.7: Comparison measured V-THD before and after installation of extra 1600 kVA transformers

Location	V_{THD} (95% limit)					
	Lecture and conference hall connected			Lecture and conference hall disconnected		
	V_{A}	V_{B}	V_{C}	V_{A}	V_{B}	V_{C}
Main switchboard M_1	5.3	5.4	5.7	2.4	2.3	2.3
Distribution board M_2	5.8	5.9	6.7	×	×	×
Office M_3	×	×	6.7	×	×	3.1

In the design only the DPF $\cos\theta$ was taken into account when evaluating the PF. Ironically, the technicians of University of Twente foresaw the problems in the design phase already and advised against the consulting companys recommended 4 MVA. However, the owner approved the advice based on estimated costs. As a result of the current distortion of each piece of modern energy saving equipment, the multitude of such equipment resulted in a much higher level of V-THD than expected in the design. The distorted current drawn by the nonlinear loads results in a voltage drop across the transformers and feeding lines of the PDUN. This eventually resulted in a distorted voltage feeding the equipment connected to the PDUN and overheating of transformers.

Waveform measurements on one dimmed fluorescent lamp reveal glitches in the current waveform around the zero crossings of the voltage waveform, as shown in Figure 4.20. In the Carré building, every office has 8 and every laboratory has 12 modern fluorescent light-units consisting of 2 lamps. Despite each light-unit fulfills the IEC 61000-3-2 Class C equipment emission requirements discussed in Section 3.3, the contribution of these lamps to the harmonic distortion should not be ignored.

The conventional approach in design of PDUN, and in general for power distribution networks, is to use the DPF and simultaneity factor. Simultaneity factor is a measure for coinciding use of equipment. This approach cannot be applied anymore, because the distortion will significantly contribute to the total apparent power. The modern low power equipment do not have high rated

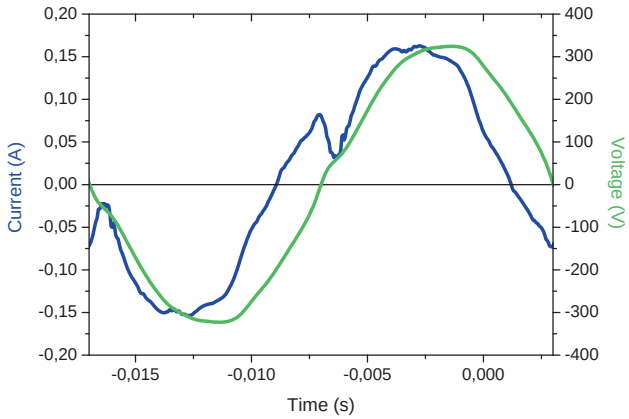

Figure 4.20: Waveforms dimmed fluorescent light-unit

real power, but still high apparent power needs to be available and transported through the PDUN. As discussed in Section 3.4, the PDUN has to cope with sharp, short and high current peaks. Any resulting deviation in voltage waveform due to voltage drop over transformers and feeding lines of the PDUN will in turn influence the current waveform and vice versa.

4.5 PV systems in PDUN in rural areas

The number of PDUNs with distributed energy generation is increasing. In the Netherlands PV systems are very popular with farmers. They are living in rural areas where the grid is weaker compared to the urban areas. The distance between the last transformer in the grid and the POI can range from several hundreds up to thousand meters. Moreover, the number of nonlinear electrical equipment is also increasing in PDUNs in rural areas. This might make these PDUNs extra vulnerable for EMI.

In [24] a farm in a rural area near Enschede with its own PV system is studied. The PQ in terms of V-THD is evaluated and compared to evaluation performed at others places, as already discussed in Section 4.1. Current measurements which were also performed will be discussed in this section. Besides two other case studies with a PV at a farm are briefly discussed in this section. One is about overheated equipment due to over voltage generated by a PV system and another about a disturbed PV system.

4.5.1 Injection of distorted current waveforms by PV system

A PQ analyzer monitors the line from PV to the bus feeding conventional machines as shown in Figure 4.21. The PDUN is connected to the grid via a power cable rated at 63 A of at least 500 m. The installed PV system can deliver a maximum power of 13 kW. During the monitoring various weather conditions occurred such that different operation modes of the PV system can be studied.

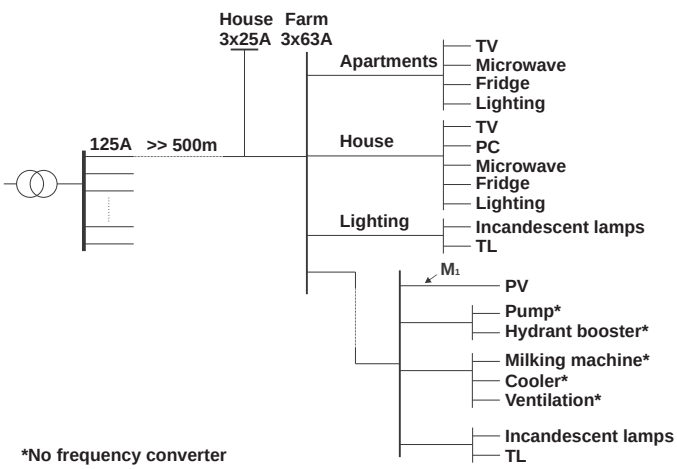

Figure 4.21: Scheme of distribution of power supply: voltage and current are monitored at location M_1

Waveforms captured during cloudy conditions corresponding to low power generation are shown in Figure 4.22. The injected current waveforms are distorted and contain a DC component. Also during sunny periods when the PV system is operating in a higher power mode the injected current waveforms can be rather distorted as well. Figures 4.23(a) and 4.23(b) respectively show relative distorted and clean current waveforms for higher injected powers.

Distorted current waveforms during moderate power injection have frequently been measured during two measurements periods of respectively 3 weeks and 2 months. Representative trends in voltage and current distortions together with apparent and active power are shown in Figures 4.24(a) and 4.24(b). There is no strong relation between current distortion and the amount of injected current. Moreover, the voltage is not significantly affected by the injected current. However, more PV systems are installed and as a result the total injected current will rise. A similar scenario as in the case of the Carré building supply discussed in Section 4.4 is not inconceivable.

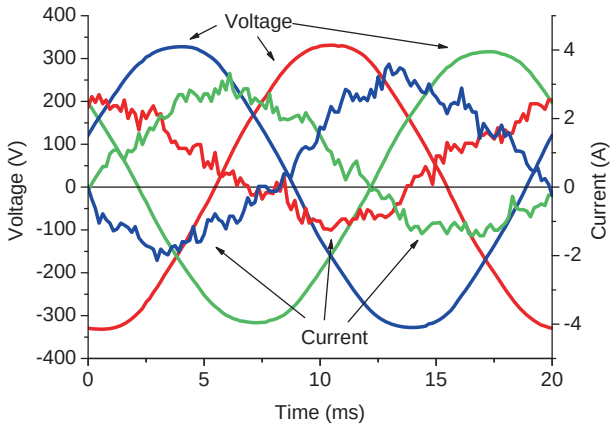

Figure 4.22: Current injected by PV-inverter in low power injection mode: high distortion

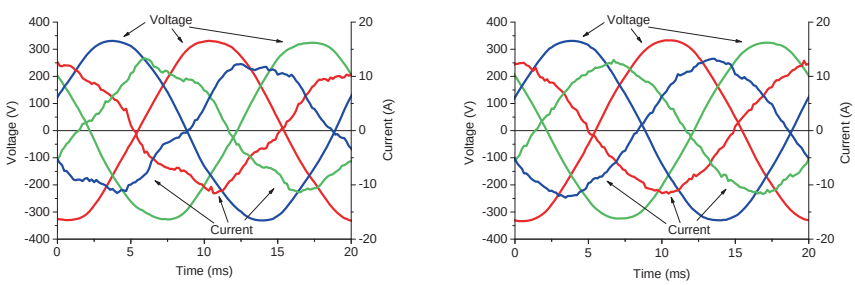

(a) (b)

Figure 4.23: Current injected by PV-inverter in moderate power mode: (a) high distortion; and, (b) low distortion.

4.5.2 Over voltage by PV system

Irrespective of shapes of current waveform injected by power generator in PDUN it is of importance to account for impedance at all times. It is common practice to account for voltage drop over long cables between the last transformer of the grid and the POI. With the introduction of distributed energy resources voltage rise over the same long cables should also be accounted for as illustrated by Figure 4.25. In this figure the voltage and current waveforms are assumed to be sinusoidal and in phase. Complaints arise about the functioning of a vintage food weighing machine at a farm with a 45 kW PV system. These complaints coincided with sunny periods and after long periods of sun

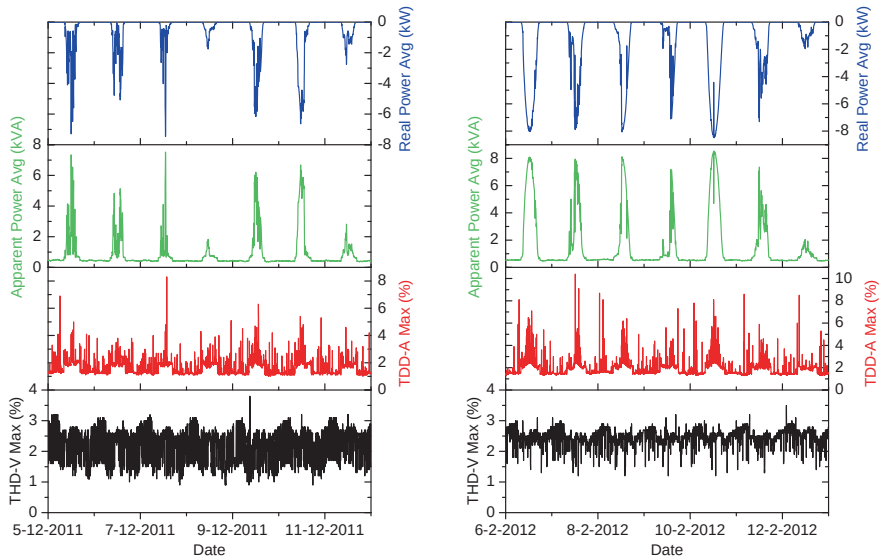

(a) (b)

Figure 4.24: Weekly trends PV-inverter: real power (top), apparent power (top-middle), current distortion (bottom-middle) and voltage distortion (bottom): (a) week 49 2011; and, (b) week 06 2012.

the food weighing machine became defective. It was designed for a nominal RMS voltage of 220 V. Depending on operating loads the supply RMS voltage was about 230 V without power generation, but the voltage could rise by 30 V due to power injection. The food weighing machine has an passive conventional supply and the electrical components behind the voltage transformer got overheated. Figure 4.26 shows an example of the voltage rise at the terminals of a socket in a room of the farm. By controlling the injected current over voltage can be avoided. An alternative solution is decreasing the grid impedance. Besides, the input of the vintage food weighing machine can be adapted such that it can withstand higher voltages. In this way its nominal voltage can be increased to at least 230 V.

4.5.3 Disturbance of PV system

Instead of disturbing existing equipment in the PDUN a PV systems can also be disturbed by already installed equipment. A 50 kW PV system does not generated more than 25 kW during sunny periods. In addition large fluctuations of injected power occurs and the PV inverters loses synchronization to the power frequency and disconnect themselves from the PDUN. The owner, a

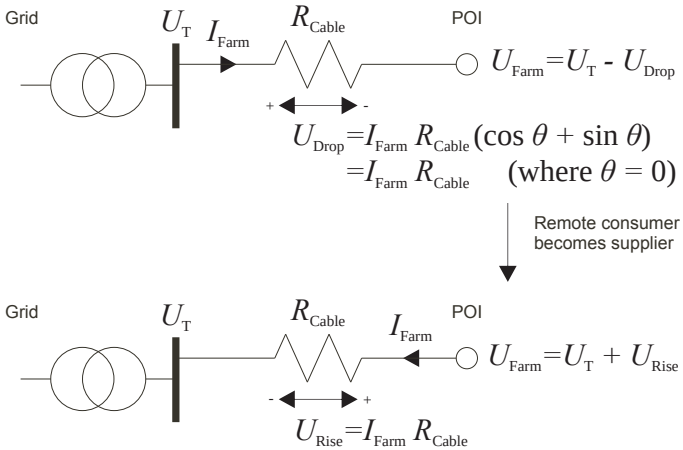

Figure 4.25: Voltage drop over long cables between last transformer of the grid and remote POI

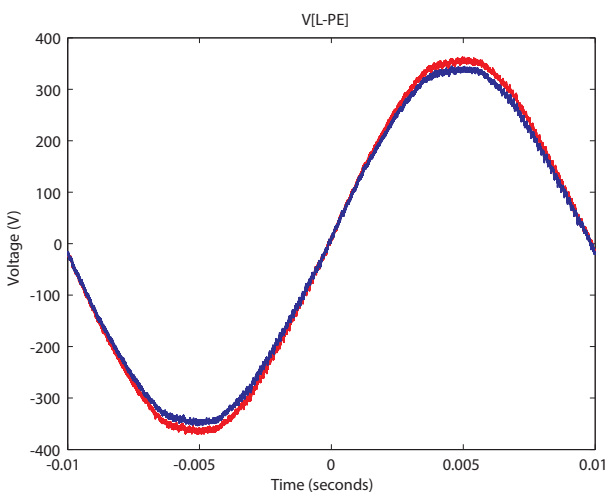

Figure 4.26: Voltage waveforms at terminals of a socket in an room of the farm with (red: 242 V) and without (blue: 228 V) current injection by PV-inverters

farmer, states that the PV system functions well when the ventilation system of the piggery is operating in manual mode. Operating in manual mode means that the Power Drive System (PDS) of the ventilation system is disconnected and bypassed. Furthermore, in the past, the feeding machine was malfunctioning due to the emission from the PDS. After extending the power cord of the feeding machine the disturbance was eliminated.

A schematic overview of the PDUN is given in Figure 4.27. 75% of the installed power is injected into the POI and the remainig 25% is directly injected into busbar of the new piggery. Measurements have been performed on a socket of the new piggery. Results of reference measurements, PDS is not active, are shown in Figures 4.28(a) and 4.28(c). The first figure shows a clean voltage waveform and the second figure shows no significant background emission. Whether the PV inverters are connected to the PDUN or not, the reference measurements do not change significantly. However, when the PDS drives the fans at 17 Hz the voltage waveform gets distorted as shown in Figures 4.28(b) and 4.28(d). At the time of measurement the visible distortion of the waveform is highest at this operation frequency. Just before and after the peaks and around the zero crossings distortion appear. The PV inverters have no significant effect on the results. Also at the POI the distortion is present when the PDS is active.

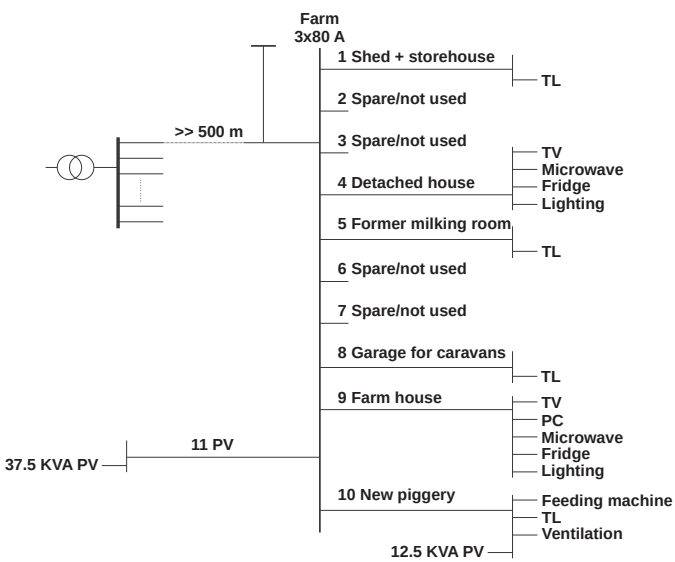

Figure 4.27: Scheme of distribution of power supply farm

Furthermore, Fast Fourier Transforms were performed on the waveforms of Figure 4.28. The results of the reference measurements are shown in Figures 4.29(a) and 4.29(c). When the PDS was active there is a significant increase (upto 20 dB) in the frequency band from 3 kHz to 100 kHz. Regarding conducted emissions there are no criteria for the frequency band from 2 kHz to 150 kHz. The frequency band upto 2 kHz is considered as harmonics and from 150 kHz protection of radio applications starts.

Both PV inverters and previous PDS comply with the applicable Declaration of Conformity (DoC) and have the Conformité Européenne (CE) marking. This means that they are compliant with their own product standards for EMC.

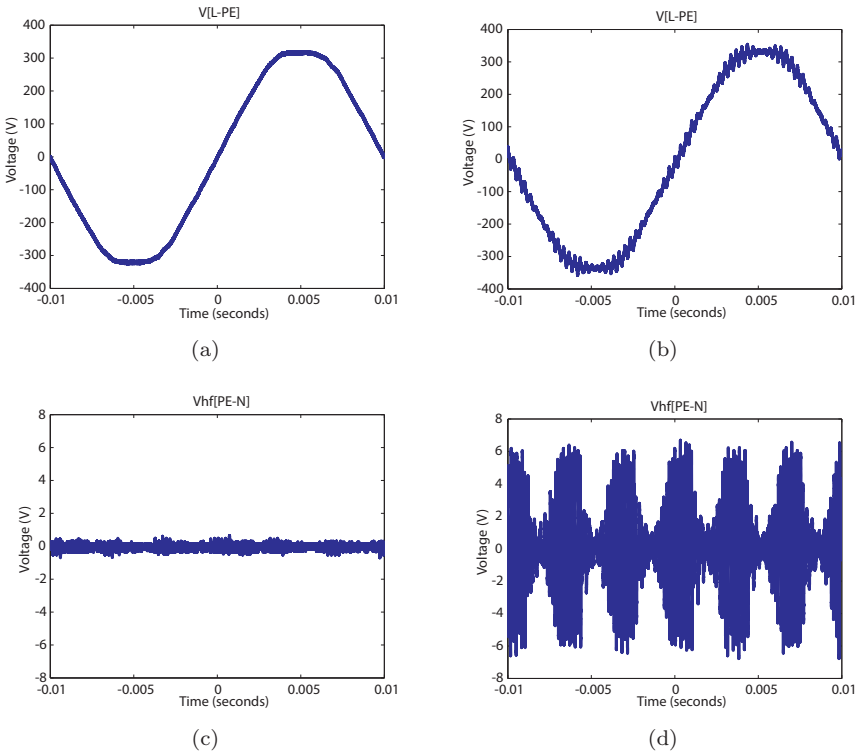

Figure 4.28: Voltage waveforms: (a) voltage waveform $V_{\text{L-PE}}$ PDS not active (reference); (b) voltage waveform $V_{\text{L-PE}}$ PDS active (17 Hz); (c) high-pass filtered (-3 dB point at 10 kHz) voltage waveform $V_{\text{PE-N}}$ PDS not active (reference); and, (d) high-pass filtered (-3 dB point at 10 kHz) voltage waveform $V_{\text{PE-N}}$ PDS active (17 Hz).

No guarantees are given for being EMC when the products are used in an arbitrary environment, like the case of the farm. Within the European Union, however, all equipment put on the market shall fulfill the essential requirements of the European Directive on EMC [1]. This means that the product standards for EMC fail to cover the essential requirements of the European Directive on EMC.

The PDS has been replaced by a similar one but from a new series to suppress the voltage distortion. The PV inverters deliver the maximum output under good weather conditions and their operation is stable. Furthermore, the conducted emission to the grid has been reduced.

Not only consumption of power but also injection of power by power electronics affect the PQ in the PDUN [31]. Especially rural areas are susceptible for EMI as the grid impedance and consequently the impedance in the PDUN

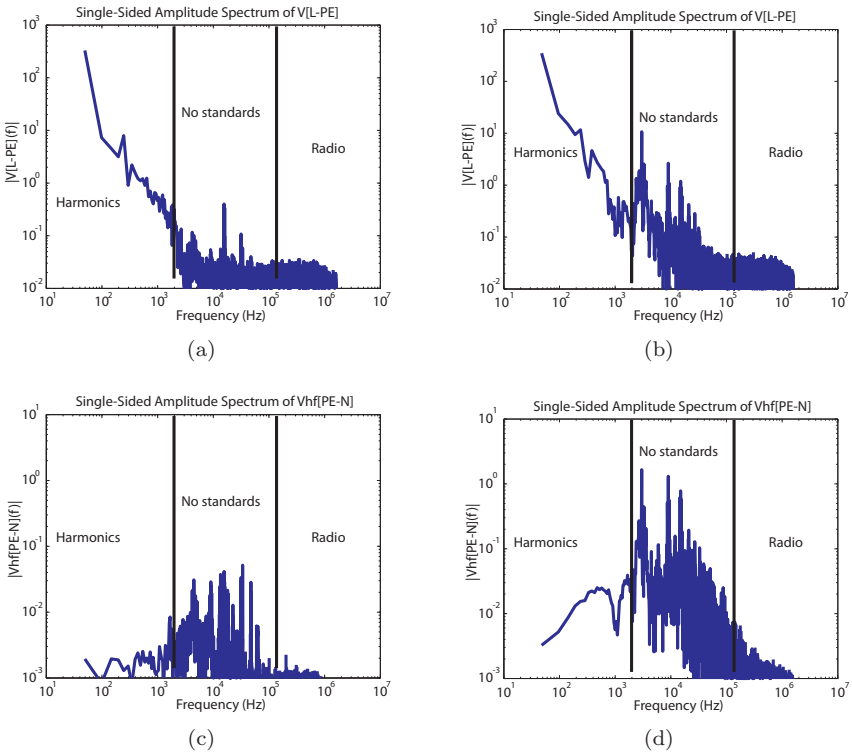

Figure 4.29: Spectra voltage waveforms in Figure 4.28: (a) spectrum waveform Figure 4.28(a); (b) spectrum waveform Figure 4.28(b); (c) spectrum waveform Figure 4.28(c); and, (d) spectrum waveform Figure 4.28(d).

in those areas is higher. The higher the grid impedance, the more isolated the PDUN becomes, the less is its coupling to the grid.

4.6 PDUN in island operation

In decentralized or micro grids there are local power generation systems only. The amount of available power is typical lower and the impedance is typical higher than in the centralized main grid. Section 4.3 already showed an example of a mobile 2-stroke power generator. This section focus on a larger isolated system, the PDUN onboard of the Hr. Ms. Holland patrol ship of the Royal Netherlands Navy. Very typical for the Hr. Ms. Holland patrol ship is the integrated mast I-MAST 400 [32]. The I-MAST 400 is the first member of the family with various sizes, each one intended for a different class of naval vessels [33]. The integrated mast has many observation, radar, communication and lots of other modern electronic systems.

The PDUNs and equipment onboard of naval ships are required to meet the STANAG 1008 military standard 'Characteristics of Shipboard Electrical Power Systems in Warships of the Nato Navies [12]. The technology in the commercial market grows very fast and, although not certified, Commercial Off the Shelf (COTS) products are economically interesting for use on a naval vessel. In [34] and [35] the interaction between the PDUN and the connected equipment is analyzed via measurements. The measurements are performed during the 'setting to work phase, so the starting up and testing phase implying many on/off switching events. This means the PDUN is not stable. In [34] the integrated mast has not been installed and the objective was to investigate the risk of EMI to many COTS products. In [35] the measurements are repeated after installation of the integrated mast to verify the effect of the integrated mast on the PQ. To justify the employment of COTS on naval vessels regarding PQ the results are analyzed with respect to both military and civil standards. An overview of these standards was given in Section 2.3.

The voltage margins in EN 50160 cannot be used for equipment voltage immunity curves. For COTS equipment the Information Technology Industry Council (ITI) curve is used [25]. In Figure 4.30 the STANAG 1008 and ITI curves are respectively shown in red and black. In the tolerable region the equipment should operate properly. In the interruption region the equipment may temporarily malfunction or stop operation. The prohibited region should be avoided as in this region permanent malfunctioning or loss of functioning of equipment may occur.

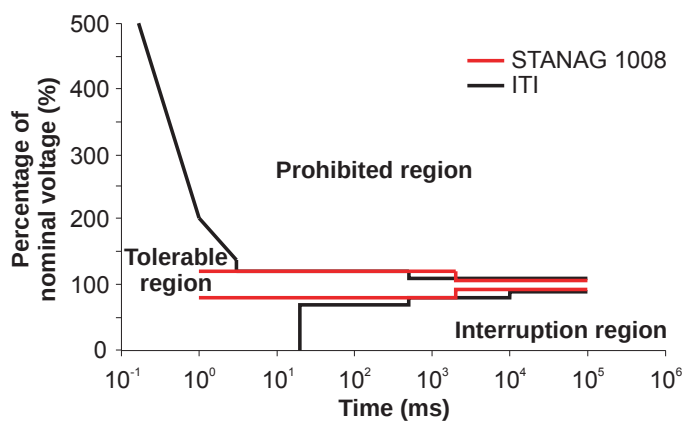

Figure 4.30: STANAG 1008 [12] and ITI [25] curves specifying the input voltage envelopes which must be tolerated by equipment, $f = 60$ Hz

The PDUN of the Hr. Ms. Holland patrol ship of the Royal Netherlands Navy is fed by three 450 V_{ac} 60 Hz diesel generators, having a total apparent power of 1150 kVA. The PDUN itself has 440 V_{ac}, 230 V_{ac} and 115 V_{ac} three phase delta supply networks. The 230 V_{ac} 60 Hz supply network is not a basis supply network for a naval vessel and is therefore not included in Table 2.4

Section 2.3. STANAG indicates that for 230 V_{ac} 60 Hz supply network provided for operational systems the same limits apply as given for 440 V_{ac} and 115 V_{ac} 60 Hz supply networks. The limit for voltage transient is set to 1400 V.

In each supply network PQ analyzer monitors are installed. In this way simultaneous measurements at different locations can be performed. The next 3 quantities have been monitored:

- voltage fluctuations,
- power frequency fluctuations, and
- harmonic distortion.

The measurement data logged by PQ analyzer monitors on the Hr. Ms. Holland patrol ship without integrated mast is summarized in Table 4.8. These devices show that voltage as well as frequency fluctuations are within the limits of the EN 50160 standard for each supply network. Switching loads on and off resulted in changes of voltage level, but the voltage control mechanism compensates within tenths of seconds. Comparing the mobile generator in Subsection 4.3.2 with the performance of these high-end generators it can be learned that the quality of those mobile generators is really poor. Figure 4.31 shows the effect of the control mechanism for a dip in the 440 V_{ac} supply network. Within tenths of seconds a surge follows and the voltage level restores. This also occurred simultaneously in the 115 V_{ac} and 230 V_{ac} supply networks. As a result no variations outside the ITI curve occurs, despite the many switching actions as is shown in the ITI curve for the 230 V_{ac} supply network in Figure 4.32. However, in all supply networks the V-THD and 11^{th} voltage harmonic component exceeds the maximum limit given in EN 50160. Furthermore, in both 115 V_{ac} and 440 V_{ac} supply networks the 13^{th} voltage harmonic component is too high.

The summary of measurement data logged by another PQ analyzer monitor installed in the 440 V_{ac} is listed in Table 4.9. The device was set to log any exceeding of the EN 50160 limits, but using its raw data, it is also possible to perform a confined STANAG 1008 evaluation. This has been done for the short term voltage variations, power frequency variations, and V-THD. Only a deviation in the V-THD has been monitored: the 5% STANAG 1008 limit is exceeded. Parallel to the EN 50160 measurements the Royal Netherlands Navy performed STANAG 1008 measurements using their own PQ analyzer monitors at the same locations as the PQ analyzer monitors discussed so far. Those results confirm that regarding voltage and frequency fluctuations STANAG 1008 compliance has also been met. Furthermore the level of 11^{th} and 13^{th} order components of voltage harmonics components as well as V-THD do not meet the STANAG 1008 requirements.

The exceeding of voltage harmonic distortion limits occur during operation of the electrical propulsion above 30% propulsion power. Similar observations related to electrical propulsion onboard (naval) ships are reported in [36]. The measured highest V-THD onboard the Hr. Ms. Holland patrol ship is about

Table 4.8: EN 50160 summary provided by PQ analyzer monitors (3×115 V_{ac}, 3×230 V_{ac}, 3×440 V_{ac})

115 V_{ac} supply network	
Voltage: ±10% (95%)*	Passed
Voltage: +10/-15% (100%)*	Passed
V_{THD}: 8% (95%)*	Passed 5%
Individual harmonic distortion (95%)*	Failed 11^{th} harmonic: 4.0% 13^{th} harmonic: 3.2%
Frequency: ±1% (99.5%)*	Passed
Frequency: +4/-6% (100%)*	Passed
230 V_{ac} supply network	
Voltage: ±10% (95%)*	Passed
Voltage: +10/-15% (100%)*	Passed
V_{THD}: 8% (95%)*	Passed 6%
Individual harmonic distortion (95%)*	Failed 11^{th} harmonic: 4.7%
Frequency: 1% (99.5%)*	Passed
Frequency: +4/-6% (100%)*	Passed
440 V_{ac} supply network	
Voltage: ±10% (95%)*	Passed
Voltage: +10/-15% (100%)*	Passed
V_{THD}: 8% (95%)*	Passed 5%
Individual harmonic distortion (95%)*	Failed 11^{th} harmonic: 4.1% 13^{th} harmonic: 3.1%
Frequency: 1% (99.5%)*	Passed
Frequency: +4/-6% (100%)*	Passed

* range of 10 minutes mean values for measurement period

Table 4.9: Summary confined STANAG 1008 evaluation (3×440 V_{ac})

	Minimum	Maximum
Voltage*	383.2 V / -12.9% (<2 s)	473.4 V / +7.6% (<2 s)
Frequency	57.15 Hz / -4.8% (<2 s) 59.25 Hz / -1.3%	60.86 Hz / +1.4% (<2 s) 60.86 Hz / +1.4%
V_{THD}	-	7%

* PQ analyzer monitor was not set to log voltage deviations exceeding the ±5% limits

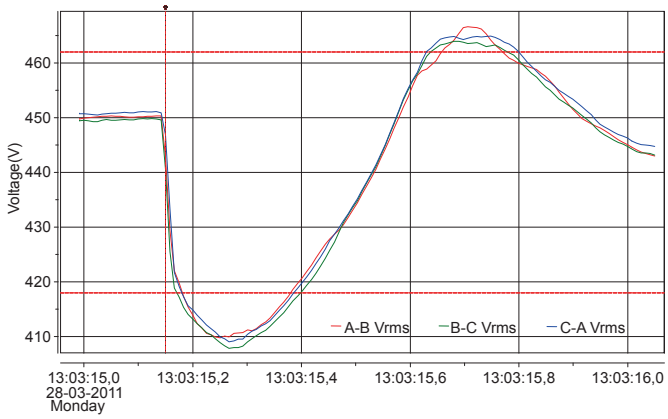

Figure 4.31: Voltage dip, immediately followed by a surge in 440 V_{ac} supply network

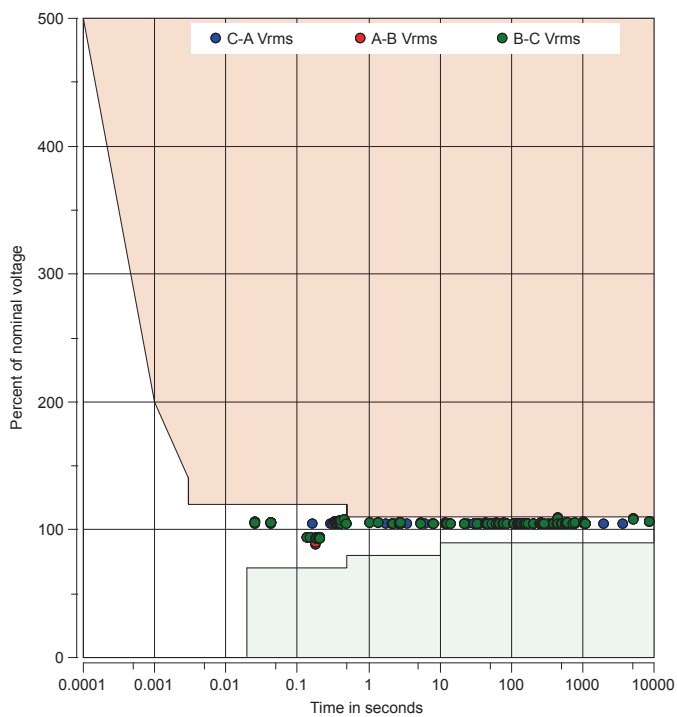

Figure 4.32: No variations outside ITI tolerance curve 230 V_{ac} supply network

10% and occurs in the 230 V_{ac} supply network. Some electric or electronic components inside equipment connected to the 230 V_{ac} supply network form part of a resonance circuit and this circuit gets excited during operation of the electrical propulsion above 30% propulsion power. An example of voltage waveforms and corresponding histogram of voltage harmonics are respectively shown in Figures 4.33(a) and 4.33(b) for the 440 V_{ac} supply network.

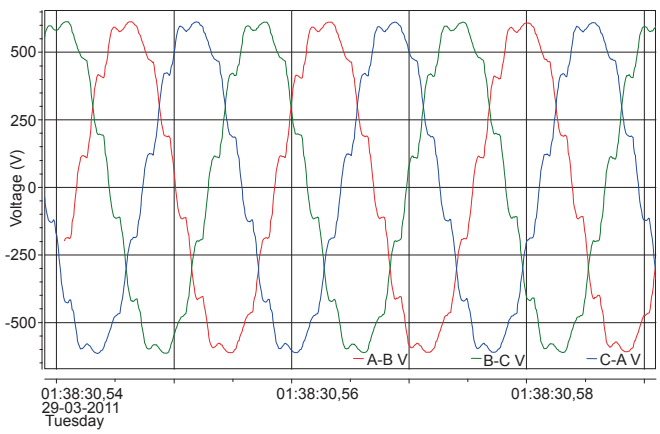

(a)

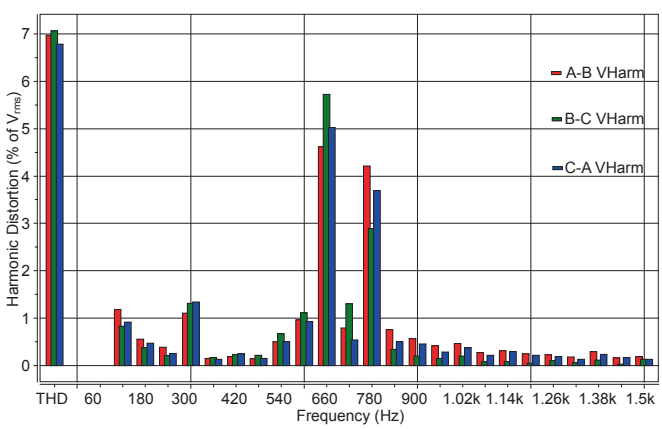

(b)

Figure 4.33: Harmonic distortion 440 V_{ac} supply network during electrical propulsion test: (a) waveforms; and, (b) corresponding histogram.

The collected data gathered during three days measurement period onboard the Hr. Ms. Holland patrol ship without integrated mast shows com-

pliance with both EN 50160 and STANAG 1008 standards for frequency and voltage fluctuations. Furthermore, no variations outside ITI tolerance curve are detected. However, the harmonic distortion during the operation results in exceeding of harmonic limits. Measures have been taken to mitigate the high levels of 11^{th} and 13^{th} order voltage components resulting in a high level V-THD.

After the first measurement run the Royal Netherlands Navy installed two filters in the 230 V_{ac} supply network to suppress the 11^{th} and 13^{th} order voltage components. Furthermore, the integrated mast was installed. Then the measurements were repeated to verify the effect of the integrated mast and installed filters on the PQ. Only if the filters are not used, the harmonic distortion appears again in all three supply networks. Furthermore, there is no significant influence of the integrated mast on the PDUN. With regard to voltage fluctuations, power frequency fluctuations and harmonic distortion, this means that if the filters are used it is possible to use COTS equipment onboard of the Hr. Ms. Holland patrol ship. Both the STANAG 1008 and EN 50160 standards are fulfilled for these three criteria and no variations outside the ITI curve are detected.

There are also other aspects not covered in this study like isolation as the power supply networks on a naval vessel are unearthed. COTS equipment with EMI filters cannot be connected to an Insulation Terre (IT) without any measures. Capacitors to earth result in leakage currents endangering the isolation. Simply cutting the capacitors results in higher risk of EMI [37]. Further research is needed to be able to determine the suitability of and the conditions for using COTS equipment on naval vessels.

The results of this study can also be used for PDUNs in general [36]. Short term voltage fluctuations and temporary high distortion levels are caused by switching actions. The severity of these phenomena is also dependent on the available power and impedance. This should also be taken into account for PDUNs in rural areas and in decentralized or micro grids with local power generation systems.

4.7 Summary

The studies in [18–20] show the need for further research on emission from PDUN feeding large numbers of electronic equipment. These studies evaluate the effects on PQ on the grid level. Rather than on grid level, the case studies presented in this chapter focus on PQ inside the PDUN. Therefore long term conditions as well as short term variations are considered as a single event may result in malfunctioning or disturbance of connected equipment.

As already discussed in Section 3.4 the IEC 61000-3-2 standard does not anticipate on synchronous switching resulting from interaction between several instances of similar equipment. The case studies show that the distortion will significantly contribute to the total apparent power and the PDUN has to cope with sharp, short and high current peaks. Therefore, connecting large numbers

of similar low power equipment can have a significant impact on the PDUN. The basic working principle of power electronics will result in an alignment of current peaks as the nonlinear behavior is basically charging of a capacitor behind a rectifier bridge. Similar low power equipment will draw currents in or around the top of voltage waveform and as a result the current peaks are synchronized in time. Any resulting deviation in voltage waveform due to voltage drop in the PDUN will in turn influence the current waveform and vice versa.

With the introduction of energy resources voltage rise should also be accounted for. In one of the case studies of a PV system at a farm the RMS voltage level increases significantly and as a result equipment get damaged. Another case study shows the injection of rather distorted current waveforms, but the voltage waveforms are not significant affected. However, more PV systems are installed and a similar scenario as synchronous switching of large number of similar loads is not inconceivable. Especially in rural areas as the grid impedance and consequently the impedance seen by equipment in the PDUN in those areas is higher.

In the civil standards there is a gap in the frequency band from 2 kHz to 150 kHz. The frequency band upto 2 kHz is considered as harmonics and from 150 kHz protection of radio applications starts. The case study with the PDS for a ventilation system showed significant conducted emission from the PDS in the uncovered frequency band. As a result the PV system in the same PDUN was malfunctioning. Both PV inverters and PDS comply with their own product standards for EMC, but do not fulfill the essential requirements of the European Directive on EMC.

The severity of the observed phenomena in the case studies is dependent on the broadband PDUN impedance and the dynamic broadband behavior of connected equipment. However, the current standards and design approaches do not anticipate dynamic broadband behavior of the PDUN with its connected equipment. The following two chapters will therefore analyze and provide models for the PDUN impedance and the PDUN as propagation medium for conducted interference. Special attention will be paid on transients which are intermittent events. Then, the dynamic behavior of equipment is analyzed and subsequently models are derived.

Chapter 5

Impedance of PDUN

The consideration of impedance faced by the equipment connected to the PDUN is very confined in standards. In Chapter 3 (Sections 3.3 and 3.4) it was stated that the reference impedance used in IEC standards is defined for the fundamental frequency only. A broader description should be applied, not only for harmonic distortion, but also for emission at higher frequencies upto and above 9 kHz as in the case presented in Section 4.5 of the PV system being disturbed by the PDS of the ventilation system. The impedance of the PDUN is in military standards described from 30 Hz upto 10 MHz, or sometimes 100 MHz even [13], [38].

In this chapter the impedance of the PDUN is further analyzed and models are developed. Section 5.1 gives an overview of describing lines by transmission line equations. Then, the limitations of the standards as discussed in Chapter 2 for the impedance of the PDUN is summarized in Section 5.2. Afterwards, Section 5.2 discusses equivalent networks used in interference testing. Section 5.4 puts the discussed material into perspective.

5.1 Cable impedance and electrical length

Cables in PDUN have lengths in the range from one to several tens of meters. A cable is electrical small as its length is much smaller than the wavelength. Often used is

$$L < \frac{\lambda}{2\pi} \tag{5.1}$$

with L and the wavelength λ in meters as criterion for electrical small dimension. For non conductive media, the velocity of wave propagation is

$$\begin{aligned} v &= \frac{1}{\sqrt{\epsilon\mu}} \\ &= \frac{1}{\sqrt{(\epsilon_0\epsilon_r)(\mu_0\mu_r)}} \end{aligned} \tag{5.2}$$

where $\epsilon_0 = 8.845 \times 10^{-12}$ F/m and $\mu_0 = 4\pi \times 10^{-7}$ H/m and ϵ_r the relative permittivity of the dielectric and μ_r the relative permeability of the metal. The frequency f can be calculated using

$$f = \frac{v}{\lambda} \tag{5.3}$$

Electrical small cables are considered as electrical short lines and modeled using single circuit elements as in Figure 5.1 [39]. The figure represents a cable consisting of line conductor and neutral conductor with line series resistance R_{L}, neutral series resistance R_{N}, line series inductance L_{L}, neutral series inductance L_{N}, shunt conductance G and shunt capacitance C.

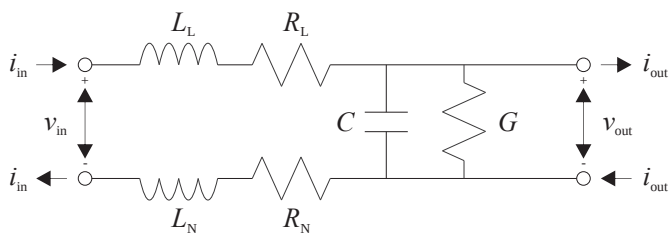

Figure 5.1: Representation of electrical short line for a cable consisting of line conductor and neutral conductor

When the cable is not electrical small the model in Figure 5.1 cannot be applied. Then transmission line equations can be used for describing the propagation of voltage and current along the z axis of the line as function of time t [39]:

$$\frac{\partial \mathbf{v}(z,t)}{\partial z} = -\mathbf{R}\mathbf{i}(z,t) - \mathbf{L}\frac{\partial \mathbf{i}(z,t)}{\partial t} \tag{5.4a}$$

$$\frac{\partial \mathbf{i}(z,t)}{\partial z} = -\mathbf{G}\mathbf{v}(z,t) - \mathbf{C}\frac{\partial \mathbf{v}(z,t)}{\partial t} \tag{5.4b}$$

where $\mathbf{R}$ denotes the resistance, $\mathbf{L}$ denotes the inductance, $\mathbf{G}$ denotes the conductance and the $\mathbf{C}$ denotes the capacitance matrices per unit length of transmission line. An infinite small piece of transmission line represented by the 4 distributed lumped circuit elements is shown in Figure 5.2, where the resistance of signal and return conductors have been lumped in a single resistance and furthermore the inductance of signal and return conductors have been lumped in a single inductance. The voltage $v(z,t)$ and current $i(z,t)$ are exponential function of z and t expressed as:

$$v(z,t) = V\mathrm{e}^{\mathrm{j}\omega t - \gamma z} \tag{5.5a}$$

$$i(z,t) = I\mathrm{e}^{\mathrm{j}\omega t - \gamma z} \tag{5.5b}$$

where γ is the complex propagation constant with real part α the attenuation constant per unit length and imaginary part β the phase constant per unit length expressed as:

$$\gamma = \alpha + \mathrm{j}\beta = \pm\sqrt{(R + \mathrm{j}\omega L)(G + \mathrm{j}\omega C)} \tag{5.6}$$

Inserting Equation 5.6 in Equation 5.5 results in:

$$v(z,t) = V\mathrm{e}^{-\alpha z}\mathrm{e}^{\mathrm{j}(\omega t - \beta z)} \tag{5.7a}$$

$$i(z,t) = I\mathrm{e}^{-\alpha z}\mathrm{e}^{\mathrm{j}(\omega t - \beta z)} \tag{5.7b}$$

Equation 5.7 represents traveling waves of which the amplitudes decrease exponentially with α. The ratio V over I is named characteristics impedance Z_c and is given by:

$$Z_c = \sqrt{\frac{R + \mathrm{j}\omega L}{G + \mathrm{j}\omega C}} \tag{5.8}$$

Backward traveling waves result from reflection of forward traveling waves due to a mismatch between this characteristic impedance of the transmission line Z_c and the impedance of its load Z_l. The reflection ρ_l at the load is expressed as:

$$\rho_l = \frac{Z_l - Z_c}{Z_l + Z_c} \tag{5.9}$$

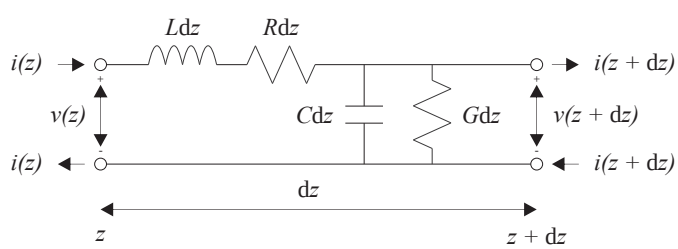

Figure 5.2: Representation of infinite small piece of transmission line

In case the cable consisting of line conductor and neutral conductor being represented in Figure 5.1 is electrical long, its circuit has to be split up in smaller circuits resulting in distributed lumped element circuits as shown in Figure 5.3 where each subcircuit is electrical small. In this figure the elements in the return conductor are explicitly taken into account such that Common Mode (CM) to Differential Mode (DM) conversions and radiation can be modeled. The return path of the CM current is the environment which is not shown in Figure 5.3. Also the return path of the CM consists of distributed lumped elements where shunt conductances and capacitances are between return path and line as well as return path and neutral. The CM to DM conversions are described using transfer impedance Z_T giving the voltage in one mode resulting

from the current in the other mode. Also Longitudinal Conversion Loss (LCL) is used which express the conversion of the voltage in one mode into voltage in the other mode. CM to DM conversions and radiation are beyond the scope of this thesis. An elaborate description of these phenomena is given in [40], where a global behavior model of the motor drive is presented including designable parameters for EMI filters.

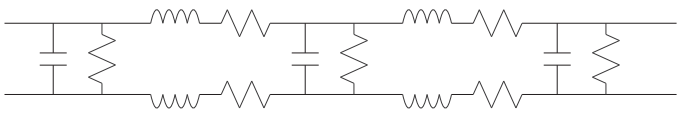

Figure 5.3: Electrical long transmission lines are modeled using distributed electrical small lumped elements circuits

5.2 Limitation of reference impedance in standards

In [41] an extensive description for cable models used for distribution of electrical power is presented. Resistive, capacitive and inductive elements are included in the cable parameters. However, the impedance of cables is split into a DC components and power frequency components. This is a typical approach in power distribution engineering which is also applied in the definition of reference impedance. The IEC 60725 'Consideration of reference impedances and public supply network impedances for use in determining disturbance characteristics of electrical equipment having a rated current $\leq$ 75 A per phase' [17] defines the reference impedance at the POI. This generic network impedance is defined for the fundamental frequency only. For 50 Hz power frequency this is 0.24 + j0.15 Ω for phase and 0.16 + j0.1 Ω for neutral, which is equivalent to 0.24 Ω + 477 μH for phase and 0.16 Ω + 318 μH for neutral. As illustrated in Figure 5.4, this reference impedance can not be used for defining and evaluating emission parameters because it does not represent the impedance inside the PDUN. Therefore, the impedance of the PDUN has to be defined as function of frequency and distance.

Measurement results on the impedance of PDUN in Thales Nederland BV in Hengelo are shown in Figure 5.5. The measurements have been performed by putting a constant voltage level of 90 dBμV from a 50 Ω source and measuring the current flowing into the PDUN. Curves are shown for different test sites in or near the buildings spread over the company premises. Local variations with frequency exist. The impedance is a function of location and time [42], [43]. On average the impedance is, rather not monotonic, increasing with frequency in the frequency band from 20 kHz to 30 MHz [42], [43]. The frequency dependent behavior of the impedance of the PDUN is accounted for in standardized setups for conducted interference tests. In order to get insight in the use of these standardized setups, a brief overview of historical developments of these setups is given in the next section.

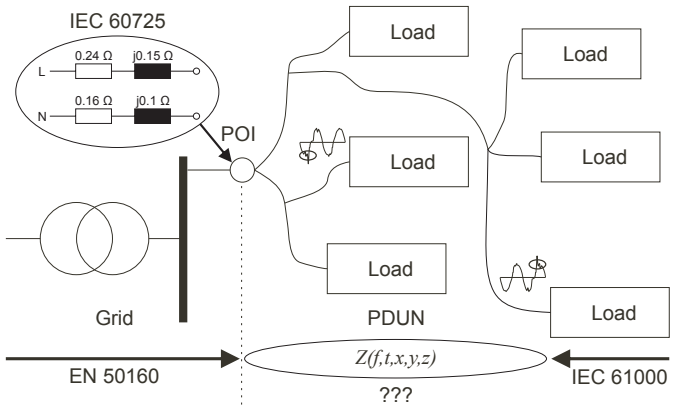

Figure 5.4: Reference network impedance is defined for the power frequency and does not include the PDUN [17]

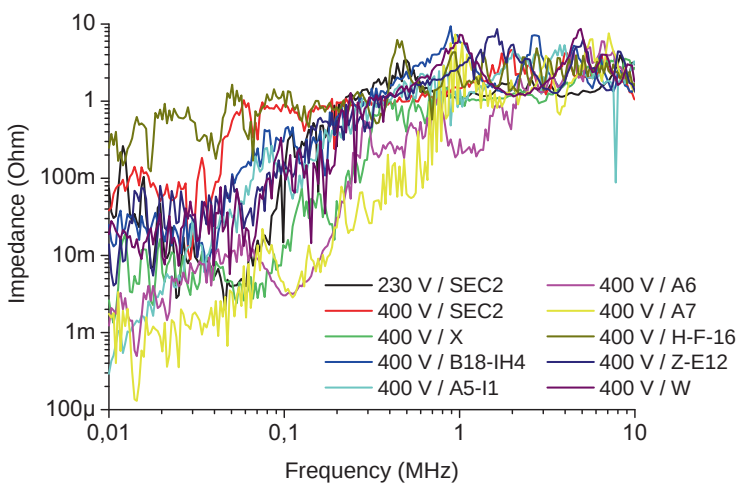

Figure 5.5: Line impedance measured at different locations within a PDUN

5.3 Equivalent networks for conducted interference in RF bands

For interference measurements a Line Impedance Stabilization Network (LISN) for professional applications and an Artificial Mains Network (AMN) for civil applications is used. The purpose of an AMN or LISN is to provide a defined impedance at RF at the terminals of the Device Under Test (DUT). Furthermore, it prevents unwanted RF signals being present on the power supply

reaching the test circuit including the DUT. Finally it couples the disturbance voltage resulting from the DUT to the measuring receiver.

The specification for the AMN was drafted as part of a measurement set in 1935 [44] by the International Special Committee on Radio Interference (CISPR) which had its first meeting in 1934. After this different countries produced measurement sets based on the specification. The data produced was different from country to country. Therefore, the Belgian Electrotechnical Committee constructed the standard CISPR measurement set. This standard set was distributed among the countries in 1939.

No meetings were held during WW II. The work on the standard measurement set was continued in 1946. In 1958 an updated measurement specification was approved in The Hague and the covered frequencies ranged from 150 kHz to 30 MHz. The work on the measurement specification and herewith the specification of the AMN is kept ongoing.

The specifications of the AMN are given in CISPR 16 [45]. CISPR is part of the IEC and prepares standards covering protection of radio bands from 9 kHz. In Europe CENELEC and in the United States of America (USA) American National Standards Institute (ANSI) and Federal Communications Commission (FCC) use and refer to CISPR publications. In Figures 5.6 to 5.8 are shown the specifications of the AMN. The AMN is a V-network type coupling the unsymmetric voltage, that is the voltage between line and reference or neutral and reference, to the measurement receiver. The transfer and inserted equivalent network shown represent the impedance between phase and reference or neutral and reference as seen by the DUT. The corresponding bands are defined as:

- Band A: 9 kHz to 150 kHz,
- Band B: 150 kHz to 30 MHz, and
- Band C: 150 kHz to 100 MHz.

Depending on the frequency band the component values of the corresponding equivalent circuit differ.

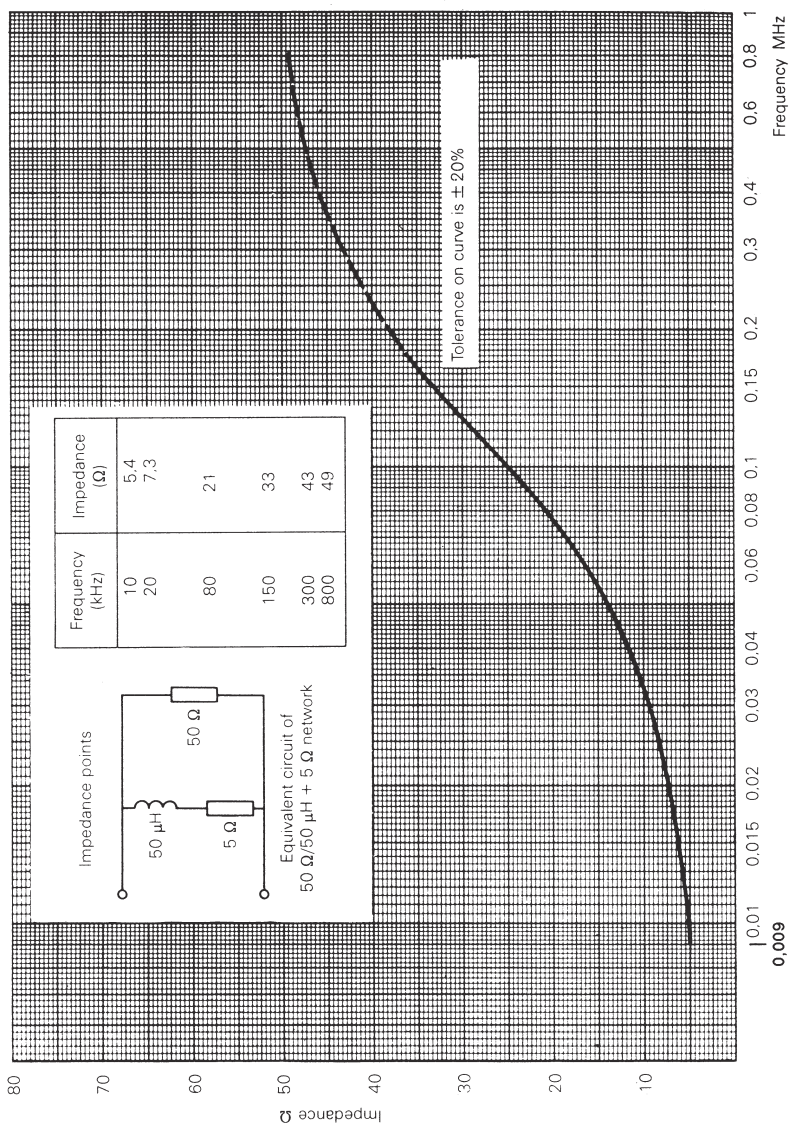

Figure 5.6: Impedance of AMN for band A as in CISPR 16 [45]

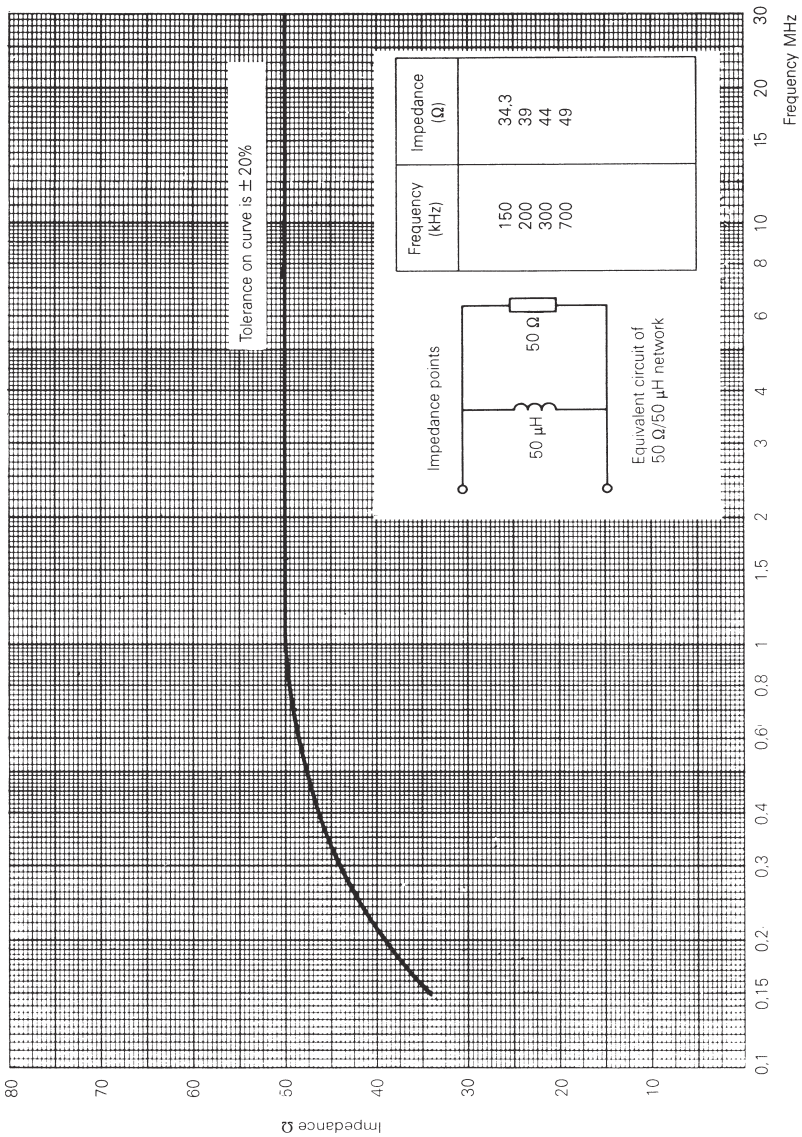

Figure 5.7: Impedance of AMN for band B as in CISPR 16 [45]

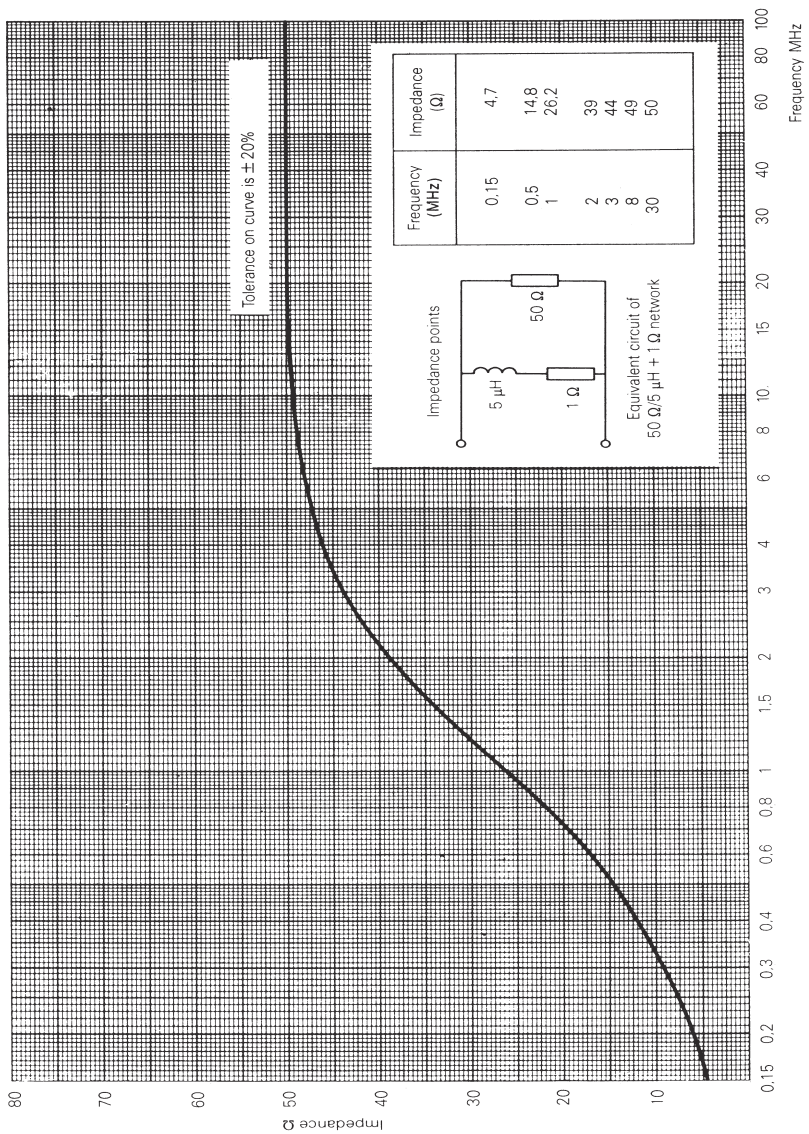

Figure 5.8: Impedance of AMN for band B, 0.15 MHz to 30 MHz or band C, 30 MHz to 100 MHz, as in CISPR 16 [45]

In the Military Handbook (MIL-HDBK) 241, which was used till the end of 2000 [46] in the USA, similar curves and equivalent circuits are used for the impedance of the power line or PDUN. In [47] is shown Figure 5.9 for the 'in-house filter designer' to give a reference for the impedance seen by the equipment in design at its terminals. The graph shows measured mean values of many power lines and the curves of three equivalent parallel RL circuits. The upper curve represents a circuit with $R = 150\ \Omega$ and $L = 50\ \mu$H, the middle curve a circuit with $R = 50\ \Omega$ and $L = 30\ \mu$H and the lower curve a circuit with $R = 23\ \Omega$ and $L = 13\ \mu$H.

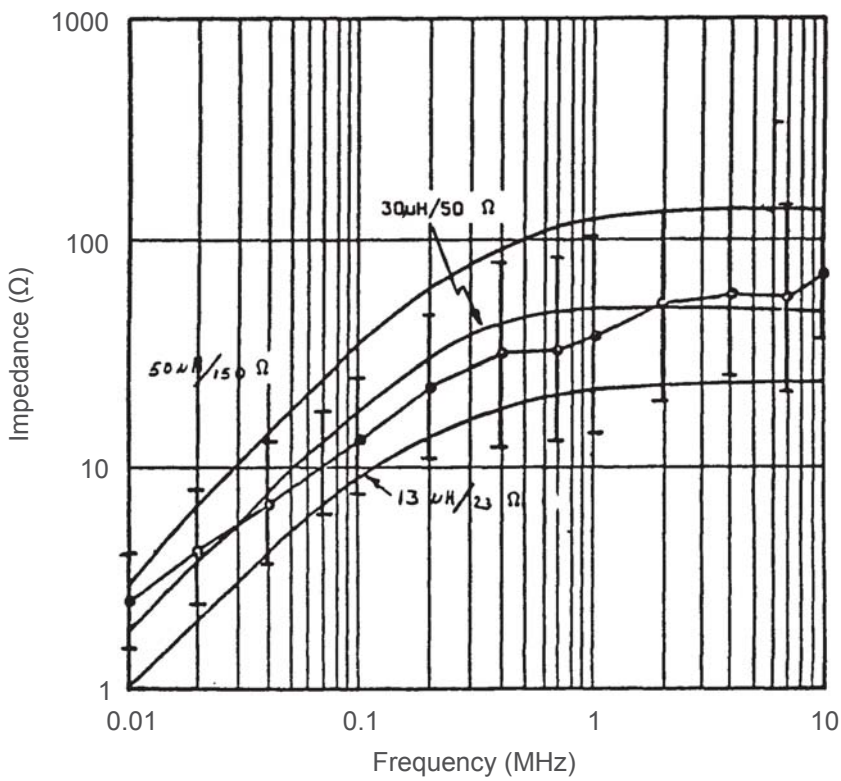

Figure 5.9: Power impedance data and circuit curves as in MIL-HDBK 241A [47]

The specifications of the LISN is part of the developments of the Military Standards (MIL-STDs) 461, 462 and 463. The United States (US) Army, US Navy and US Air Force had their own standards up to 1967. In 1967 MIL-STD 461 and 462 were published to provide a single 'Tri-Service' standard. MIL-STD 461 was intended to describe the requirements for which the US Navy had responsibility [48]. MIL-STD 462 was intended to describe the procedures for which the US Air Force had responsibility [49]. The US Army was responsible

for the definitions described in MIL-STD 463 [50] already published in 1966. Three years after the initial release of MIL-STD 461 and 462, the US Air Force had issued Notice 2. Then, the US Army had issued their own Notice 3 one year later. The odd thing was that Notice 2 and 3 were entirely different standards. This means that different requirements hold for different departments. As a result manufacturers had to comply with significant different specifications for each department. In 1999, MIL-STD 461 and 462 were merged into MIL-STD 461 Revision E [51], [52]. In 1995 MIL-STD 463 was canceled and the ANSI C63.14 'Standard Dictionary for Technologies of Electromagnetic Compatibility (EMC), Electromagnetic Pulse (EMP) and Electrostatic Discharge (ESD)' is used as reference [53].

The schematic and an implementation of the LISN as used in MIL-STD 462 Notice 3 is shown in Figures 5.10 and 5.11 [54]. The impedance seen between line and reference or neutral and reference is shown in Figure 5.12. [54]

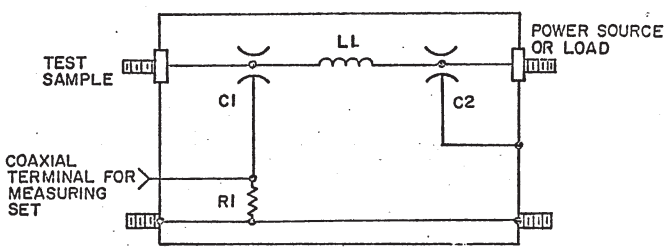

Figure 5.10: Schematic of LISN as in MIL-STD 462 Notice 3 [54]

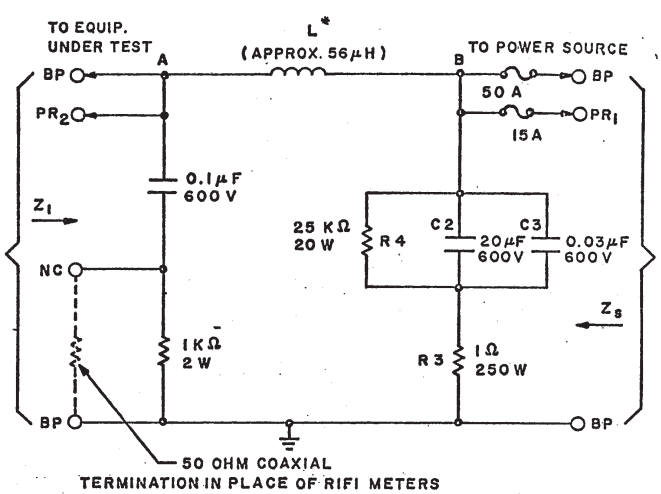

Figure 5.11: Implementation of LISN, as in MIL-STD 462 Notice 3 [54]

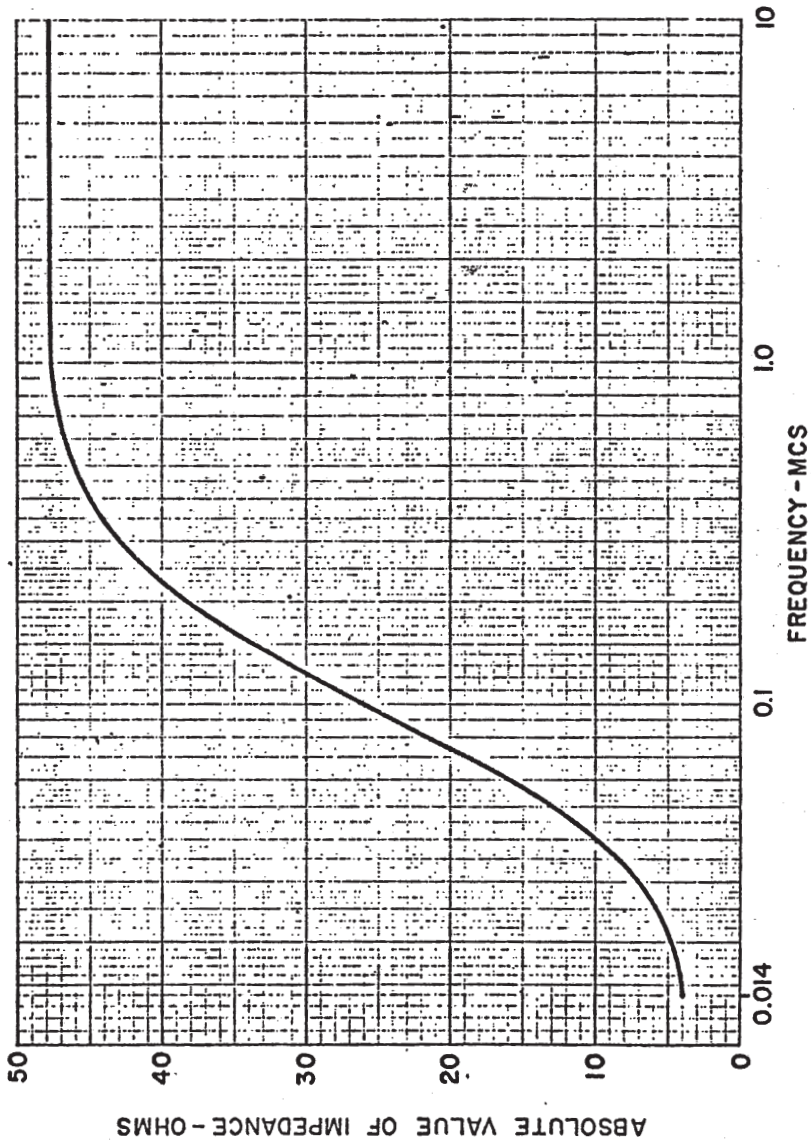

Figure 5.12: Impedance of LISN, as in MIL-STD 462 Notice 3 [54]

MIL-STD 461 Revision E and F provides background regarding the development of the LISN [51], [38]. In MIL-STD 462 10 μF feed through capacitors were used on the power leads. The purpose of these capacitors was to determine the current generator contribution of a Norton current source model. To this end, the impedance of the interference source needed also to be known. Otherwise, the interference potential of the source can not be analyt-

ically determined. However, no requirements were established for measuring the impedance portion of the Norton current source model. The influence of the test configuration on the filter design was a cause of concern. An optimized filter design is based on the impedances on its load and source side. The 10 μF feed through capacitors in series to the DUT will influence the filter design of equipment.

Before the definition of the LISN a number of experiments were performed in order to determine typical power line impedances present in a shielded room. Various power input types with and without power line filters were used. Furthermore, methods for controlling the impedance were investigated. Initially, it was considered to specify only the impedance curve for the frequency range from 30 Hz to 100 MHz without giving a way of obtaining the impedance curve. However, the experiments lead to the conclusion that a straightforward technique to maintain significant control over the entire frequency range was not practical.

In the past, 5 μH LISNs were common use and they did not provide sufficient control below 100 kHz. Several 50 μH LISNs were evaluated under various circumstances and the LISN shown in Figure 5.13 is now used in the standard. The impedance curve of this LISN is shown in Figure 5.14. This figure does not show the frequency range from 30 Hz upto 10 kHz where the 8 μF capacitor and 5 Ω resistor are active. Near 10 kHz, the 50 μH inductor and 8 μF capacitor cancel each other resulting in effectively a 5 Ω resistive load over a line and reference. Above 150 kHz, the DUT sees the 50 Ω input impedance of the measuring receiver. The frequency range goes not beyond 10 MHz as the interconnecting cables between LISN and DUT starts dominating the test results. Beyond 10 MHz these cables give rise to resonances.

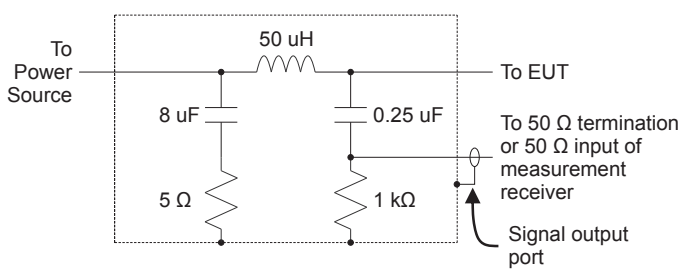

Figure 5.13: Schematic 50 μH LISN, as in MIL-STD 461 Revision E and F [51], [38]

The 50 μH inductor in the LISN represents the inductance of a wire in a power cable of 50 m length. For small platforms, this might not be representative for the actual installation like a PDUN on a small aircraft. An alternative LISN design might be used in which among other the issue of impedance control and frequency range must be addressed.

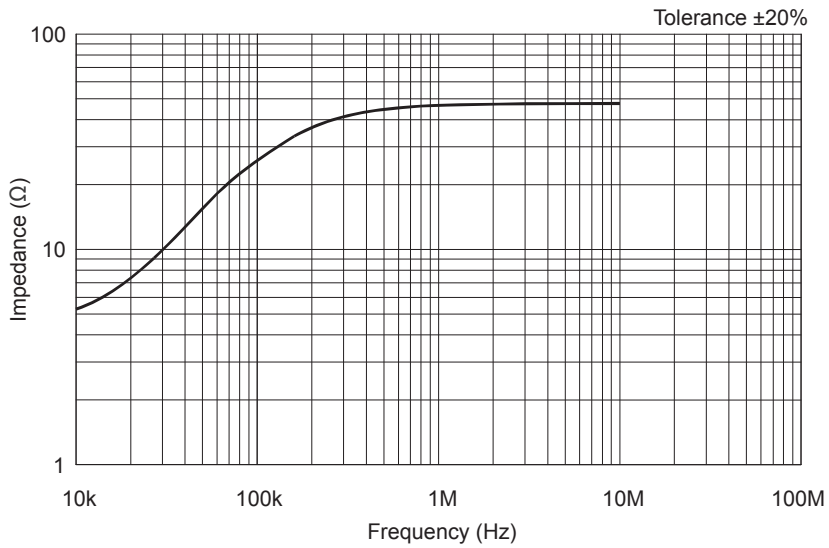

Figure 5.14: Impedance 50 μH LISN, as in MIL-STD 461 Revision E and F [51], [38]

5.4 Discussion

The description of cables being components of the PDUN using only DC components and power frequency components is too limited for describing conducted emission in PDUN. A better approach is to extend the frequency range like in the equivalent networks for the LISN or AMN. These standardized networks represents the impedance between line and reference or neutral and reference as seen by the connected equipment. The civilian standard CISPR 16 defines impedance curves for three frequency ranges: from 9 kHz to 150 kHz (band A), from 150 kHz to 30 MHz (band B), and from 150 kHz to 100 MHz (band C). As CISPR is part of the IEC, the publications on specifications of the LISN serve as base for developing standards. The military standard MIL-STD 461 covers the frequency range from 30 Hz to 10 MHz. The approach followed is to use an 8 μF capacitor with 5 Ω resistor in series for the lower part of the frequency range and a 50 μH inductor with 50 Ω impedance in parallel for the upper part of the frequency range. Around 10 kHz, a 5 Ω resistive load over a line and reference is seen as the 50 μH inductor and 8 μF capacitor cancel each other. This approach can also be found in many other standards series for automotive and aerospace (SAE), aircraft (RTCA and EuroCAE), space industry (ECCS from ESA) and many national defense standards. A sketch of the impedance is shown in Figure 5.15.

The cable length as well as the considered frequency range determines the components, as series resistance, series inductance, shunt conductance and

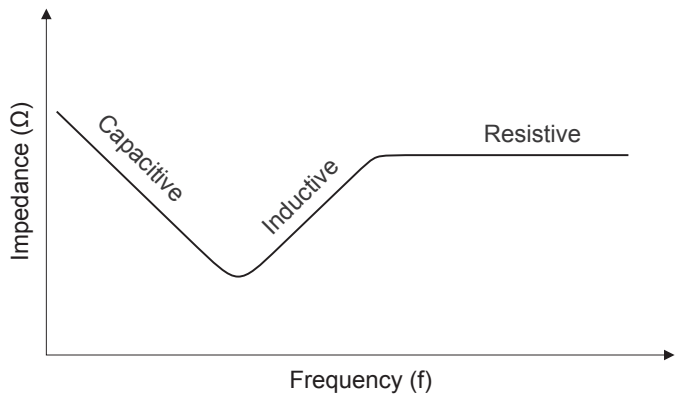

Figure 5.15: The impedance of the LISN seen by connected equipment consist of a capacitive (8 μF capacitor), inductive (50 μH) and resistive (50 Ω) parts

shunt capacitance, to be modeled and the values of those components. These are extracted from transmission line equations. When the electrical length of the cable is long, propagation delay and reflection need to be included. This is done by splitting up the cable into smaller sections each represented by a subcircuit. The cable is then modeled by distributed lumped element circuits where each subcircuit is electrical small.

Modeling the PDUN means modeling each cable and interconnection of cables. Depending on the electrical length and physical length it might be necessary to model all cable parts using distributed lumped element circuits. When the physical length is such that high frequency components are sufficiently attenuated, the distributed lumped element circuits might be replaced by one single circuit. However, when considering a subpart of the PDUN again the approach of distributed lumped element circuits has to be applied.

5.5 Summary

Each cable and interconnection of cables in the PDUN has to be modeled in order to analyze conducted interference between equipment. Depending on the electrical length and physical length it might be necessary to model all or a subpart of it using distributed lumped element circuits to account for propagation delay and reflection. The 4 lumped elements, series resistance R, series inductance L, shunt conductance G and shunt capacitance C, are expressed per unit length of transmission line. The lumped elements are extracted from transmission line equations for describing the propagation of voltage and current along the axis of the line as function of time.

The conventional approach in power engineering is to split the impedance

of cables into a DC components and power frequency components. The generic network impedance is defined for the fundamental frequency only as 0.24 + j0.15 Ω for phase and 0.16 + j0.1 Ω for neutral. This reference impedance can not be used for defining and evaluating emission parameters containing other frequencies.

For interference measurements an AMN or LISN is used to provide a defined impedance at the terminals of the DUT. The covered frequency bands start at 9 kHz and end between 10 to 100 MHz for AMN and start at 30 Hz and end at 10 MHz for LISN. These standardized networks represent the impedance between phase and reference or neutral and reference as seen by the DUT. It prevents unwanted RF signals being present on the power supply reaching the test circuit including the DUT thereby coupling the disturbance voltage resulting from the DUT to the measuring receiver. The AMN is specified in CISPR 16 and the specification of the LISN is developed by the US Army, US Navy and US Air Force. The equivalent impedance of the standardized networks is a single circuit with lumped components.

An AMN or LISN is basically a capacitor at low frequencies, a resistor (often 50 Ω) for high frequencies and an inductor, which represents the power cables, for medium frequencies. The description is based on measurements performed several decades ago when linear equipment was dominant. Nowadays nonlinear equipment is dominant and has a time dependent impedance. When the rectifier bridge in the power electronic interface is conducting and charging the bulk capacitor, the impedance is much lower than when the bridge is not conducting. This means that more measurements are needed to characterize the PDUN, especially for the low frequency range which is dominated by periodically charging of bulk capacitors. Then a description can be developed of the PDUN as seen by the DUT for a frequency range starting from below the fundamental power frequency upto 100 MHz or even higher.

The following chapter studies the propagation of transients on short cables. Also the effect of nonlinear equipment is taken into account by including varistors representing the power electronic interfaces of equipment. In the chapter thereafter, the dynamic behavior of equipment is analyzed and subsequently models are derived. Using these models in combination with the models for the infrastructure of the PDUN, which is in essence a combination of lumped element circuits, the entire PDUN can be modeled.

Chapter 6

CM and DM transients

The majority of transient analyses in power distribution systems focus on transients generated in the grid [55]. Transients usually do not have a widespread effect in contrast to voltage interruptions and dips. The consequences of a transient is mainly limited to local equipment and therefore transients are not commonly discussed in PQ literature [56]. Transients generated by switching actions in the end-user equipment have the potential of equipment malfunction and damage. For the most part in PQ data logging transient capturing is not done as a higher sampling rate and wider bandwidth is needed. However for EMI tests on equipment, transients, bursts and surges as described in the IEC 61000-4-4 and 61000-4-5 have to be applied. The risetime of the transient voltage is 5 ns, which is much faster than any of the phenomena taken into account by PQ analyzers.

Inside large PDUNs transients and surges are induced by disconnecting cables carrying high current. This disconnection can be intentional switching off a system or an accidental cutting from the supply due to an overloaded fuse. Voltage transients will propagate on the disconnected cable to the electric equipment connected to it. Also crosstalk due to coupling between cables occur which can result in EMI. An example of equipment malfunctioning by crosstalk is the disturbance of data links [57].

Chapter 5 gave a brief overview of transmission lines, reflections and the basics of propagation on transmission lines. The history of research on transients in PDUN is discussed in Section 6.1. Section 6.2 discusses the limitations of the PQ analyzers used in the case studies of Chapter 4 with respect to occurrence of transients on cables in PDUN. Furthermore, it introduces an alternative for PQ analyzers to capture fast transients. Due to time constraints the design has not been implemented and a setup for measuring propagation of transients on cables is used in Section 6.3. In this setup connected electronic equipment is represented by varistors to investigate the impact of transients on electronic equipment and vice versa. In Section 6.4 the measurement results are compared to reported findings in literature on intentional ultra wideband voltage transients.

6.1 Transients and surges

In May 1987 a comprehensive study has been published on the occurrence of transients in PDUN [58]. In four different areas transient measurements had been performed between line and protective earth. The voltage between line and protective earth is also called nonsymmetrical voltage as defined in Figure 6.1. Table 6.1 summarizes the areas, number of measurement points, measurement time and average occurrence of transients in excess of the mains voltage. Furthermore, the transients were categorized according to maximum peak amplitude in the transient in excess of the mains voltage. The bottom limit of the range is 100 V and the upper limit is 3000 V. Transients having a larger peak than 3000 V were counted together. Table 6.2 lists for every area the number of transients per maximum peak amplitude range.

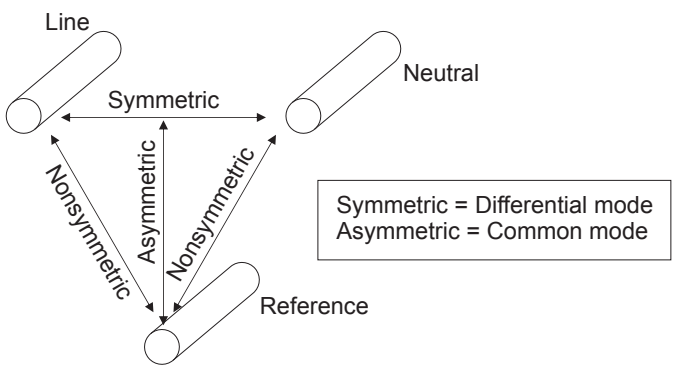

Figure 6.1: Definition of symmetrical, nonsymmetrical and asymmetrical voltage

Table 6.1: Overview transient measurement results as published in [58]

Area	# points	# transients	Time (hr)	Average rate ($\frac{1}{\text{hr}}$)
Industrial	14	23054	1317	17.5
Business	9	3401	1202	2.8
Domestic	6	287	447	0.6
Laboratory	11	1069	462	2.3
Total	40	27811	3428	8.1

The results from Table 6.2 includes transients which do not result in an instantaneous voltage level exceeding the swing of the nominal voltage. For the range of transient peaks upto about 650 V it is in theory possible that the instantaneous voltage does not exceed the swing. Exceeding is unavoidable for higher ranges. However, the measurement system used in [58] has a bandwidth

Table 6.2: Range of transient peaks as published in [58]

Peak value	Area				
(V)	Industrial	Business	Domestic	Laboratory	Total
100 - 140	11666	1826	148	589	14229
140 - 180	7408	877	68	197	8550
180 - 230	2635	467	37	145	3284
230 - 300	751	98	21	94	964
300 - 390	229	41	10	27	307
390 - 500	94	5	2	10	111
500 - 650	66	-	1	3	70
650 - 840	54	3	-	-	57
840 - 1000	35	1	-	-	36
1000 - 1400	39	8	-	1	48
1400 - 1800	25	3	-	-	28
1800 - 2300	13	7	-	-	20
2300 - 3000	11	4	-	1	16
> 3000	28	61	-	2	91

of 20 MHz and a sampling interval of 10 ns. This means it is able to detect transients shorter than 1 μs in contradiction to the PQ analyzers used in the case studies of Chapter 4. This may imply there were transients occurring during the case studies, but all of them were so fast that they kept undetected for the PQ analyzers. However, as a result of the work in [58] electronic equipment is equipped with a certain level of protection against electrical fast transients and bursts as well as surges. These phenomena result from lightning and switching events and are covered in the following two IEC publications [59] and [60]:

- IEC 61000-4-4 'Testing and measurement techniques - Electrical fast transient/burst immunity test', and
- IEC 61000-4-5 'Testing and measurement techniques - Surge immunity test'.

As stated in Section 5.1 two modes of propagation exist: DM and CM propagation. Figures 6.2 and 6.3 respectively illustrate DM and CM propagation on a single phase power cable. The DM signal flows over line and neutral in opposite directions. One of the two wires act as return for the DM signal, resulting in a voltage difference between the wires. Protection against DM transients makes use of monitoring the voltage between the wires. The CM signal flows over line and neutral in same direction. The environment provides the return path for the CM signal, resulting in a voltage difference between the cable and the environment. It is not easy if not virtually impossible to trace this return path as the environment provides various ways for the CM signal to split up and to flow back. The CM transient does not occur between the wires within

the cable. Detection of and protection against CM cannot be based on simply monitoring the voltage between the wires.

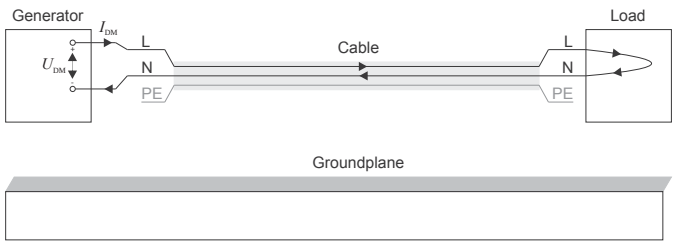

Figure 6.2: DM propagation on power cable

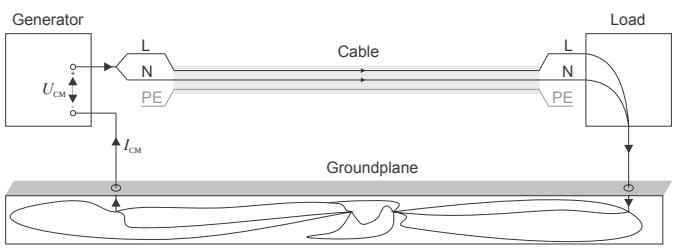

Figure 6.3: CM propagation on power cable

The predecessor of the IEC 61000-4-4 covered only nonsymmetrical transients [61]. When having only a single nonsymmetrical voltage transient, one cannot deduce the type of mode from it. Referring to Figure 6.1 when having a DM transient, there is a nonzero symmetrical voltage, a zero asymmetrical voltage and the nonsymmetrical voltages have opposite sign. When having a CM transient, there is a zero symmetrical voltage, a nonzero asymmetrical voltage and the nonsymmetrical voltages are equal and nonzero.

6.2 Design of high-speed multichannel data logger for PQ measurements

During all the cases studies, the instantaneous voltage level maintained in the swing of the nominal voltage. No transients exceeding several hundred of volts were detected. This holds for transients between line and neutral (symmetric), line and protective earth (nonsymmetric), and neutral and protective earth (nonsymmetric). It should be noted that the PQ analyzers used in the case studies of Chapter 4 and PQ analyzers in general are not designed for detection of high frequency phenomena. One of the two types of PQ analyzers used, a PQube, can detect transients as short as 1 μs, but its maximum sampling rate

is 256 samples per cycle of power frequency. The other one used, a Power Explorer, is capable to capture events as short as 1 μs.

In large systems, transients, bursts and surges can occur due to switching effects of parts of the systems. An example is switching of one radar inside an integrated mast. Because PQ analyzers are not capable to capture fast transients the design of a transient analyzer, combined with a conventional PQ analyzer, was foreseen. In the course of this research project low cost PQ analyzers became available, such as the PQube. Therefore a high-speed multichannel data logger was designed. The design is performed in collaboration with a bachelor student from the University of Twente [62]. This data logger is able to capture high frequency phenomena. The requirements on the data logger are listed in Table 6.3. In transient measurements performed on a power cable for defining the requirements showed spectral content up to 110 MHz resulting in a minimal sample rate of 220 MS per second. For the purpose of analyzing events, the data logger has to capture events in a window of several periods of power frequency.

Table 6.3: Minimal requirements high-speed multichannel data logger for PQ measurements

Specification	Requirement
# channels	8
Resolution per channel	8 bit
Sample frequency	$>$ 220 MS per second
Measurement sample length	100 ms
Storage	non-volatile long term
Input protection	transient and surge resilient
Autonomous functioning	yes
Build in power functionality	long enough to store data

The block diagram of the data logger design is shown in Figure 6.4. The processor unit being based on an Field Programmable Gate Array (FPGA) processor is connected to two Analog to Digital Converters (ADCs). Each ADC is connected to 4 inputs via protection circuits. Cache memory and storage are connected to the processing for short term and long term data storage. Furthermore, an user input provides the user interface. The design is based on the commercial availability of the different building blocks.

At time of designing the high-speed multichannel data logger, Texas Instruments was the only manufacturer offering high-speed ADC boards with multiple connectors for high-speed data transfer. The fastest boards in their collection were a board with a four channel 200 MS per seconds ADC, a board with a two channel 250 MS per second ADC and a board with an one channel 500 MS per second ADC. Despite the sampling rate is rather lower than required, the four channel 200 MS per second option is chosen as this board has the highest number of channels. The board is shown in Figure 6.5 and con-

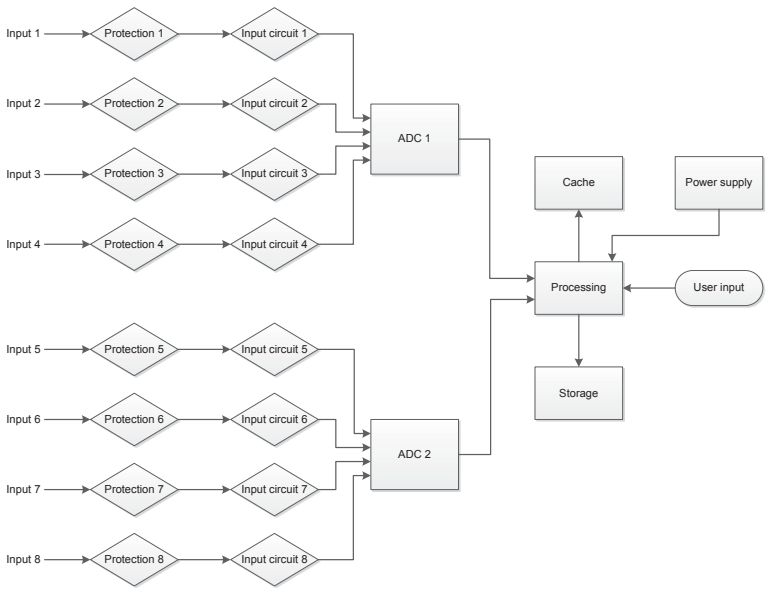

Figure 6.4: Block diagram design high-speed multichannel data logger for PQ measurements

tains an ADS58C48 chip from Texas Instruments with a four channel, 11 bit, 200 MS per second ADC. The board on which the ADS58C48 ADC is placed has a Double Data Rate (DDR) Low Voltage Differential Signaling (LVDS) data output. This data output can be connected to a high speed connector of an FPGA development board via a High Speed Mezzanine Card (HSMC) ADC bridge. This bridge is an interface between the high speed data output of the ADC evaluation module an HSMC connector of the FPGA development board. Furthermore several transformers are placed on the module as input circuits. These inputs are modified for the data logger.

The specifications of the original and modified input circuit are listed in Table 6.4. The main characteristics of the input circuit is to convert the input signal from a single-ended to a differential signal and to prevent aliasing by low pass filtering. The sampling rate of the ADC board is 200 MS per second. Therefore, the -20 dB point is specified to be between 90 MHz and 100 MHz in order to have enough attenuation at 100 MHz and still having a large passband. The original circuit has large attenuation at low frequencies and a non constant transfer and its upper -20 dB point is located at 160 MHz.

The design in building blocks of the input circuit is shown in Figure 6.6. The first building block contains a low pass suppressing high frequency signals. The second block is active converting the single-ended input signal to a differential

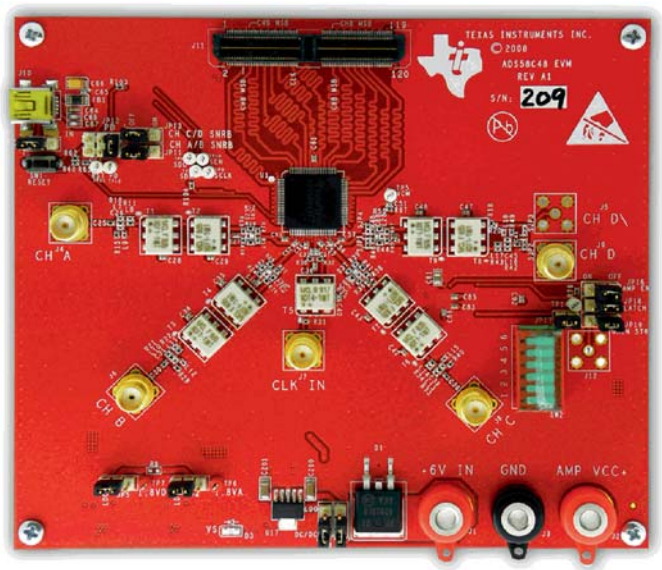

Figure 6.5: ADS58C48 Evaluation Module

Table 6.4: The specifications of the original and new input circuit of ADC board

Specification	Requirement	Original input	Modified input
Input signal type	single-ended	single-ended	single-ended
Output signal type	differential	differential	differential
Output voltage	$>$ -0.3 V, $<$ 1.9 V	not restricted	$>$ 0 V, $<$ 1.9 V
Input impedance	50 Ω	unknown	50 Ω
Output impedance	matching network	matching network	matching network
Passband frequency	0 - 90 MHz	20 kHz - 20 MHz	0 - 90 MHz
Passband ripple	$<\pm 1$ dB	$<\pm 1$ dB	$<\pm 1$ dB
-20 dB point	$>$ 90 MHz, $\leq$ 100 MHz	$>$ 160 MHz	100 MHz

output signal. This block includes a second low pass filter to further suppress high frequency signals. The last block contains a notch filter to ensure rapid

attenuation in frequency transfer around 100 MHz.

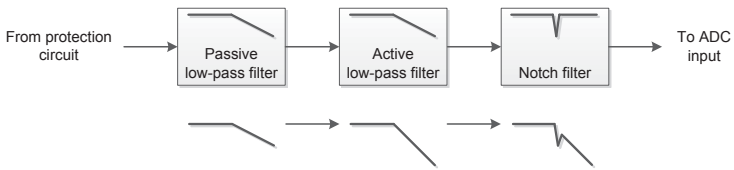

Figure 6.6: The concept of the input circuit filtering

The measured transfer functions of the original and modified input circuit are shown in Figure 6.7. The passband transfer of the modified circuit is constant within ± 1.0 dB over a large range of the passband and the -20 dB point is located at 97 MHz. The required and obtained specifications of the modified input circuit are listed in Table 6.5. Most obtained specifications are within the requirements. However, the upper frequency of the passband is much too low due to a slowly increasing attenuation for frequencies higher than 5 MHz. This can be compensated for by changing the design or of the input circuit or by incorporating compensated weighting coefficients in the data processing. The input impedance is constant within the passband, but not 50 Ω. When necessary for the protection circuit an impedance matching network can be used. Each input has a protection block to prevent over voltages in the measured signal from damaging the input circuit or other circuits following it. The protection circuit attenuates or limits the input voltage range to the usable input range of the input circuit. It is chosen not to design an universal protection circuit due to the variety in measurement configurations as different input voltages, measurement connectors or sockets. The output voltage range of the modified input circuit of the ADC has not been measured and can therefore not be verified.

As the ADCs sample each channel at 200 MS per second with 8 bit resolution, the minimum data rate to be handled will be 12.8 Gbit per second. Most commercially available data connections like Universal Serial Bus (USB), Serial Advanced Technology Attachment (SATA) and Ethernet can not handle this data rate. Even though using multiple links in parallel, like three USB 3.0 connections combined or two 10 Gbit Ethernet links combined or an 8 lane Peripheral Component Interconnect (PCI) express connection are capable of handling this data rate, the data has to be stored what might become the bottleneck of the data transfer rate in the system. The (internal) SATA connections of the storage medium can not handle the data throughput. An option is to use cache memory. A measurement sample length of 100 ms to capture multiple periods of power frequency at a data rate of 12.8 Gbit per second results in a minimum size of 160 MB. For the capability of measuring repeatably within a short timespan and for future functionality a larger capacity is used.

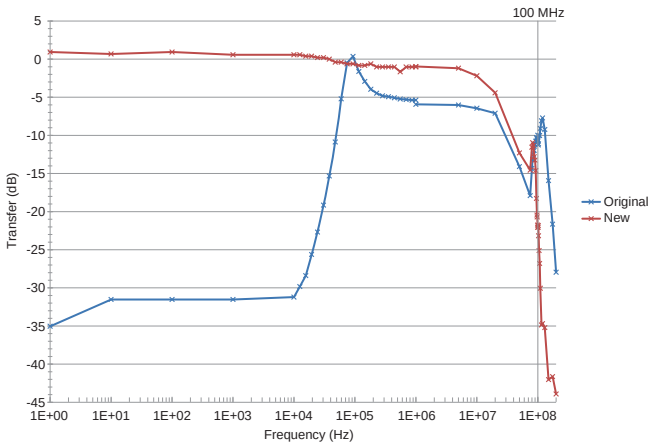

Figure 6.7: Frequency transfer of the original and modified input circuits

Table 6.5: The obtained specifications of the modified input circuit of ADC board

Specification	Requirement	Modified input
Input signal type	single-ended	single-ended
Output signal type	differential	differential
Output voltage	$>$ -0.3 V, $<$ 1.9 V	not measured
Input impedance	50 Ω	constant
Output impedance	matching network	matching network
Passband frequency	0 - 90 MHz	0 - 5 MHz
Passband ripple	$<\pm 1$ dB	$<\pm 1.02$ dB
-20 dB point	$>$ 90 MHz, $\leq$ 100 MHz	97 MHz

In the design a DDR 2 Small Outline Dual Inline Memory Module (SODIMM) is used, which can handle the high data rate and has a large capacity.

For the data processing itself an FPGA is used. Is has the capability to handle a high data rate and the ability to connect to the ADC boards and DDR 2 SODIMMs. The Altera DE4-230 development board is used in the design of the high-speed multichannel data logger. It is capable to handle

two DDR 2 SODIMM and a maximum data rate of 102 Gbit per second. It also has 48 full-duplex transceivers which are necessary for PCI express bus, gigabit Ethernet, fiber channel communication, and other interfaces which can be used in the future. The Altera DE4-230 development board supports Secure Digital (SD) cards, but also has USB 2.0 and SATA ports such that a Solid State Disk (SSD) can be connected. An SD or SSD can be used for long term storage of the large size of measurement data and to protect the data in case of a power supply failure.

The power supply on the Altera DE4-230 development board has a maximum power rating of 250 W. Considering a shutdown time of 5 minutes using maximum power 21 Wh is consumed. This can be supplied by two rechargeable D-cells or a small lead-acid battery. A commercially available Uninterruptible Power Supply (UPS) is an alternative which can also be used to power possible peripheral equipment in future.

The Altera DE4-230 development board together with two ADS58C48 evaluation modules and two HSMC ADC bridge boards are the base for the high-speed multichannel data logger. The input circuit and the protection circuit need to be designed completely. An overview of all components proposed for the data logger is listed in Table 6.6.

Table 6.6: Proposed components for high-speed multichannel data logger for PQ measurements

Design part	Proposed component
Protection circuit	to be designed for specific situation
Input circuit	modified circuit for low pass filtering
ADC	two ADS58C48 evaluation modules
Processing	Altera DE4-230 development board
Cache	two DDR2 SODIMMs
Storage	(SSD) harddisk or SD card
Power supply	rechargeable battery or UPS

The required and obtained specifications of the data logger are summarized in Table 6.7. At the time of design, the commercially available ADCs had not sufficient sampling rate or not a sufficient number of channels. Multichannel ADCs with higher sample rates can be expected in the near future. The usage of faster ADCs will also reduce the complexity of the input circuit. This makes it easier to shift the upper frequency of the low pass band filter to a higher frequency. The input protection circuit has still to be designed. Further details on the design and design considerations can be found in [62].

Table 6.7: Obtained specification in design of high-speed multichannel data logger for PQ measurements

Specification	Obtained in design
# channels	8
Resolution per channel	11 bit
Sample frequency	200 MS per second
Measurement sample length	$\geq$ 100 ms
Storage	(SSD) harddisk or SD card
Input protection	to be designed for specific situation
Autonomous functioning	yes
Build in power functionality	$\geq$ 5 minutes

6.3 Propagation of fast transients on short cables

The high-speed multichannel data logger has not been implemented yet and measurements on propagation of transients shorter than 1 μs are performed using the measurement setup shown in Figure 6.8. It consist of an Schaffner interference simulator NSG 222A as transient generator and an Agilent DSO-X 3024A oscilloscope for measuring the nonsymmetric L-PE and N-PE voltage waveforms on a 64 meter extension cable connected to the generator as shown in Figure 6.9. The sample rate of the oscilloscope is 2 GS per second and the input bandwidth of a channel is 200 MHz. A resistive voltage probe is used as interface between extension cable and oscilloscope input channels. Furthermore, a 60 W incandescent lamp used as resistive load and 230 V varistors are available for studying the effect of loads and over voltage protection on the propagation of transients. The specifications of the varistors are listed in Table 6.8. The varistors and resistive load will be used later on in this section.

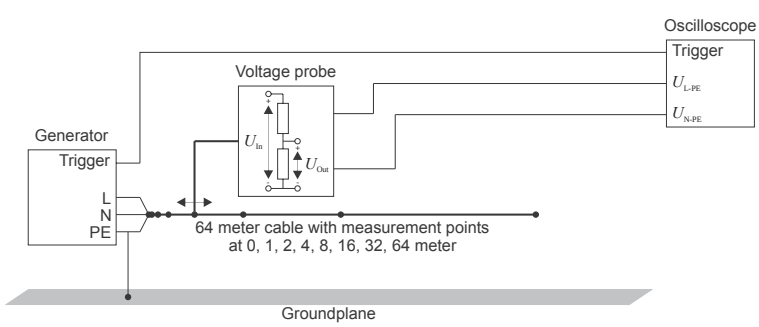

Figure 6.8: Setup for measuring propagation of transients over 64 meter cable

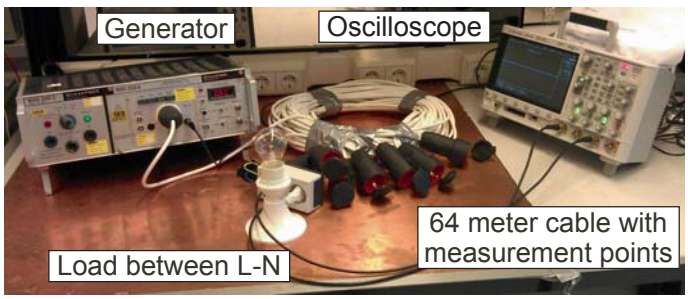

Figure 6.9: Picture of setup for measuring propagation of transients over 64 meter cable

Table 6.8: Specifications varistors used in modified versions of the setup in Figure 6.8

Working voltage (V_{AC})	Breakdown voltage (V)	Clamping voltage (V)	Capacitance at 1 kHz (pF)
230	360	595	530

The transient generator can be operated in symmetrical mode and asymmetrical mode with rise times about 5 ns. The transient voltage waveforms L-PE and N-PE have opposite sign in symmetrical mode or DM and equal sign in asymmetrical mode or CM. The transient voltage waveforms for both modes are shown in Figure 6.10. The waveforms consist of a single large peak with a number of trailing smaller peaks. As the cable has open termination reflection occurs at the end of the cable resulting in a bump about 8×10^{-4} ms = 0.8 μs. The transient voltage pulses and the transient voltage waveform could not be detected by PQ analyzers mentioned in Section 6.2 as the transient voltage pulse durations are in the order of several nanoseconds and the transient voltage waveform duration is a fraction of 1 μs.

Moving the voltage probe along the 64 meter cable give the results in Figure 6.11. As expected from the earlier analysis of cables in Section 5.1 transient voltage waveforms are dampened with distance. In symmetrical mode the transient pulses at 16 meter are a dampened version of the original pulses in Figure 6.10(a). At 32 meter the pulses combine to one broad pulse. As at the end of the cable reflection occurs resulting in a peak amplitude at 64 meter just as high as at 32 meter. The surface area of the waveform at 64 meter is approximately the surface area of the waveform at 32 meter. In asymmetrical mode the decrease of high frequency components is slower than in the symmetrical mode. Again the transient pulses at 16 meter are dampened version of the original pulses in Figure 6.10(b). The amplitude of the pulses at 32 meter are significantly lower and the trailing pulses combine into one large pulse. At

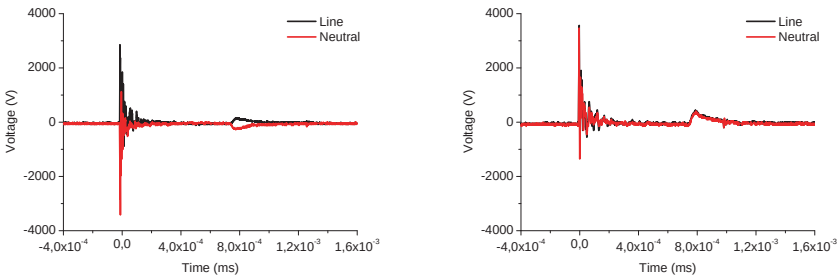

Figure 6.10: Waveforms of transients generated by generator: (a) Symmetric mode (= DM); and, (b) Asymmetric mode (= CM).

64 meter reflections occurs and the peak amplitude of the voltage waveform as well as the waveform surface area are about the same as at 32 meter.

In the measurement results obtained using the setup of Figure 6.8 crosstalk will be present as the 64 meter cable is coiled up. Capacitive coupling occurs between the windings of the coil. This crosstalk is measured with a pick-up coil of 32 meter cable length as in Figure 6.12. The results are shown in Figure 6.13 for symmetric and asymmetric modes and agree with the measured voltage waveforms in Figure 6.11. Since the hight of the coil is about 10 cm, negligible compared to the length of the cable, the crosstalk virtually appears at 0 seconds in all voltage waveforms captured using the measurement setup in Figure 6.8 and modified versions of this setup used in the remaining part of this section.

To further explorer the propagation of fast transients the setup of Figure 6.8 is modified. The modified setups are shown in Figures 6.14 - 6.20. First the effect of resistive load on the propagation of transients is investigated. Then the effect of varistors is investigated and finally combinations of resistive load and varistors are investigated. As varistors are used in electronic equipment for protection against over voltage, varistors are used in the setups to represent connected electronic equipment. The varistors used will clamp when they detect the transients. In this way, the impact of transients on equipment and vice versa can be investigated without using electronic equipment.

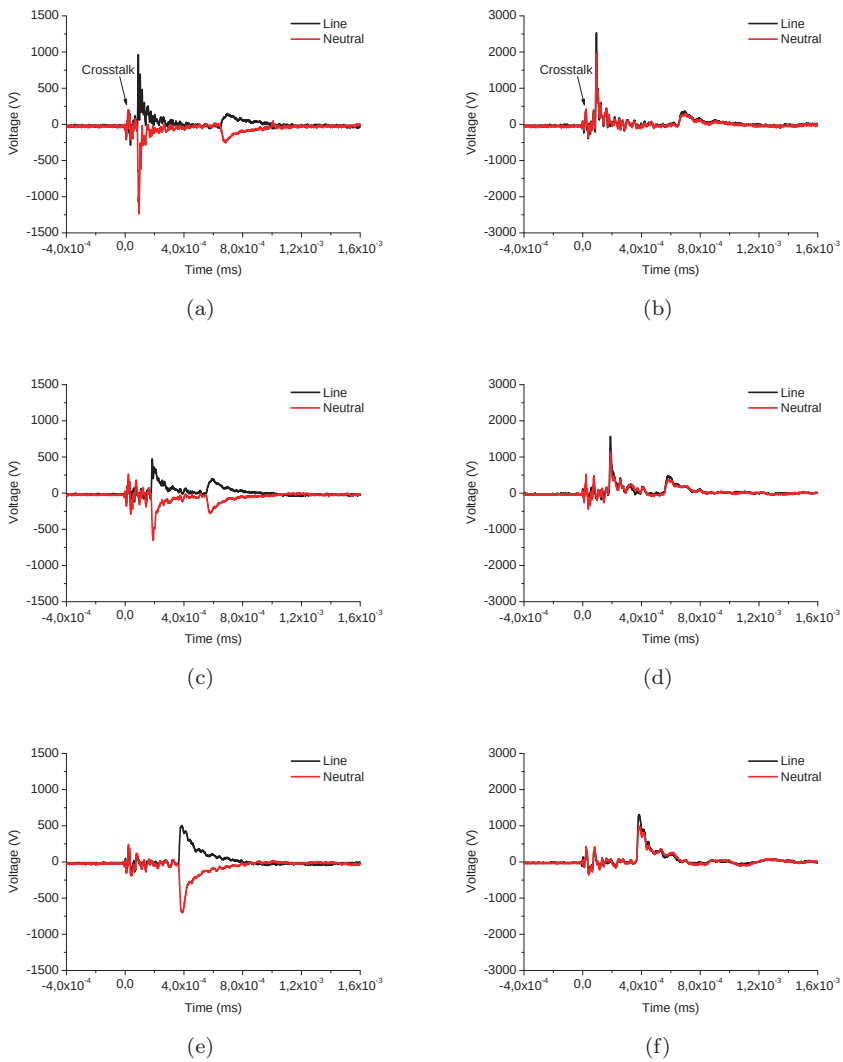

Figure 6.11: Propagation of transients over 64 meter cable with open termination: (a) Symmetric mode 16 meter; (b) Asymmetric mode 16 meter; (c) Symmetric mode 32 meter; (d) Asymmetric mode 32 meter; (e) Symmetric mode 64 meter; and, (f) Asymmetric mode 64 meter.

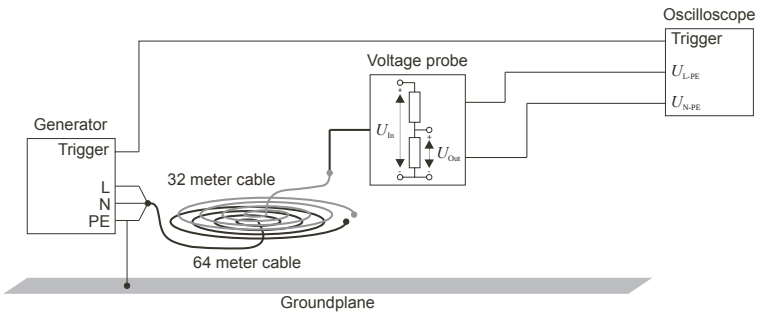

Figure 6.12: Setup for measuring crosstalk between two cables coiled up

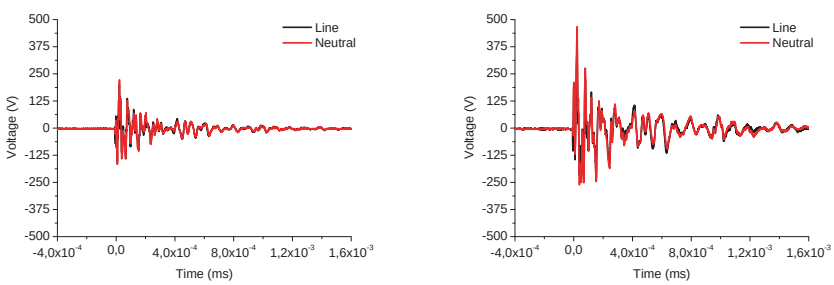

(a) (b)

Figure 6.13: Crosstalk between two cables coiled up: (a) Symmetric mode; and, (b) Asymmetric mode.

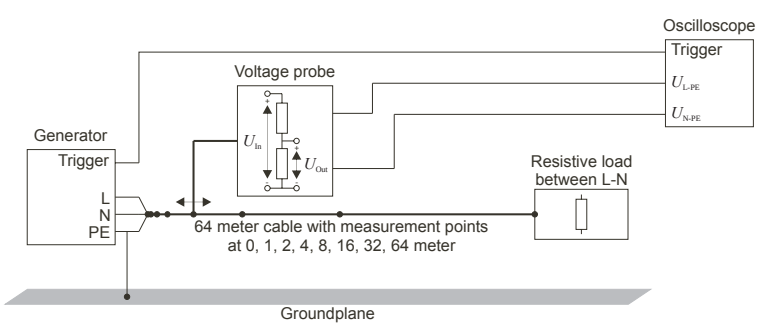

Figure 6.14: Setup for measuring propagation of transients over 64 meter cable with 60 W resistive termination

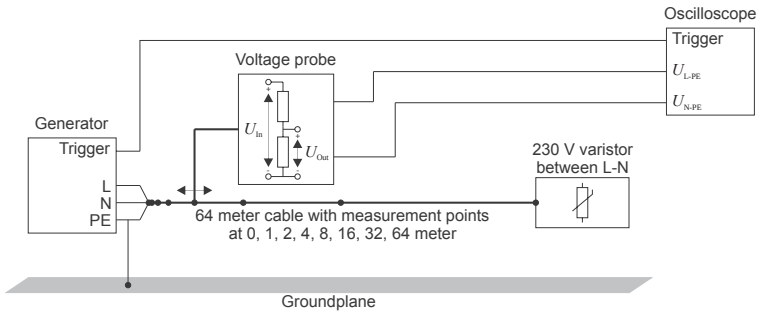

Figure 6.15: Setup for measuring propagation of transients over 64 meter cable with varistor between L-N as termination

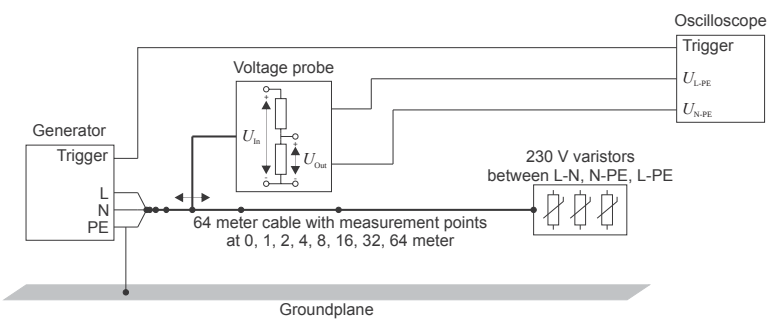

Figure 6.16: Setup for measuring propagation of transients over 64 meter cable with varistors between L-N, N-PE and L-PE as termination

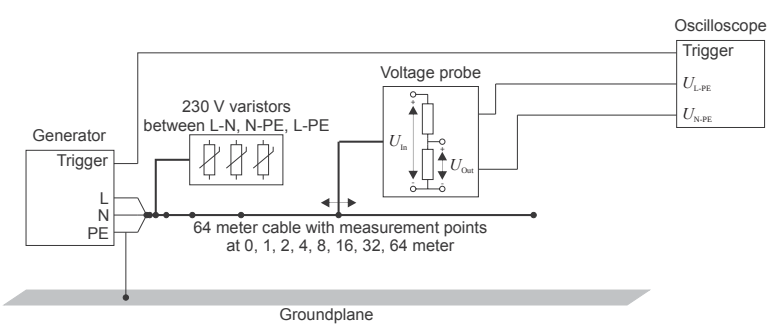

Figure 6.17: Setup for measuring propagation of transients over 64 meter cable with open termination and varistors between L-N, N-PE and L-PE at 2 meter

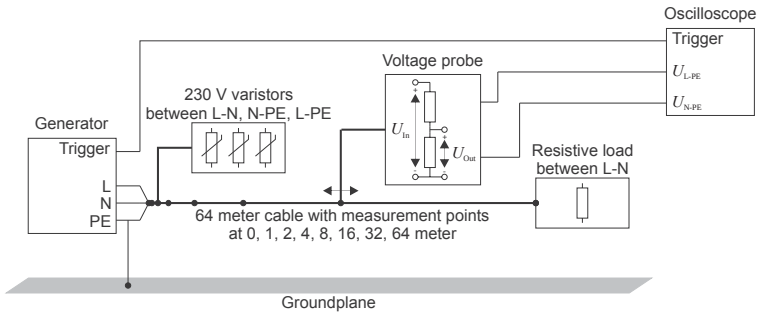

Figure 6.18: Setup for measuring propagation of transients over 64 meter cable with 60 W resistive termination and varistors between L-N, N-PE and L-PE at 2 meter

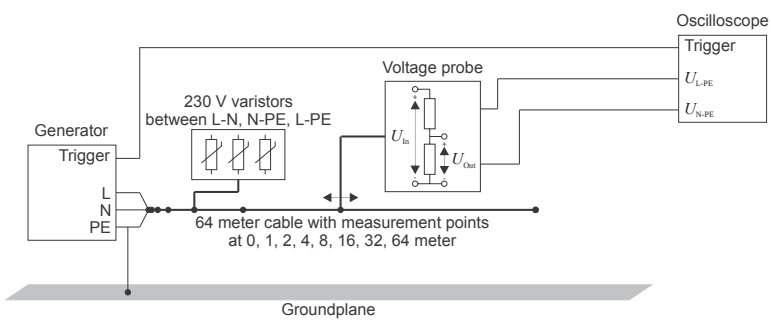

Figure 6.19: Setup for measuring propagation of transients over 64 meter cable with open termination and varistors between L-N, N-PE and L-PE at 8 meter

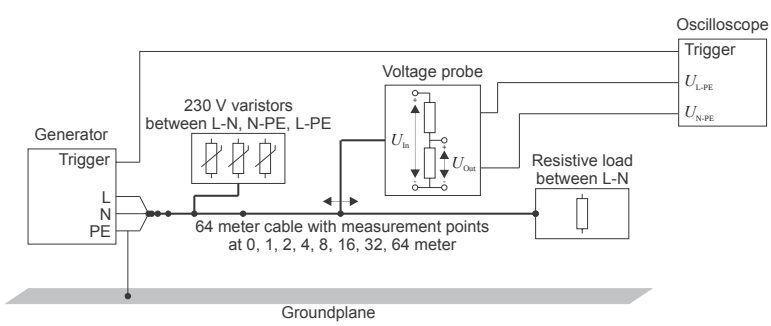

Figure 6.20: Setup for measuring propagation of transients over 64 meter cable with 60 W resistive termination and varistors between L-N, N-PE and L-PE at 8 meter

By terminating the cable the reflection will be affected. A 60 W load is connected between L-N at the end of the cable in the measurement setup of Figure 6.14. For symmetrical mode transients the transient voltage waveforms are the same as in the previous case with open termination except for the absence of reflections. This is shown for the measurement at 32 meter in Figure 6.21(a). At the end of the cable the transient is absorbed by the load. As a result, the peak amplitude of the voltage waveform pulse and its surface area are both smaller at 64 meter than at 32 meter. For the asymmetric mode the transient voltage waveforms are the same as in the previous case with open termination. As the transient waveforms have an equal sign, there is no voltage across the load and the reflection is still present. This is shown for the measurement at 32 meter in Figure 6.21(b).

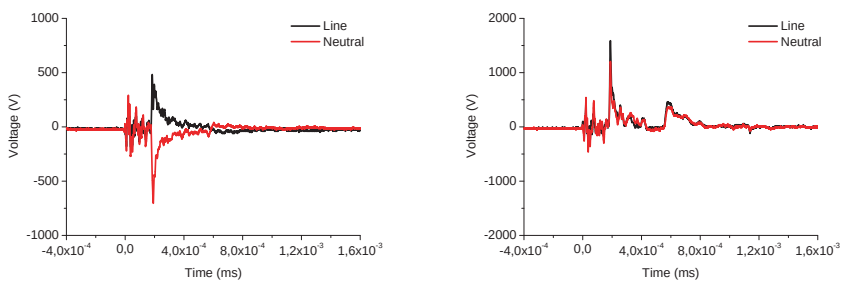

(a) (b)

Figure 6.21: Propagation of transients over 64 meter cable with 60 W resistive termination: (a) Symmetric mode 32 meter; and, (b) Asymmetric mode 32 meter.

Replacing the resistive load between L-N by a 230 V varistor gives different results for the symmetric mode transients. The measurement setup for this situation is shown in Figure 6.15. Up to 32 meter the transient voltage waveform is unaffected, but the reflection is different. The reflecting pulse consists of two parts. The first part is a peak with the opposite sign as the reflection had in the previous cases. The second part has the original sign. The result for 32 meter is shown in Figure 6.22(a). At 64 meter a dip arise in the L-PE voltage waveform where the varistor conducts. This results in a total voltage waveform with first a narrow peak with an amplitude about 220 V, then a sharp dip followed by a large and broad pulse with about 350 V as shown in Figure 6.22(b) for the 230 V varistor. As in the case of the resistive load between L-N a varistor between L-N does not affect the asymmetric transient voltage waveform because there is no significant voltage over the varistor.

Replacing the varistor between L-N by 230 V varistors between L-N, L-PE and N-PE also the asymmetric mode transient voltage waveforms are affected. Figure 6.16 shows the modified setup. For the symmetric mode up to 64 meter

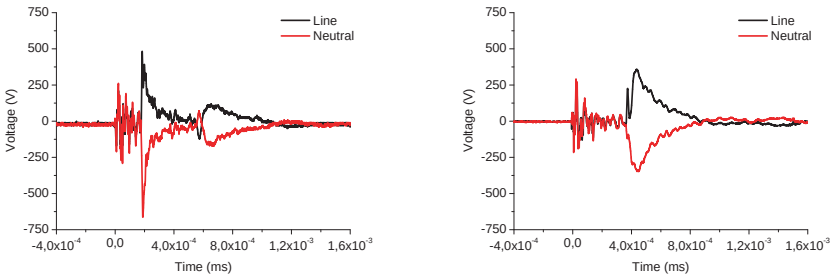

(a) (b)

Figure 6.22: Propagation of transients over 64 meter cable with varistor between L-N as termination: (a) Symmetric mode 32 meter (230 V varistor); and, (b) Symmetric mode 64 meter (230 V varistor).

the transient voltage waveforms are similar to those of the previous setup with a single varistor. At 64 meter only the amplitude is lower. The first peak is about 180 V and the amplitude of the broad pulse is about 290 V. The voltage waveform shape is also smoother. For the asymmetric mode up to 64 meter the transient voltage waveforms are similar to the previous cases apart from the reflection. The reflection consists of a negative peak with half the amplitude of the original reflection followed by a broader pulse with the original positive sign and also half the amplitude of the original reflection. The voltage waveform at 32 meter is shown in Figure 6.23(a). At 64 meter the transient voltage waveform consists of a narrow peak with an amplitude of about 180 V followed by a steep dip which is followed by a broad pulse with an amplitude about 600 V. The voltage waveform at 64 meter is shown in Figure 6.23(b).

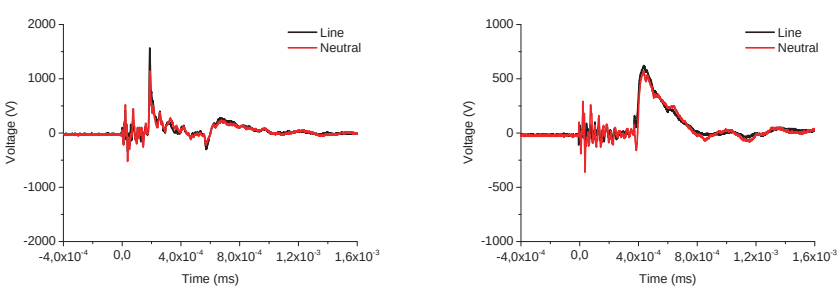

(a) (b)

Figure 6.23: Propagation of transients over 64 meter cable with varistors between L-N, N-PE and L-PE as termination: (a) Asymmetric mode 32 meter; and, (b) Asymmetric mode 64 meter.

More details of the effect of varistors on the propagation of transients are revealed when the varistors are moved along the cable. Figure 6.17 shows the setup in which the 230 V varistors between L-N, L-PE and N-PE are placed at 2 meter. The voltage waveform for symmetric mode at 0 meter is shown in Figure 6.24(a) which is similar to the original transient voltage waveform at 0 meter in Figure 6.10(a) except for the smaller reflection. At 2 meter, shown in Figure 6.24(c), the first pulse is about 20% smaller than in the original case of the setup with open cable termination and the trailing pulses start to combine in one broad pulse. Figure 6.24(e) shows the voltage waveform at 4 meter. The first pulse is three times as small as in the original case with open cable termination. The trailing pulses are much more apparent than at 2 meter. At 8 meter, shown in Figure 6.25(c), the pulses are combined and the peak amplitude is halved compared to the case at 4 meter. The voltage waveform is much wider and has an peak amplitude which is about half of the peak amplitude in the original case with open cable termination. At 64 meter reflection occurs resulting in a voltage waveform with smaller peak amplitude and surface area as in the original case with open cable termination. Besides reflection reoccurs at the varistor resulting in extra bumps with negative sign around 1.2×10^{-3} ms as shown in Figure 6.25(c).

For the asymmetric mode at 0 meter the reflection has a smaller amplitude than in the original case of the setup with open cable termination. Furthermore, as shown in Figure 6.24(b), there is also a large negative pulse present corresponding to the location of the varistors at 2 meter. Figure 6.24(d) shows the voltage waveform at 2 meter. The pulses combine to a broad pulse with lower amplitude. At 4 meter, shown in Figure 6.24(f) the broad pulse decomposes into pulses and the maximum amplitude is larger than at 2 meter. The negative part of the voltage waveform is significantly reduced. At 8 meter the maximum amplitude is about the same order as at 4 meter. The negative part of the voltage waveform is growing as shown in Figure 6.25(b). Figure 6.25(d) shows the voltage waveform at the end of the cable. Reflection occurs and the maximum amplitude of the waveform as well as the surface area are larger than in the case with the three varistors as a load but smaller than in the original case with open termination. Like in the symmetric mode, reflection reoccurs at the varistor resulting in extra bumps with negative sign around 1.2×10^{-3} ms as shown in Figure 6.25(d).

Adding the 60 W resistive load between L-N at the end of the cable as in Figure 6.18 reduces the reflection for symmetric mode as the load dissipates the transient. Up to 64 meter the transient voltage waveforms in this setup is similar to those of the previous setup, but now the reflection is not present. This is shown for the 0 meter case shown in Figure 6.26(a) where the bump around 8×10^{-4} ms in Figure 6.24(a) is not present anymore. The voltage waveform measured at 64 meter is shown in Figure 6.26(b) and the amplitude and surface area are halved compared to the result in Figure 6.25(c) of the previous setup. The transient voltage waveforms for the asymmetric mode are not influenced by the resistive load.

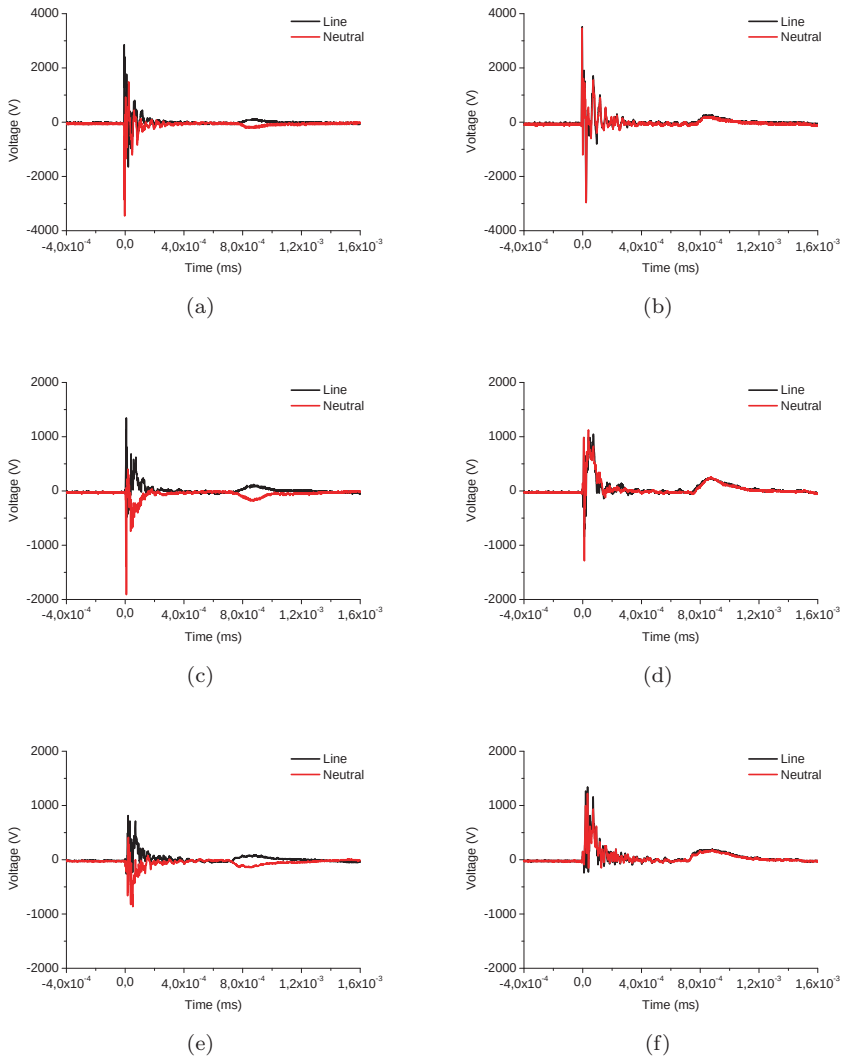

Figure 6.24: Propagation of transients over 64 meter cable with open termination and varistors between L-N, N-PE and L-PE at 2 meter (1): (a) Symmetric mode 0 meter; (b) Asymmetric mode 0 meter; (c) Symmetric mode 2 meter; (d) Asymmetric mode 2 meter; (e) Symmetric mode 4 meter; and, (f) Asymmetric mode 4 meter.

Removing the load and moving the varistors between L-N, N-PE and L-PE to 8 meter results in the setup of Figure 6.19. For symmetric mode until 8 meter the voltage waveform is very similar to original case with open termination,

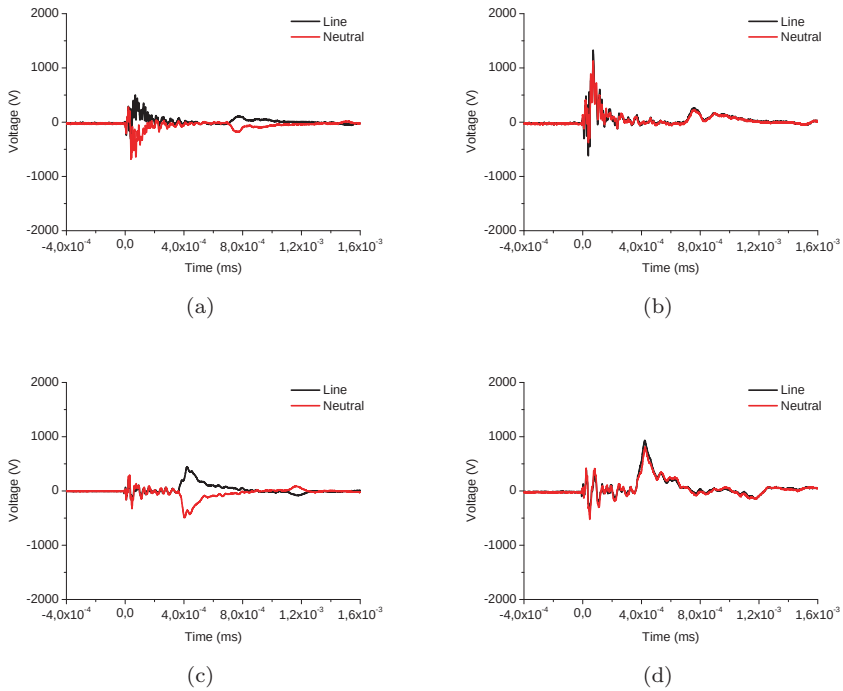

Figure 6.25: Propagation of transients over 64 meter cable with open termination and varistors between L-N, N-PE and L-PE at 2 meter (2): (a) Symmetric mode 8 meter; (b) Asymmetric mode 8 meter; (c) Symmetric mode 64 meter; and, (d) Asymmetric mode 64 meter.

except that the amplitude of the reflection is smaller. At 8 meter the amplitude of the first large peak is three-quarters of the case with no load, and the trailing peaks are changed to a broad pulse with a much lower amplitude. At 16 meter the large peak is gone. At 64 meter reflection occurs and the maximum amplitude is three-quarters of the the amplitude of the original case with open termination. Compared with the case with the three varistors at 2 meter with open termination, the voltage waveforms at 16 meter and 32 meter look similar, but at 64 meter the maximum amplitude of the voltage waveform is three-quarters of the the maximum amplitude of the case with the three varistors at 2 meter with open termination. The voltage waveforms at 8 meter, 16 meter and 64 meter are respectively shown in Figures 6.27(a), 6.27(c) and 6.27(e).

The results for asymmetric mode are similar to the case with the three varistors at 2 meter with open termination except for the large negative peak which is now occurring later and the time between reflections is shorter as the varistors are positioned at 8 meter. Except for the negative peak the voltage

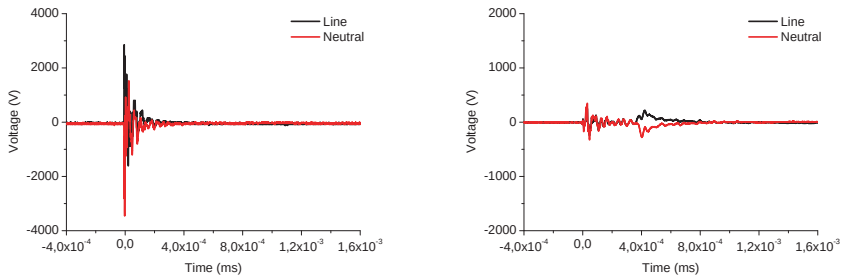

(a) (b)

Figure 6.26: Propagation of transients over 64 meter cable with 60 W resistive termination and varistors between L-N, N-PE and L-PE at 2 meter: (a) Symmetric mode 0 meter; and, (b) Symmetric mode 64 meter.

waveform at 0 meter is similar to the original case with open termination but with a smaller reflection. At 8 meter the first large peaks significantly decrease in amplitude and the trailing peaks combine in a broad pulse. At 16 meter the first peak has disappeared and the amplitude of the broad pulse is lower. At 64 meter the maximum amplitude is almost 15% smaller than the maximum amplitude in the case with the three varistors at 2 meter with open termination. The voltage waveform at 0 meter, 8 meter and 16 meter are respectively shown in Figure 6.27(b), 6.27(d) and 6.27(f).

Connecting the 60 W resistive load between L-N at the end of the cable as in Figure 6.20 reduces the reflection for symmetric mode as the load dissipates the transient. At 64 meter the voltage waveform is half the height and surface area of the previous case with open termination. The voltage waveform at 8 meter and 64 meter are shown in Figure 6.28. The transient voltage waveforms for the asymmetric mode are not influenced by the resistive load.

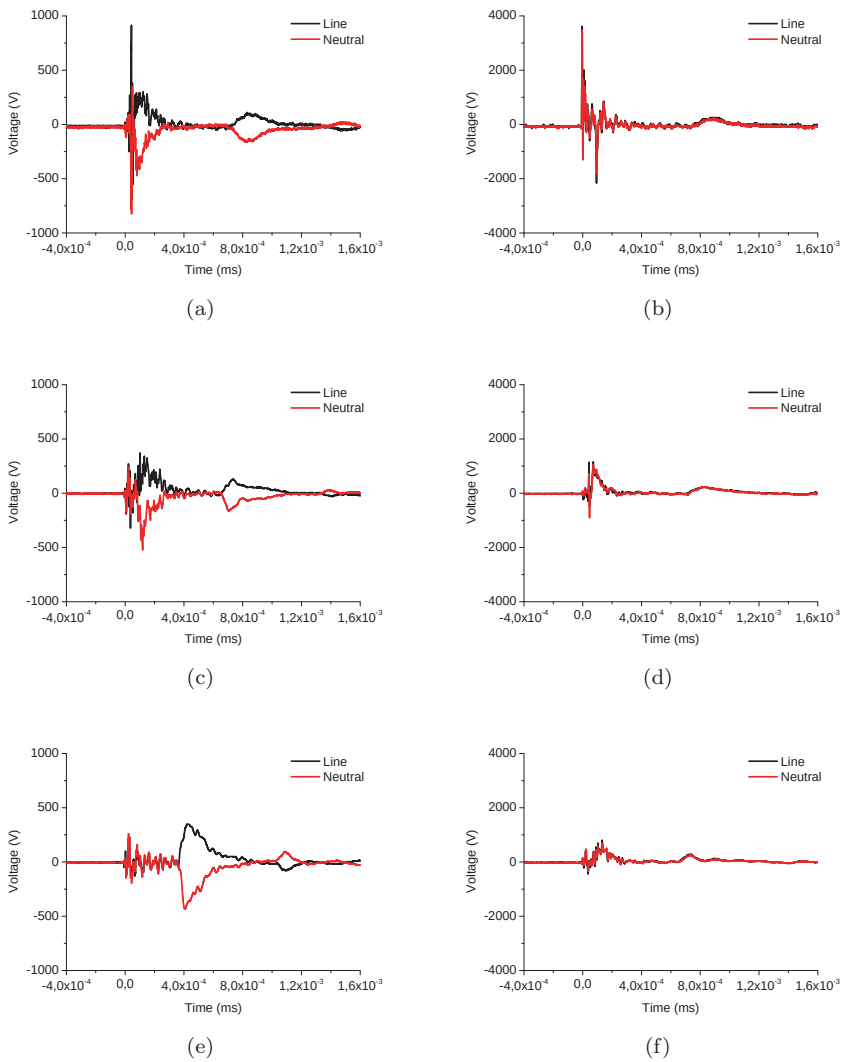

Figure 6.27: Propagation of transients over 64 meter cable with open termination and varistors between L-N, N-PE and L-PE at 8 meter: (a) Symmetric mode 8 meter; (b) Asymmetric mode 0 meter; (c) Symmetric mode 16 meter; (d) Asymmetric mode 8 meter; (e) Symmetric mode 64 meter; and, (f) Asymmetric mode 16 meter.

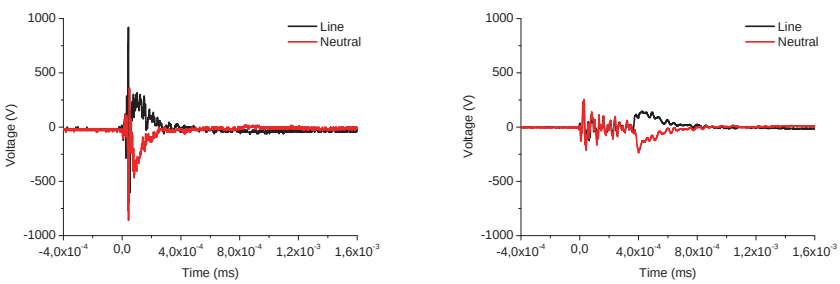

Figure 6.28: Propagation of transients over 64 meter cable with 60 W resistive termination and varistors between L-N, N-PE and L-PE at 8 meter: (a) Symmetric mode 8 meter; and, (b) Symmetric mode 64 meter.

The results of the measurements on transient propagation is listed as follows:

- Symmetrical mode transients:

  The 60 W resistive load dissipates the transients as it is connected between L-N and no reflection occurs.

  The reflection has a negative sign when encountering a varistor between L-N (lower impedance).

  Between the generator and the varistor a dip in the voltage waveform arise corresponding to the location of the varistor.

  After passing the varistors temporary pulse broadening occurs and increase of maximum amplitude of the voltage waveform occurs.

  When the cable is open, reflection occurs at the end of the cable as well as at the varistors, resulting in a voltage waveform becoming a sum of incoming and reflecting voltage waveforms.

- Asymmetric mode transients:

  The 60 W resistive load does not influence the voltage waveform as it is not connected between L-PE and N-PE.

  The reflection has a negative sign when encountering varistors between L-PE and N-PE (lower impedance).

  Between the generator and the varistor pulses with opposite sign arise corresponding to the location of the varistor.

  After passing the varistors temporary pulse broadening occurs and increase of maximum amplitude of the voltage waveform occurs.

  Reflection occurs at the end of the cable as well as at the varistors, resulting in a voltage waveform becoming a sum of incoming and reflecting voltage waveforms.

- General:

  Symmetric mode voltage transients or DM voltage transients are dampened faster than the asymmetric mode voltage transients or CM voltage transients.

These results show that on one hand the varistors suppress the fast transients, but on the other hand transients find a way to by-pass the varistors. CM to DM conversions and vice versa occur at the varistors. This means that on equipment level inside the PDUN these fast transient may have a negative effect on the performance of equipment as the distance between equipment becomes smaller and the switching and operation frequencies of equipment is increasing.

In the measurements the incandescent lamp of 60 W is used as resistive load. As the measurements are performed in the absence of a 230 V supply voltage, the resistive load is cold. As a result its resistance is lower than when it

is at operating temperature. The cold incandescent lamp is a perfect matching load between L-N when connected at the end of the extension cable as then no reflections of symmetric mode transients occur.

6.4 Transients as intentional EMI

This study on the propagation of transients is limited and it does not take into account among others CM current, which varies according the layout of cabling and equipment, characteristic impedance of the cable, and existing equipment connected to the PDUN. More details can be found in [63], [64] and [65] where transients are put on the PDUN by intention in an act of terrorism or sabotage. The work in [63] investigates the propagation of subnanosecond rise time or ultra wideband voltage transients on cables present in the PDUN based on tests in a laboratory. The main mode of propagation is DM. The transients on cables propagate in a quasi transverse electromagnetic mode. These DM transients can spread to any junction and connected equipment on relatively short distance as the attenuation per meter of cable is approximately 1 dB. The losses are mainly ohmic and no significant power is lost in bends. Mainly impedance mismatches and resulting reflections limited the received power. Also CM transients are taken into account in [63]. By its nature of CM propagation, the return path and impedance of this return path is unknown and as a result the measurement conditions are not fully controllable. This is schematically shown in Figure 6.29. However, only a fraction of the injected power appears between the ground of the load and the conductors of the cable, which is also a nature of CM propagation.

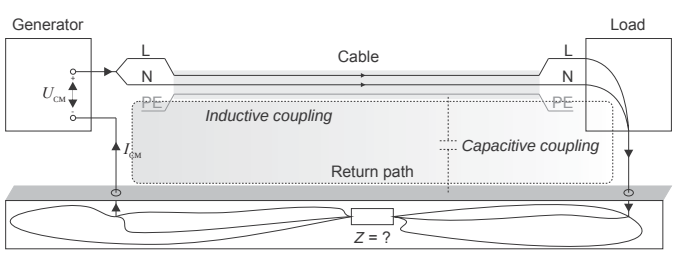

Figure 6.29: For CM propagation the return path is unknown

The continuation of the work in [63] is reported in [64]. It investigates the propagation of ultra wideband transients through different types of junctions of cables. The main mode of propagation is transverse electromagnetic. As a result no measurable power is lost at the junction in the form of radiation. The impedance mismatch between the different sides of the junction result in decrease of received voltage level. Reflections causes redistribution of energy between the different loads and branches.

Furthermore in [64], the propagation of ultra wideband voltage transients

in a PDUN of a building is investigated. DM transients are directly injected into an outside positioned socket. The transverse electromagnetic field structures breaks down and the transient propagates mostly outside the dielectric of cables, so it propagates mostly in free air. However, compared to the injected transients relatively large voltage amplitudes arrive at the inside power sockets. The farther the injection point in the PDUN the lower these voltage amplitudes become.

In [65] the focus is on propagation of high voltage transients from a COTS pulse source, based on a stun gun and a pulse forming circuit. The voltage rise time of the pulse from the stun gun is long and therefore having a low frequency range. To produce fast transients with a high voltage a pulse forming circuit is used. A choice for pulses to be generated is made based on cables and filter networks inside equipment connected to the PDUN. The analysis includes cable impedance, dispersion and high voltage nonlinear behavior. The work shows measurements in which damped sinusoidal pulses with a resonant frequency of 170 MHz are generated. These pulses are applied on a power supply network feeding a PC. Depending on the numbers of pulses applied, the PC shows failure symptoms like, resets, graphic card break downs. Applying higher amplitude pulses results in damaging of components on the power supply Printed Circuit Board (PCB) of the PC.

6.5 Summary

Electronic equipment is equipped with a protection against electrical fast transients and bursts covered in IEC 61000-4-4 [59] standard as well as surges covered in IEC 61000-4-5 [60] standard. The predecessor of the IEC 61000-4-4 defined only nonsymmetrical transients and later on CM transients have been included.

The PQ analyzers used in the case studies of Chapter 4 and PQ analyzers in general are not designed for detection of high frequency phenomena with rise and durations time shorter than 1 μs. Therefore the propagation of faster transients inside the PDUN cannot be evaluated using conventional PQ analyzers and a high-speed multichannel data logger for PQ measurements has been designed for future measurements. The high-speed multichannel data logger for PQ measurements can be used for further research on fast transients including CM transients.

Measurements using an oscilloscope, transient generator and varistors representing electronic equipment are performed. The results show that on one hand the varistors suppress the fast transients, but on the other hand there is a mechanism that converts DM transients to CM transients and vice versa. Due to these conversions, transients by-pass the varistors. The work in [63], [64] and [65] is performed to assess the impact of fast transients generated in an act of terrorism or sabotage. It shows that propagation of fast transients inside the PDUN can happen if the fast transients are generated inside or near the system. For PQ it is imperative to consider other ways to generate fast

transients. An option is to switch high currents on a cable. The inductance of the cable carrying a high current gives rise to voltage transients when this cable is cut from the supply. These voltage transients will propagate on the disconnected cable to the electrical equipment connected to it.

In 1987 many nonsymmetrical transients were measured, but nowadays it seems that they do not occur that often anymore. Protection by varistors in equipment on the PDUN suppresses the transients. However, due to mode conversions occuring when the varistors are clamping, transients can still propagate. As a result of these mode conversions and coupling mechanism between cables, there is still a risk of EMI.

Chapter 7

Nonlinear behavior of equipment

In Chapter 5 models are developed for the infrastructure of the PDUN. In order to simulate the entire PDUN the equipment connected to the PDUN need also to be modeled. In the measurements on propagation of transient in Chapter 6 varistors have been used to represent the input circuit of equipment. These are nonlinear devices. Modern electrical loads and sources are also nonlinear as they have power electronic interfaces. To reduce the complexity in the design of PDUNs and to simulate large PDUNs feeding thousands of small electronic devices, behavior models are developed in [66]. The advantage of a behavior model over a circuit model is that the circuit of the DUM does not need to be known and simulated. The work in [66] is performed in collaboration with a master student from the University of Twente and a scientific staff member from Polytechnic University of Turin (Politecnico di Torino). Models are developed for two kinds of nonlinear loads commonly found. The first DUM is a load with a rectifier bridge without PFC, and the second a load with a rectifier bridge with active PFC. The models describe the steady state behavior of loads.

Section 7.1 introduces the DUM and the requirements on the model, after which the models are presented. Parameterization of the models based on measurements and the simulation results are briefly discussed in Section 7.2. Section 7.3 gives some indicative figures on the computational load of the models. The procedure from model development to simulation results is evaluated in Section 7.4.

7.1 Model of low frequency steady state behavior

The purpose of the models developed in [66] is to simulate the steady state behavior of loads connected to the PDUN. Emission beyond 10 kHz due to fast switching circuits as the Switched Mode Power Supply (SMPS) in the PC supply or the PDS in Subsection 4.5.3 is not included in the modeling. This

work distinguishes two types of transient currents caused by nonlinear loads. The first type is inrush currents occurring when the load is switched on or connected. An inrush current is considered to be a single event which can have a large impact, but it is not taken into account. The second type is current transients occurring as function of the power frequency, usually even multiples of the power frequency period. These current transients are generally much smaller than the inrush currents, but they are produced continuously and by every connected nonlinear load at a given instance of time. They take part in the interaction between current and voltage or synchronization switching as discussed in Section 3.4.

The models developed in [66] are intended to take into account synchronous switching effects. From the wide range of nonlinear loads two common loads are chosen for modeling: a CFL and a SMPS for PCs. The CFL has rated active power of 11 W and is from the house brand of the Karwei hardware store. It has a double sided rectifier which is present in virtual all electronic loads. The SMPS for PC with active PFC has rated active power of 300 W and is from the Pure Power L7 series of Be Quiet. SMPSs with active PFC is commonly found in computers and other appliances that consume more than 75 W of active power.

The models are constructed such that they can be parameterized to represent any DUM. It is not desirable to have to take apart every DUM to parameterize its model. Therefore, the parameterization needs to be performed based purely on (nondestructive) measurements. The requirements are listed as follows:

- the models need to be able to be parameterized to represent a wide variety of DUMs,
- the parameterization should be based on measurements,
- the models need to be computationally light,
- the models should accurately simulate steady state behavior, and
- the models should react realistically to distortions in the voltage waveform.

In [67] a brief overview is given on the approaches for characterization and modeling of conducted EMI noise sources. A model can be categorized as device physics based model or device behavioral model [68], [69], [70], [71]. The device physics based model is also referred to as white box model. White box models contain the full design of the DUM. All electrical components are present in the model. Also parasitic effects, like leakage capacities, can be taken into account. A common example of a white model is a SPICE model containing a complete design of a DUM [72]. The advantage of the white box model is that it provides full insight into the behavior of the DUM. It has a physical meaning and is valid for different operating conditions. It is very accurate since all nonlinearities and

dynamic behavior can be simulated including unusual circumstances. However, the intellectual property of the DUM will be revealed in the model. Another disadvantage is the complexity and dimension of the model. It takes a very long time to simulate it, making it impossible to simulate large systems that contain many white box models of (sub)systems, or to simulate the interaction between a large number of DUMs.

Device behavioral model is also referred to as black box model. Black box models are equivalent circuits of the DUM and contain no information on the internal structure. They only describe the behavior on the electrical terminals without revealing the intellectual properties. These descriptions can be mathematical formulas relating voltage, current and time as well as voltage-current (V-I), voltage-time (V-t) or current-time (I-t) graphs. A common example of black box models in integrated circuits is the Input/Output Buffer Information Specification (IBIS) model [73]. It is computationally more simple and efficient than the white box model as the complete internal circuits including parasitic effects do not have to be taken into account. This makes the simulation of the interaction of many DUMs less complex. Even if the manufacturer of the DUM does not provide models, black models can be obtained. By performing measurements on the electrical terminals the behavior of the DUM can be analyzed. However, the model has not a physical meaning and is strictly related to the operating conditions.

The IBIS modeling method is developed for describing the behavior of input and output buffer ports on an integrated circuit [66]. These methods are particularly designed for ports with a few states and state transitions. Therefore they cannot be applied right away when modeling equipment connected to the PDUN as these operate on an AC system. In [70] a device behavior modeling method is introduced for modeling the impedance of a low voltage DC motor. It also takes into account main physical features as brushes, windings, iron core, shaft and casing. Furthermore, the most important physical phenomena as skin effect on the windings and the eddy currents on the iron are taken into account. The reported results show that the impedance model closely match the motor impedance in the frequency band from DC to 1 GHz. In [71] a device behavior model is developed for switching power converters. A generalized terminal modeling technique for a DC-DC boost converter is extended to cover a three phase voltage source inverter. Use is made of the presence of input capacitor and parasitic input inductances. The developed model shows, apart from some frequencies, good matching of predicted and measured results in the frequency band from 20 kHz and 100 MHz. The behavior models proposed in [70] and [71] are categorized as gray box models as they contain a mixture of properties from white and black box models.

The models developed in [66] also contain a mixture of properties from white and black box models. The models contain some information of the design of the DUM, as far as it is relevant to the behavior observed at the terminals. The knowledge of the design of the DUM contained can be based on what is commonly found in devices similar to the DUM. Looking into the a CFL at

the terminals one can find a series resistor, a diode bridge rectifier, a capacitor and then a load on the DC bus. By performing measurements these elements can be parameterized. The advantage of this gray box model is the high degree of accuracy in simulation of the dynamic and nonlinear behavior while still hiding the intellectual property of the manufacturer. Gray box models are more simple than the white box models, but still more complex than the black box models.

7.1.1 CFL

A CFL can be considered as a two terminal port, or a two terminal impedance, with nonlinear and not static behavior. V-I curves for 115, 211, 230 and 253 V_{RMS} are shown in Figure 7.1. The rising part of the 50 Hz sinusoidal voltage waveform gives a different V-I curve than the falling part. A model based on static V-I data will not respond accurately to different RMS voltage levels and voltage waveforms. Therefore, the first electrical components of the DUM are modeled. The basis of the model is shown in Figure 7.2. Z_{In} is a resistor, followed by the diodes D_1 to D_4 forming a rectifier bridge and capacitor C_{DC} feeding the DC bus. These model components are found when opening the CFL lamp. Still the structure and behavior of the components behind the capacitor are unknown. This remaining part of the DUM is represented by Z_{Load}. Z_{Load} can be modeled as a resistor, as a constant DC current source, as a constant power load or using a V-I characteristic.

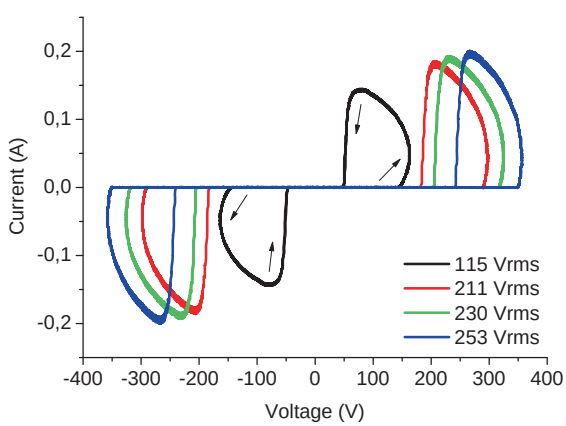

Figure 7.1: V-I curves of a CFL lamp for different RMS voltages at 50 Hz

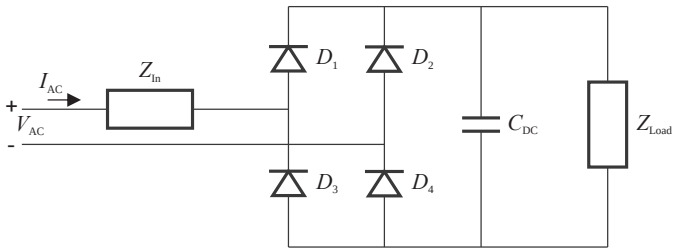

Figure 7.2: Simplified schematic of gray box model for CFL lamp

7.1.2 SMPS for PC

The basis of the model of the SMPS for PC with active PFC is shown in Figure 7.3. It consist of a line filter and rectifier with capacitor at the front and a DC capacitor and load at the end. Between the capacitors is the section implementing fast current switching and active PFC. This section draws a current proportional to the voltage waveform V_{AC} and is based on the boost converter [74]. Current needs to be drawn across the rectifier bridge, even if the absolute voltage to the left of it, $|V_{\mathrm{AC}}|$, is lower than the DC bus voltage on the right V_{DC}. The transistor S_1 acts as a switch. In closed position, current I_{Closed} will flow through the switch S_1 and through the inductor L_1, as long as V_{Pulse} is greater than 0 V. V_{Pulse} is the voltage over the capacitor on the right of the rectifier bridge and for its value yields $V_{\mathrm{Pulse}} \approx |V_{\mathrm{AC}}|$. One instance in time later, the switch will open and the stored magnetic energy inductor inductor L_1 will try to keep the current flowing. Current I_{Open} will flow through diode on the right D_6 and the buffer capacitor C_{DC} feeding the load Z_{Load}. In this way current is 'pumped' from AC side of the circuit to the DC side of the circuit.

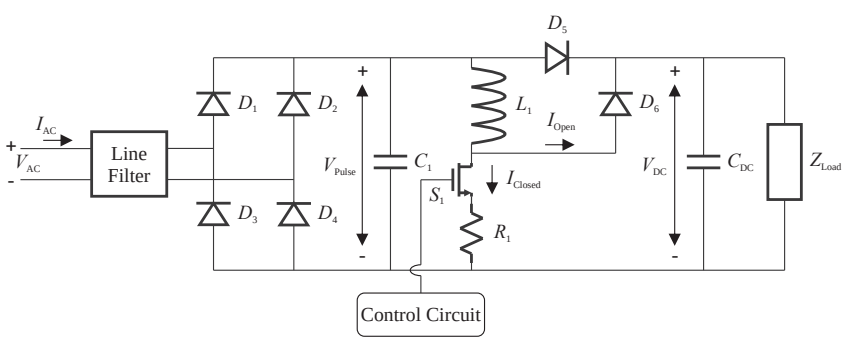

Figure 7.3: Simplified schematic of gray box model for SMPS for PC with active PFC

Details of the components inside the control circuit of the DUM are unknown. Fortunately, some fundamental relations can be deduced for modeling.

The current drawn by the DUM I_{AC} should be proportional to the input voltage V_{AC} and therefore V_{Pulse} is an input parameter of the control circuit. Furthermore, the DC voltage V_{DC} and current pumped into buffer capacitor C_{DC} are bounded. If the current charging C_{DC} is greater than the current that the load draws then V_{DC} become infinitely large. V_{DC} is an input factor for the control circuit. Finally, the instantaneous voltage difference between V_{DC} and V_{Pulse} determines the maximum current the circuit can pump.

The scheme in Figure 7.3 does include switching of current at the switching frequency. This switching frequency is about 55 kHz for the DUM. As emission beyond 10 kHz is not taken into account, a low frequency equivalent model is developed taking the aforementioned aspects into account, without actually simulating at a 55 kHz switching frequency. The basic functional schematic of the low frequency equivalent model is shown in Figure 7.4. The section between the capacitors has been replaced by current sources. Only diode D_5 is left as it was. The static behavior of the section is defined by its prototype current waveform controlling currents $I_{\mathrm{Horizontal}}$ and I_{Vertical}. This prototype current waveform is the the measured current waveform drawn by the SMPS for PCs when being fed by a clean voltage waveform. As the current sources are behind the rectifier, the prototype current waveform is rectified. The remaining part of the section adapts the current waveform to react dynamically to the voltage waveform V_{AC} and load Z_{Load}. Z_{Load} can be modeled as a resistor, as a constant DC current source, as a constant power load or using a V-I characteristic.

The value of V_{DC} in the actual DUM is larger than the amplitude of V_{Pulse} which is $\check{V}_{\mathrm{Pulse}}$. In steady state operation diode D_5 does not conduct and is always reverse biased. In [66] reference voltage V_{REF} has been taken to be 10% higher than $\check{V}_{\mathrm{Pulse}}$ and the control loop will attempt to let V_{DC} follow V_{REF}. The reference voltage V_{REF} is created by a max hold circuit and an ideal amplifier with amplification $A_1 = 1.1$. The power dissipated in the load is a parameter set by the user. To control the V_{DC} the prototype current waveform is scaled as function of the difference between V_{REF} and V_{DC} or V_{Error}. To this end amplification A_2 is set to 1 and the result is low pass filtered to ensure the ripple on V_{DC} does not directly influence the current waveform. Furthermore, amplification A_3 is of the form $a + b \times V_{\mathrm{Error}}$ and controls the feedback amplification. The result is denoted as V_{PFC} and goes to the controlled current sources. The horizontal source pushes current $I_{\mathrm{Horizontal}}$ from lower voltage to higher voltage thereby delivering power into the circuit. As all the power should come from the PDUN, the vertical current source pushes current I_{Vertical} into sink thereby dissipating the same amount of power delivered to the circuit. The current magnitude of both sources are generally not equal as the voltage across them is not equal either. To avoid hidden amplification the sum of the amplification $(1 - G + G)$ of both voltage controlled current sources is unity. As the ratio of $\check{V}_{\mathrm{Pulse}}$ and V_{DC} is fixed, the ratio of the amplification factors of the current sources is also fixed. This eventually enables the model to adapt the current I_{AC} it draws automatically to the voltage V_{AC} at the input as long as the power conversion efficiency is constant.

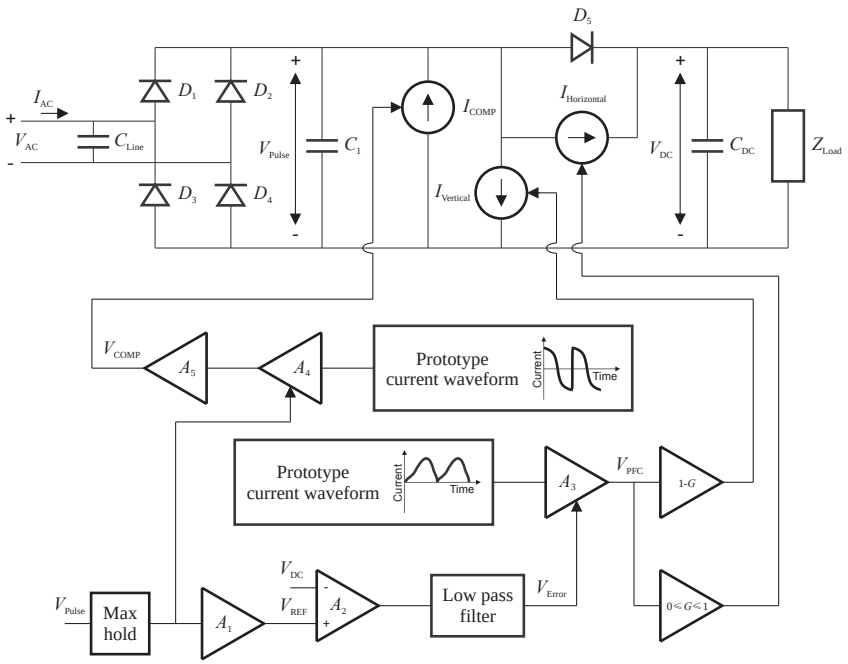

Figure 7.4: Low frequency equivalent of model in Figure 7.3

The prototype current waveform controlling the currents $I_{\text{Horizontal}}$ and I_{Vertical} is measured at the terminals of the DUM while the current sources are placed behind the rectifier. The effect of the capacitors C_{Line} and C_1 on the current waveform needs to be compensated for, otherwise this effect would be present twice: first in the measured prototype current waveform and second in the model by placing the controlled current sources behind the capacitors C_{Line} and C_1. In [66] an extra voltage controlled current source is placed in parallel to capacitor C_1 injecting a compensating current I_{Comp} such that the total current seen at the terminals of capacitor C_1 is the same as the current at this point during the measurement of the prototype current waveform under clean voltage waveform condition. The dynamic behavior of the model is retained, as capacitors C_1 and C_{Line} still respond to distortions in the voltage waveform, while the current waveform of I_{Comp} is fixed. The basic current waveform is based on a sinusoidal voltage waveform with unity amplitude and 50 Hz power frequency. This waveform is then multiplied by V_{Pulse}, amplification A_4, and by the sum of the values of C_1 and C_{Line}, amplification A_5. This setup is flexible with respect to voltage amplitude V_{AC} and capacitor size.

By introducing an extra voltage controlled current source the computational load of the model becomes heavier. Therefore in [66], I_{Comp} is included in the prototype current waveform controlling currents $I_{\text{Horizontal}}$ and I_{Vertical}. This way, compensation of current is established without adding extra complexity

to the model. The resulting scheme is shown in Figure 7.5.

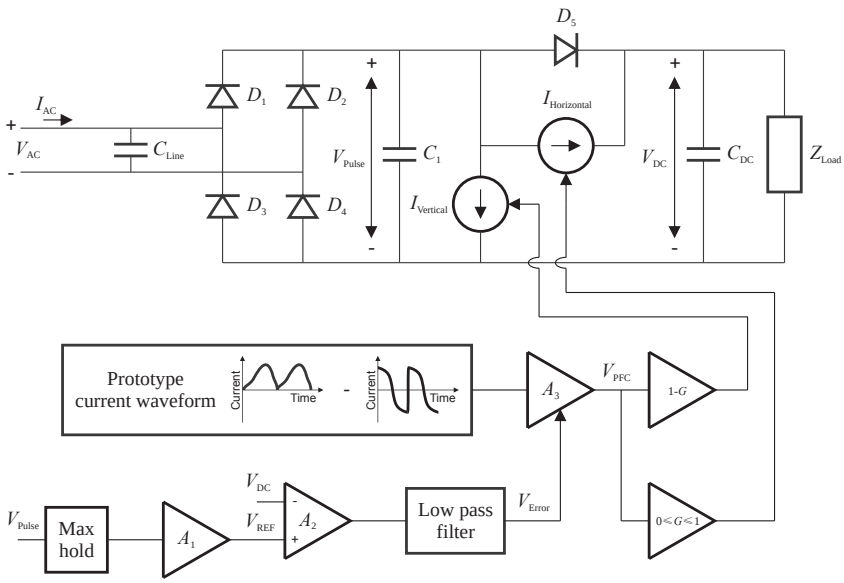

Figure 7.5: Low frequency equivalent of model in Figure 7.3 in which compensation for capacitive current is included in the prototype current waveform controlling currents $I_{\text{Horizontal}}$ and I_{Vertical}

7.2 Parameterization and simulation

Parameterizing of the components in the models shown Figures 7.2 and 7.5 is based on measurement setup in Figure 7.6 and scripts developed in [66]. The programmable power supply can feed the DUM by various waveforms such as sinusoidal voltages of different frequency and amplitude or an arbitrary waveform from a file to measure the behavior of the DUM. A brief description of the procedure for parameter extraction for the CFL including results are presented in [37]. Using the scripts in [66] parameter values are computed from measured responses. The validation of simulation results for the CFL based on the model in Figure 7.2 and the SMPS for PC with active PFC based on the model in Figure 7.5 is discussed in [66]. The validation is performed on a basic level as it compares the measured and simulated waveforms by visual inspection. This simple approach is sufficient to evaluate the suitability of the modeling method.

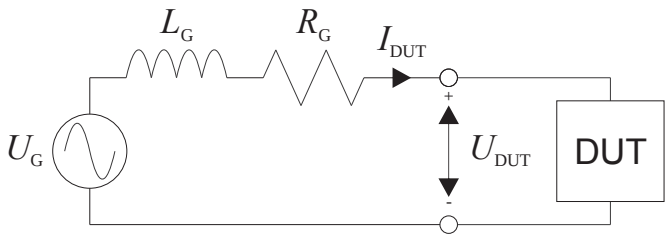

Figure 7.6: Measurement setup for parameterization of DUM and validation of the model

7.2.1 CFL

The simulated and measured responses to sinusoidal voltage waveforms with low (211 V), nominal (230 V) and high (253 V) RMS voltages of the CFL are shown in Figure 7.7. The simulated current fits to a high degree the measured current as the current waveforms are coinciding. Also for different power frequencies the simulated current is in good agreement with measured current as shown in Figure 7.8. Measured and simulated responses to distorted voltage waveforms are shown in Figure 7.9. These voltage waveforms are reconstructions from measured voltage waveforms in the Environmental and Competence Centre laboratory of Thales Nederland BV in Hengelo (voltage waveform 1) and in an office in the Carré building of University of Twente (voltage waveform 2). The simulated current waveforms match to a large extent the measured current waveforms.

7.2.2 SMPS for PC

The parameterization of the model of the SMPS for PC with active PFC including prototype current waveforms is based on measurements with 150 W load. The 230 V_{RMS} sinusoidal voltage waveform and voltage waveform 2 are used for excitation in these measurements. Simulated and measured current waveforms for 230 V_{RMS} sinusoidal voltage waveform and for voltage waveform 2 are shown in Figure 7.10. The level of fitting between simulated and measured current waveforms is high. Deviation from the circumstances of the prototype current measurement result in decreasing level of fitting. The responses to sinusoidal voltage waveforms with low and high voltages are shown in Figure 7.11. To keep the power consumption at 150 W, the model changes the scale factor of current thereby mainly leaving the shape of the current waveform as it was. The actual DUM also changes the shape of the current waveform. Changing the load has similar effects. For 90 W and 270 W load, the response to 230 V_{RMS} sinusoidal voltage waveform and voltage waveform 2 are shown in Figure 7.12. The model mainly changes the scale factor, while the actual DUM also changes the shape of the current waveform.

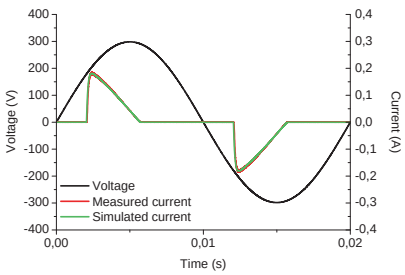

(a)

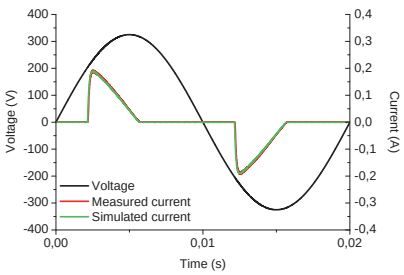

(b)

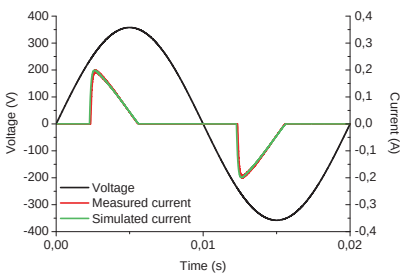

(c)

Figure 7.7: Simulation results for CFL supplied by sinusoidal voltage waveforms: (a) 211 V_{RMS}; (b) 230 V_{RMS}; and, (c) 253 V_{RMS}.

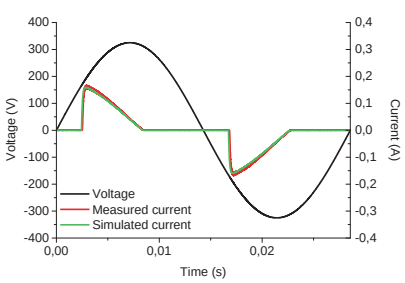

(a)

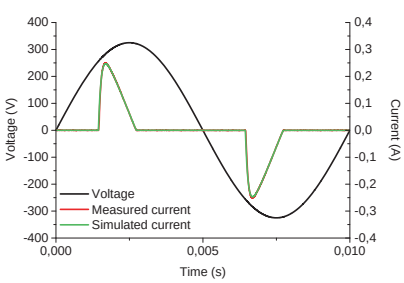

(b)

Figure 7.8: Simulation results for CFL supplied by 230 V_{RMS} sinusoidal voltage waveforms: (a) $f = 35$ Hz; and, (b) $f = 100$ Hz.

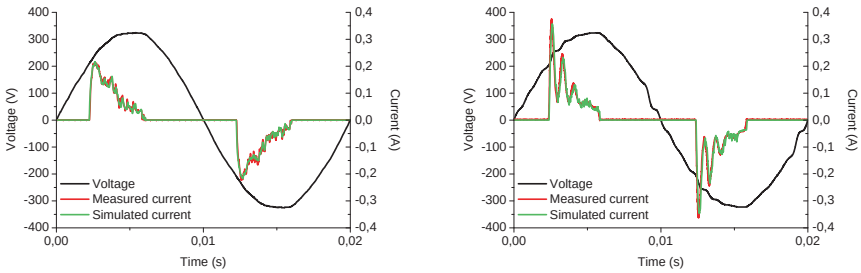

Figure 7.9: Simulation results for CFL supplied by: (a) voltage waveform 1; and, (b) voltage waveform 2.

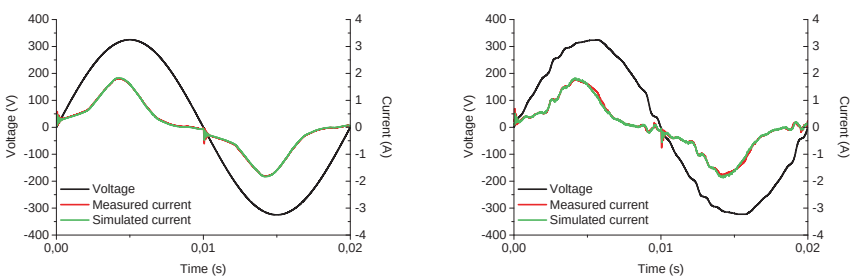

Figure 7.10: Simulation results for SMPS for PC with active PFC supplied by: (a) 230 V_{RMS} sinusoidal voltage waveform; and, (b) voltage waveform 2.

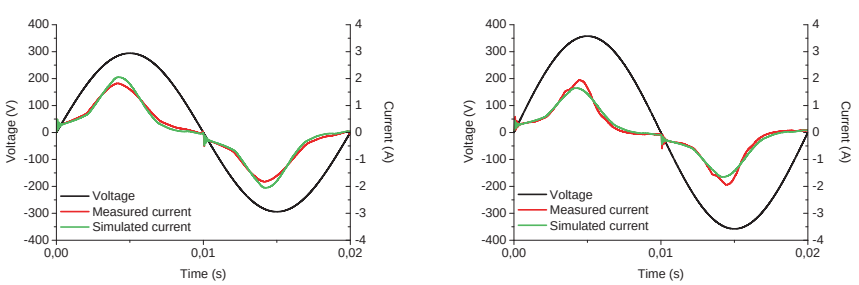

Figure 7.11: Simulation results for SMPS for PC with active PFC supplied by: (a) 208 V_{RMS} sinusoidal voltage waveform; and, (b) 253 V_{RMS} sinusoidal voltage waveform.

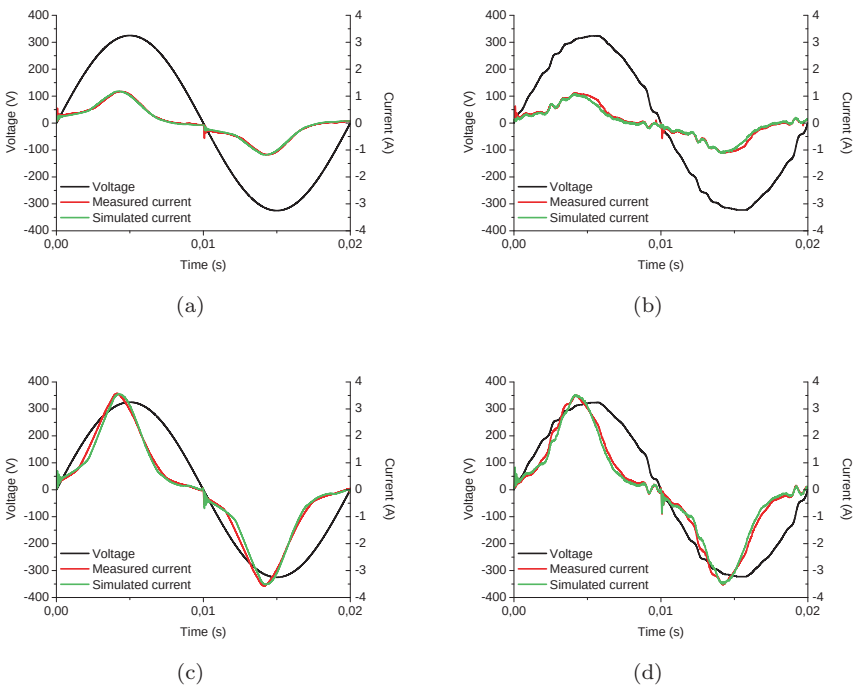

Figure 7.12: Simulation results for SMPS for PC with active PFC: (a) with 90 W load supplied by 230 V_{RMS} sinusoidal voltage waveform; (b) with 90 W load supplied by voltage waveform 2; (c) with 270 W load supplied by 230 V_{RMS} sinusoidal voltage waveform; and, (d) with 270 W load supplied by voltage waveform 2.

7.3 Computational complexity of models

The PC used for simulation is a Toshiba Portégé M700 tablet PC laptop, with a Core2Duo T8100 CPU (2 cores) at 2.10 GHz, 2 GB of RAM, running Windows 7 (32 bit version). This PC is a business model that was sold until the end of 2009. During simulations, the PC is AC powered and it is running in high performance mode. The simulation software used is LTspice IV (version 4.16h). In Table 7.1 simulation run time and speed are listed for different simulated times of CFL and SMPS for PC with active PFC. Voltage waveform 2 is used as excitation voltage. The reconstruction of this voltage is not included in the listed results.

Table 7.1: Simulation time performance of model of CFL and SMPS for PC with active PFC

DUM	Simulated real time (s)	Simulation run time (s)	Average simulation speed (ms/s)
CFL	0.25	14	17.9
	0.5	32	15.6
	1.0	70	14.3
SMPS for PC with active PFC	0.25	28	8.9
	0.5	56	8.9
	1.0	121	8.3

As the simulation run time is larger for the model of the SMPS for PC with active PFC, it is more complex than the model of CFL, the simulation speed of it is compared to the simulation speed of a more elaborate SPICE model. This SPICE model serves as benchmark. A white box model is not available, because of intellectual property issues. Furthermore, a full design could not be reconstructed from studying the hardware. The benchmark model is based on the boost circuit inside the DUM as shown in Figure 7.3. For the control circuit the control loop scheme in [75] is used for generating a pulse width modulated signal for the transistor. It contains the primary switching element in the DUM instead of a control loop using a prototype current waveform. The transistor is modeled by an ideal switch and a constant power load is used.

The simulation of the benchmark model is run on the same tablet PC laptop as was used for the DUMs in Table 7.1. Simulating the first 20 ms takes 64 s resulting in an average simulation speed of 0.3 ms/s. This is mainly the result of numerical difficulties, where the simulation would nearly halt several times, for several seconds at a time. In the brief periods where the simulation is running smoothly, the simulation tool reported average speed value of 1.2 ms/s. The benchmark model is at least 7.5 times slower than the developed gray box model. This means that the gray box model is significantly computational lighter than a full white box model.

7.4 Discussion

Two basic models are introduced in [66] to capture the steady state behavior of loads connected to the PDUN. The basic components exist of a rectifier and load. This load can be modeled as resistor, constant current load or constant power load. Active PFC is modeled by adding current sources, between rectifier and load, drawing currents defined by a prototype current waveform. Parameterization of the models is done by measurements on the PDUN interface of the DUM and parameterization scripts. The conditions of the parameterization measurements determine the accuracy of the simulations.

Simulations of the DUM of rectifier without PFC shows very good agreement with measurements. The model for the DUM with active PFC is more complex and has more restrictions than the model of the DUM without active PFC. The prototype current waveform is fixed in shape. Whereas changing the RMS voltage values and power frequency values did not significantly change the resemblance of the simulated current to the measured current of the CFL, the level of fitting of simulated current to the measured current does decrease for the PC with active PFC. Using several prototype currents under different conditions might be necessary to gain higher levels of fitting between simulations and measurements. Therefore several measurements under different supply and load conditions might be necessary to obtain satisfactory results.

As the model for the DUM with active PFC is complexer than the one without PFC it has a higher computational load. Still the computational load is significant lower than an elaborated SPICE model which is much simpler than a white-box. This means that the developed gray box models are relatively computational light.

The developed gray box models offer simulation results being close to the measurement results, while being computational light. For these models no considerable intellectual properties are needed or revealed as they are based on basic components commonly found in loads. Therefore, they can represent a diversity of loads. Besides, model parameters can be found by measurements and using the parameterization scripts without opening and examining the loads. Macro models can be created from the gray box models, such that the gray box models can be used in simulation tools. In [66], this has been done in SPICE. Using macro models in simulation tools large groups of loads can be simulated. Large groups of loads can be an integrated mast, lighting systems in large buildings or an offshore platform. The simulations also have to include the models in Chapter 5 for the infrastructure of the PDUN. The obtained results can be used to convert the developed gray box modeling with parameterization scripts and models for the infrastructure of the PDUN into design tools for PDUNs.

7.5 Summary

Modern electrical loads and sources are nonlinear as they have power electronic interfaces. To reduce the complexity in the design of PDUNs and to simulate large PDUNs feeding thousands of small electronic devices, gray box models are developed in [66]. They describe the steady state behavior of nonlinear loads and take into account synchronous switching effects. They do not cover emission above 10 kHz. The models are developed for two kinds of nonlinear loads commonly found: a load with a rectifier bridge without PFC and a load with a rectifier bridge with active PFC. The first DUM is a CFL and the second a SMPS for a PC. The models contain only information of the design of the DUM as far as it is relevant to the behavior observed at the terminals. Therefore they can represent a diversity of loads.

The electrical components commonly found in loads similar to the DUMs, like diode bridge and capacitor feeding DC bus, are used in the gray box models. Current sources controlled by prototype current waveforms represent the active PFC. To maintain a satisfactory accuracy several prototype currents under different conditions might be necessary. Parameterization of the models is done by measurements on the PDUN interface of the DUM and parameterization scripts. The developed gray box models produce simulation results being close to the measurement results, while being computational light. As the models are based on basic components commonly found in loads they do not need considerable intellectual properties. The model parameters can be found without opening and examining the loads.

Macro models can be created from the developed gray box models to use them in simulation tools. Then, the macro models together with the models in Chapter 5 for the infrastructure of the PDUN can be used in simulation tools to simulate large groups of loads. Based on the obtained results, the models for the infrastructure of the PDUN and the developed gray box modeling with parameterization scripts can be converted into design tools for PDUNs.

By combining the broadband models for the infrastructure of the PDUN and broadband behavior models for the nonlinear equipment, one has the basics for simulating the interaction between voltage and current in the PDUN. Despite the simulation tools are not available yet, the concept can be illustrated as in Figure 7.13. For this purpose, a simplification is made by leaving variations in loads and voltage drop over the cable sections out of consideration. Similar loads are connected at one point in Figure 7.13(a). Since every load is supplied by the same voltage, all the loads draw the same current at the same time. Therefore all spectral current components will add up. When loads are connected to a long cable, there is a distance between the connection points of the loads as shown in Figure 7.13(b). This is modeled by including lumped elements circuits representing the cable distance between the loads. Each cable section represents a propagation delay. For low frequency components these propagation delays are relatively small and the spectral components will add up. For higher frequency components, the propagation delays become relatively

larger, resulting in diversity of these components. Diversity is also a function of variation in products and voltage drop over cables, but this can be included in the models. This means that diversity could be modeled.

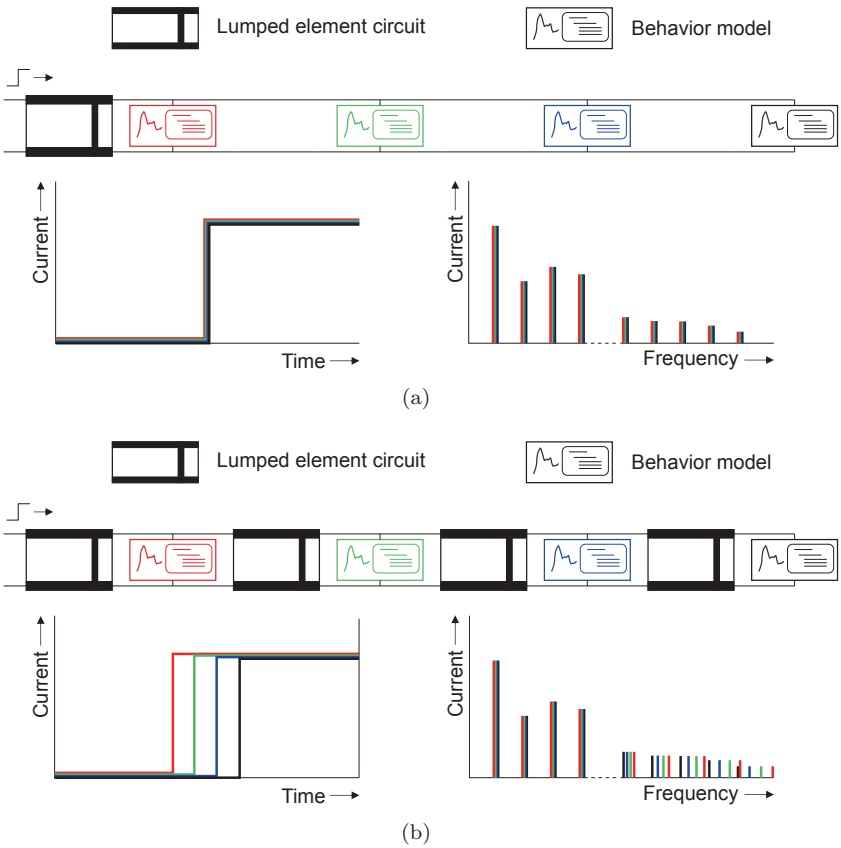

Figure 7.13: Application of the modeling concept: (a) similar loads connected in parallel at one point; and, (b) similar loads distributed along cable.

Chapter 8

Conclusions and directions for further research

This chapter will summarize the conclusions that can be drawn from the research that has been described in this thesis. Moreover some directions for further research will be suggested.

8.1 Main results of thesis

The grid operator is responsible for the voltage quality and the consumer of electrical power is responsible for the current quality, but both are strongly related. Standards are supposed to reflect these responsibilities, but evaluation of the standards shows that the voltage quality requirements and the equipment Electromagnetic Interference (EMI) requirements are weakly connected. Voltage requirements consider the Point of Interface (POI), but equipment EMI requirements consider the equipment terminals. This means that the Power Distribution User Network (PDUN) of for instance large complex facilities is not taken into account. Moreover, the current standards for supply and consumption of electrical power do not anticipate the use of similar nonlinear electronic equipment on a large scale. An increasing risk of conducted EMI in modern PDUNs is resulting as more interaction will occur via the PDUN. For determining the risk of EMI not only the long term conditions, but also the short term variations needs to be considered. This applies to large buildings but especially to complex installations. A single event causing a temporary but significant deviation of at least one Power Quality (PQ) parameter may result in interference (malfunctioning or disturbance) of equipment.

Standardization is based on dominant linear behavior. The International Electrotechnical Commission (IEC) 61000-3 series addresses nonlinearities, but only for large loads. The aggregation of many low power nonlinear loads switching synchronously is not covered. The interface of low power electronic loads is basically a capacitor behind a rectifier bridge. During a cold start, it is a

short causing high inrush currents. In steady state, interaction between current and voltage results in synchronization effects of low power electronic loads. Deviations in the voltage waveform are a function of impedance of PDUN and current, where the current waveform is also dependent on the distorted voltage waveform.

Steady state voltage and current waveforms can be described by Fourier series. Doing this for periodic non-sinusoidal current and voltage shows that each harmonic component and Direct Current (DC) component is included in the expressions for Root Mean Square (RMS) voltage and current as well as for power and Power Factor (PF). This means that $PF = 1$ if and only if all harmonic components, including DC, present in the voltage are also present in the current and every k^{th} harmonic current is in phase with corresponding k^{th} harmonic voltage. To describe the integrity of waveforms a combination of measures of at least harmonic distortion, Voltage Total Harmonic Distortion (V-THD) and Current Total Harmonic Distortion (I-THD), and the deviation of the peak value from the RMS value, Crest Factor (CF), is needed. However, case studies show that the current design approaches of PDUNs do not anticipate on the large contribution of harmonic distortion. The distortion significantly contribute to the total apparent power and the PDUN has to cope with sharp, short and high current peaks from large numbers of similar low power equipment. Furthermore, significant voltage rises occur due to current injection by a Photovoltaic (PV) system at a farm resulting in damaged equipment. Moreover, a case study with the Power Drive System (PDS) for a ventilation system showed significant conducted emission from the PDS in the frequency band from 2 kHz to 150 kHz. As a result the PV system in the same PDUN was malfunctioning. The severity of the observed phenomena in the case studies is dependent on the broadband PDUN impedance and the dynamic broadband behavior of connected equipment. Therefore new models are needed to cover this dynamic broadband behavior of the PDUN with its connected equipment.

Power engineers typically split up the impedance of cables into a real and an imaginary component which is valid only for 50 (or 60) Hz. The generic network impedance as in IEC 60725 is defined for the fundamental frequency as 0.24 + j0.15 Ω for phase and 0.16 + j0.1 Ω for neutral. For evaluating conducted emission parameters a broader description valid for higher frequencies is needed. An addition is found in standardized networks used to provide a defined impedance at the terminals of the Device Under Test (DUT). The covered frequency bands in civil standards start at about 9 kHz and ends between 10 to 100 MHz. These standardized networks represent the impedance between phase and reference or neutral and reference as seen by the DUT. In civil standards the standardized network is referred to as Artificial Mains Network (AMN) and is specified in International Special Committee on Radio Interference (CISPR) 16. It is based on experiments performed in the 1930's and therefore represents only networks with linear loads. Nonlinear loads create a time dependent impedance which is not taken into account. In standards for

professional applications the standardized network starts often already at 30 Hz and is referred to as Line Impedance Stabilization Network (LISN) and is specified in for instance the Military Standard (MIL-STD) 461. The LISN is applied in automotive, aerospace and many national military standards. The equivalent impedance of the standardized networks is a single circuit with lumped components. An AMN or LISN is basically a capacitor at low frequencies, a resistor (often 50 Ω) for high frequencies and an inductor, which represents the power cables, for medium frequencies. To model the cables, their length, L, has to be considered if it is electrically long, ($L > \frac{\text{shortest } \lambda}{2\pi}$). Then transmission line properties like delay and reflection need to be taken into account. This is done by using distributed lumped element circuits in which each subcircuit is electrical small. The 4 lumped elements, series resistance R, series inductance L, shunt conductance G and shunt capacitance C, are extracted from transmission line equations.

The inductance of the cable carrying high current give rise to voltage transients when this cable is cut from the supply. The transients will propagate on the disconnected cable to the electrical equipment connected to it. Transmission line equations are used for deriving parameters for describing the propagation of transients. There exist two modes of propagation, Differential Mode (DM) and Common Mode (CM). In DM the transients flow in opposite directions over the phase and neutral wires in the cable. In case of two wires one wire act as return resulting in a voltage difference between the wires. In CM the transients flow in same direction over wires in the cable and the environment acts as return. As a result there is no voltage difference between wires in the cable, but between the wires and environment. As the environment provides the CM transient various ways to split up and to flow back, it is hard to trace the return path. The combination of DM and CM create the nonsymmetrical voltage. In 1987, research on transients showed the occurrence of nonsymmetrical transients upto and larger than 3000 V in the PDUN resulting from lightning and switching events. As a result of that research, electronic equipment is equipped with protection against electrical fast transients and bursts as well as surges, covered in IEC 61000-4-4 and IEC 61000-4-5 standards. The first publication did not include CM transients as these were not measured yet. The risetime of the transient voltage defined in IEC 61000-4 series is 5 ns, which is much faster than any of the phenomena taken into account by PQ analyzers. Therefore the propagation of faster transients inside the PDUN cannot be evaluated using conventional PQ analyzers and a high-speed multichannel data logger for PQ measurements has been designed. Laboratory measurements are performed on an extension cable above ground plane showing faster dampening of the symmetric mode, or DM, voltage transients, than of asymmetric mode, or CM, voltage transients. By using varistors representing the electronic equipment shows that on one hand the varistors suppress the fast transients, but on the other hand transients by-pass the varistors due to mode conversions. Literature on assessing the impact of fast transients generated in an act of terrorism or sabotage show that propa-

gation of fast transients inside the PDUN can happen as they are generated inside or near the PDUN. Other ways for generation of fast transients inside the PDUN are switching large powers on cables feeding equipment in large complex systems. Due to mode conversions and coupling mechanism between cables, there is still a risk of EMI. The high-speed multichannel data logger which has been designed for these high-speed PQ measurements can be used for further research on fast transients including CM current measurements.

To reduce the complexity in the design of PDUNs and to simulate large PDUNs feeding thousands of small electronic devices, gray box models are developed. The models are developed for two kinds of nonlinear loads commonly found, a load with a rectifier bridge without Power Factor Correction (PFC) and a load with a rectifier bridge with active PFC. They describe the steady state behavior of nonlinear loads and take into account synchronous switching effects. The models do not cover emission above 10 kHz. The models contain only information on the design of the Device Under Modeling (DUM) as far as it is relevant to the behavior observed at the terminals. The electrical components commonly found in loads similar to the DUMs are used in the gray box models. Therefore they can represent a diversity of loads and do not need considerable intellectual properties. Parameterization of the models is done by measurements on the PDUN interface of the DUM and parameterization scripts. The developed gray box models produce simulation results being close to the measurement results, while being computational light. Macro models can be created from the developed gray box models to use them in simulation tools. Then, the macro models together with the models for the PDUN infrastructure can be used in simulation tools to simulate large groups of loads. Based on the obtained results, the models for the infrastructure of the PDUN and the developed gray box modeling with parameterization scripts can be converted into design tools for PDUNs. This will be useful for electrical design engineers who have to design a power supply network in a large and complex installation.

8.2 Impact of this research work

This section is an application note of the research results presented in this thesis. In the Introduction was mentioned that in 2007 the annual waste due to inadequate power quality management was € 150 billion. Estimation of costs due to loss of production, repair of equipment, modifications in PDUN, loss of prestige, loss of credibility and so on has not been considered in this thesis. However, the pitfalls can be elucidated as the case studies discussed in this thesis are examples which have the potential to lead to unexpected costs.

The conventional approach in design of PDUN, and in general for power distribution networks, is based on the Displacement Power Factor (DPF). The underlying assumption is that virtually all loads have linear behavior. As such, distortion will have an insignificant contribution to the total apparent power. Then, the wrong assumption is made that modern low power equipment does

have the same amount of apparent power as rated real power. The apparent power, which needs to be available and transported through the PDUN, is much higher than the rated real power. The distortion will significantly contribute to the total apparent power. A feedback loop is created as any resulting deviation in voltage waveform due to voltage drop over transformers and feeding lines of the PDUN will in turn influence the current waveform and vice versa. This was not foreseen in the design of PDUN the new Carré building of University of Twente. Its transformers got overheated and dual zero crossings were present in the voltage waveform. As zero crossing are used for synchronization interference result due to tripping equipment. Other unwanted effects which may show up are degradation of lifetime of 'Y' capacitors in EMI filters and malfunctioning of the Residual Current Device (RCD) resulting from large leakage currents, malfunction of fuses due to change in sensitivity and overheating of conductors. As a result equipment does not operate as intended, get damaged or catches on fire. To prevent this, extra transformers were installed, which on itself is a costly operation.

A mobile generator is used to simulate a weak PDUN as it has a relative high internal impedance and less available power. As a result of the peak current drawn by the power electronics in low power equipment, a significant voltage drop arose over the impedance of the PDUN. It is much easier to get the unwanted consequences mentioned above for the case of the new Carré building of University of Twente. Furthermore, the inrush currents during cold start of the low power equipment can result in stability problems. In critical systems, like power backup systems in hospitals, in Information and Communication Technology (ICT) centres and in utilities, this has to be taken into account in the design to maintain reliable operation. The importance of this is also stressed by [76] reporting failing Uninterruptible Power Supplys (UPSs) and equipment due to distortion caused by electronic equipment.

Not only consumption of power but also injection of power has an effect on the PQ in the PDUN. Especially rural areas are susceptible to EMI as the grid impedance and consequently the impedance in the PDUN in those areas is higher. The PDUN is connected to the grid via relative long power cables. The higher the grid impedance, the more isolated the PDUN becomes, the less is its coupling to the grid. In the case studies an example of over voltage due to high current injection resulted in malfunctioning and overheating of other equipment. It is very common to take into account voltage drop, but not voltage rise which is showing up with the introduction of local power generation. Now the current is flowing into the other direction.

The results of a naval vessel case study showed two effects resulting from switching actions, short term voltage fluctuations and temporary high distortion levels. The severity of these phenomena is dependent on the available power and impedance. This should also be taken into account for PDUNs in rural areas and in decentralized or micro grids with local power generation systems. Besides, the case study investigated the use of Commercial Off the Shelf (COTS) equipment onboard of the Hr. Ms. Holland patrol ship. This is

economical interesting as it may result in less expensive applications on naval vessels and therefore saving on costs for defense equipment.

Conducted emission is not limited to harmonic frequencies as is illustrated by the case study of the PDS disturbing a PV system in the frequency range above 2 kHz. Also other high frequency phenomena as for instance the propagation of transients as discussed in this thesis have to be taken into account. All the above described phenomena are not properly covered in the current design approaches and standardizations. The work in this thesis provides a broadband description of the PDUN impedance and dynamic broadband behavior of equipment. This can be used for developing new design approaches and standards. This also means that the currently uncovered area between the POI and the terminals of the equipment, the PDUN, has to be included.

8.3 Directions for further research

The thesis describes the work done, but the end of the thesis is not the end of the work described in the thesis.

The basics for modeling the PDUN with equipment are introduced. The description of cable model components is given including comments on applications of the models with respect to electrical length and physical length of cables. Gray box models are developed for two common loads found in PDUNs. Not only model components are described, but also simulations and verifications with measurements. Simulation and verification of a modeled PDUN without loads and with loads has not been performed and is left for future work. It is recommended to further develop the models for different loads as well as for different PDUNs and then to simulate and verify a complete model of a PDUN with loads. Furthermore, models have to be developed for equipment generating electrical power. It has to be checked if the same approach for developing gray box models for loads can be applied on local power generators.

The transient study is merely based on literature study and transient measurements using a transient generator. Measurements in the field are not performed. In the thesis a design for a high-speed multichannel data logger for PQ measurements is proposed. This design has to be implemented such that it can be used for further research on fast transients including CM current measurements.

Further research is needed to be able to determine the suitability of and the conditions for using COTS equipment on naval vessels. Considered are only voltage fluctuations, power frequency fluctuations and harmonic distortion. Another aspect not covered is insulation. As the power supply networks on a naval vessel are unearthed COTS equipment with EMI filters cannot be connected to an Insulation Terre (IT) without any measures. Capacitors to earth result in leakage currents degrading the insulation, but simply cutting the capacitors results in higher risks of EMI [77].

Bibliography

[1] *The Electromagnetic Compatibility (EMC) Directive*, Official Journal of the European Union, European Parliament and of the Council Std. 2004/108/EC, 2004.

[2] R. Targosz and J. Manson, "Pan-european power quality survey," in *9th International Conference on Electrical Power Quality and Utilisation (EPQU)*, Oct. 2007, pp. 1 – 6.

[3] (2013) Iop elektromagnetische vermogenstechniek (iop emvt) |agentschap nl. [Online]. Available: http://www.agentschapnl.nl/nl/programmas-regelingen/iop-elektromagnetische-vermogenstechniek-iop-emvt

[4] *Voltage characteristics of electricity supplied by public electricity networks*, CENELEC Std. EN 50 160, 2010.

[5] M. Olofsson, "Power quality and emc in smart grid," in *10th International Conference on Electrical Power Quality and Utilisation (EPQU 2009)*, Sep. 2009, pp. 1 – 6.

[6] M. Bollen, "Overview of power quality and power quality standards," in *Understanding Power Quality Problems:Voltage Sags and Interruptions*. Wiley-IEEE Press, 2000, pp. 1 – 34.

[7] (2013) Nma - netherlands competition authority. [Online]. Available: http://www.nma.nl/en/default.aspx

[8] (2013) The international electrotechnical commission website. [Online]. Available: http://www.iec.ch/

[9] *Testing and measurement techniques – Power quality measurement methods*, International Electrotechnical Commission Std. IEC 61 000-4-30, 2008.

[10] *Guide for the application of the European Standard EN 50160*, CENELEC Std. CLC/TR 50 422, 2003.

[11] *IEEE Recommended Practices and Requirements for Harmonic Control in Electrical Power Systems*, Institute of Electrical and Electronics Engineers Std. IEEE 519, 1993.

[12] *Characteristics of Shipboard Electrical Power Systems in Warships of the North Atlantic Treaty Navies*, NATO Std. STANAG 1008, Rev. Edition 9, Aug. 2004.

[13] *Electrical and Electromagnetic Environmental Conditions*, NATO Std. AECTP 250, Rev. Edition 2, Jan. 2011.

[14] L. Cividino, "Power factor, harmonic distortion; causes, effects and considerations," in *14th International Telecommunications Energy Conference (INTELEC '92)*, Oct. 1992, pp. 506 – 513.

[15] *Limits – Limits for harmonic current emissions (equipment input current $\leq$ 16 A per phase)*, International Electrotechnical Commission Std. IEC 61 000-3-2, Rev. ed. 3, 2005.

[16] *Limits – Limits for harmonic currents produced by equipment connected to public low-voltage systems with input current $>$ 16 A and $\leq$ 75 A per phase*, International Electrotechnical Commission Std. IEC 61 000-3-12, Rev. ed. 1, 2004.

[17] *Consideration of reference impedances and public supply network impedances for use in determining disturbance characteristics of electrical equipment having a rated current $\leq$ 75 A per phase*, International Electrotechnical Commission Std. IEC 60 725, Rev. ed. 2, 2005.

[18] A. Larsson and M. Bollen, "Emission (2 to 150 khz) from a light installation," in *Proceedings 21st International Conference on Electricity Distribution (CIRED 2011)*, Jun. 2011, p. paper 0250.

[19] J. Meyer, P. Schegner, and K. Heidenreich, "Harmonic summation effects of modern lamp technologies and small electronic household equipment," in *Proceedings 21st International Conference on Electricity Distribution (CIRED 2011)*, Jun. 2011, p. paper 0755.

[20] S. Rönnberg, M. Wahlberg, and M. Bollen, "Total conducted emission from a customer in the frequency range 2 to 150 khz with different types of lighting," in *Proceedings 21st International Conference on Electricity Distribution (CIRED 2011)*, Jun. 2011, p. paper 0173.

[21] R. Timens, F. Buesink, V. Cuk, J. Cobben, W. Kling, and F. Leferink, "High harmonic distortion in a new building due to a multitude of electronic equipment," in *2011 IEEE International Symposium on Electromagnetic Compatibility (EMC)*, Aug. 2011, pp. 393 – 398.

[22] ——, "Large number of small non-linear power consumers causing power quality problems," in *EMC Europe 2011 York*, Sep. 2011, pp. 592 – 596.

[23] (2013) The pqube - live world map of power quality website. [Online]. Available: http://map.pqube.com/

[24] R. Timens, F. Buesink, and F. Leferink, "Voltage quality in urban and rural areas," in *2012 IEEE International Symposium on Electromagnetic Compatibility (EMC)*, Aug. 2012, pp. 755 – 759.

[25] (2013) The information technology industry council website. [Online]. Available: http://www.itic.org/

[26] R. Timens, F. Buesink, V. Cuk, J. Cobben, and F. Leferink, "Diversity and summation of large number of energy saving lighting," in *2012 Asia-Pacific Symposium on Electromagnetic Compatibility (APEMC)*, May 2012, pp. 229 – 232.

[27] R. Timens, F. Buesink, and F. Leferink, "Effect of energy saving lights on power supply," in *2012 International Symposium on Electromagnetic Compatibility (EMC EUROPE)*, Sep. 2012, pp. 1 – 4.

[28] J. Blum and B. Kübrich, "In coburg gehen die uhren anders," in *Elektrojournal*, no. 6, Jun. 2004, pp. 77 – 79.

[29] J. Desmet, G. Vanalme, K. Stockman, and R. Belmans, "Analysis of the behaviour of fusing systems in the presence of nonlinear loads," in *International Conference on Power Electronics, Machines and Drives 2002*, Jun. 2002, pp. 616 – 619.

[30] Y. Xiang, V. Cuk, and J. Cobben, "Impact of residual harmonic current on operation of residual current devices," in *10th International Conference on Environment and Electrical Engineering (EEEIC) 2011*, May 2011, pp. 1 – 4.

[31] P. Korovesis, G. Vokas, I. Gonos, and F. Topalis, "Influence of large-scale installation of energy saving lamps on the line voltage distortion of a weak network supplied by photovoltaic station," *IEEE Transactions on Power Delivery*, vol. 19, no. 4, pp. 1787 – 1793, Oct. 2004.

[32] (2013) Ocean-going patrol vessels |ministry of defence website. [Online]. Available: http://www.defensie.nl/english/subjects/materiel/ships/ocean-going_patrol_vessels

[33] (2013) The integrated mast family website. [Online]. Available: http://www.thalesgroup.com/integratedmast/

[34] R. Timens, B. van Leersum, R. Bijman, and F. Leferink, "Voltage quality in a naval vessel power system during island configuration," in *2012 International Symposium on Electromagnetic Compatibility (EMC EUROPE)*, Sep. 2012, pp. 1 – 5.

[35] R. Bijman, R. Timens, and F. Leferink, "Effect of integrated mast on power quality of naval vessel in island configuration," in *2013 International Symposium on Electromagnetic Compatibility (EMC EUROPE)*, Sep. 2013.

[36] J. Prousalidis, I. Hatzilau, and S. Perros, "Harmonic electric power quality concepts for the electrified ships," in *Proceedings of International Conference on All Electric Ship (AES 2003)*, Feb. 2003, pp. 279 – 290.

[37] P. van Vugt, R. Timens, I. Stievano, F. Leferink, and F. Canavero, "Experimental characterization of cfl bulbs for power quality assessment," in *2013 IEEE International Symposium on Electromagnetic Compatibility (EMC)*, Aug. 2013.

[38] *Military Standard: Requirements for the Control of Electromagnetic Interference Characteristics of Subsystems and Equipment*, Departement of Defence (USA) Std. 461, Rev. F, Dec. 2007.

[39] C. Paul, *Introduction to Electromagnetic Compatibility*, 2nd ed., ser. Wiley series in microwave and optical engineering, K. Chang, Ed. Wiley-Interscience, 2006.

[40] A. Roc'h, "Behavioural models for common mode emi filters," Ph.D. dissertation, University of Twente, Enschede, Oct. 2012. [Online]. Available: http://dx.doi.org/10.3990/1.9789461914293

[41] P. Van Oirsouw, *Netten voor distributie van elektriciteit.* Phase to Phase B.V. (Self-published), 2011.

[42] J. R. Nicholson and J. Malack, "Rf impedance of power lines and line impedance stabilization networks in conducted interference measurements," *IEEE Transactions on Electromagnetic Compatibility*, vol. EMC-15, no. 2, pp. 84–86, 1973.

[43] J. Malack and J. Engstrom, "Rf impedance of united states and european power lines," *IEEE Transactions on Electromagnetic Compatibility*, vol. EMC-18, no. 1, pp. 36–38, 1976.

[44] *Specification for radio disturbance and immunity measuring apparatus and methods Part 3: Reports and recommendations of CISPR*, International Electrotechnical Commission Std. CISPR 16-3, Rev. ed. 1, 2000.

[45] *Specification for radio disturbance and immunity measuring apparatus and methods - Part 1: Radio disturbance and immunity measuring apparatus*, International Electrotechnical Commission Std. CISPR 16-1, Rev. ed. 2, 1999.

[46] *Military Handbook: Design Guide for Electromagnetic Interference Reduction in Power Supplies*, Departement of Defence (USA) Std. 241, Rev. B Notice 2, Dec. 2000.

[47] *Military Handbook: Design Guide for Electromagnetic Interference Reduction in Power Supplies*, Departement of Defence (USA) Std. 241, Rev. A, Apr. 1981.

[48] *Military Standard: Electromagnetic Interference Characteristics Requirements for Equipment*, Departement of Defence (USA) Std. 461, Jul. 1967.

[49] *Military Standard: Measurement of Electromagnetic Interference Characteristics*, Departement of Defence (USA) Std. 462, Jul. 1967.

[50] *Military Standard: Definitions and System of Units, Electromagnetic Interference and Electromagnetic Compatibility Technology*, Departement of Defence (USA) Std. 463, Jun. 1966.

[51] *Military Standard: Requirements for the Control of Electromagnetic Interference Characteristics of Subsystems and Equipment*, Departement of Defence (USA) Std. 461, Rev. E, Aug. 1999.

[52] *Military Standard: Test Method Standard for Measurement of Electromagnetic Interference Characteristics*, Departement of Defence (USA) Std. 462, Rev. D Notice 4, Aug. 1999.

[53] *Military Standard: Definitions and System of Units, Electromagnetic Interference and Electromagnetic Compatibility Technology*, Departement of Defence (USA) Std. 463, Rev. A Notice 2, Feb. 1995.

[54] *Military Standard: Measurement of Electromagnetic Interference Characteristics*, Departement of Defence (USA) Std. 462, Rev. Notice 3, Feb. 1971.

[55] J. Mahseredjian, V. Dinavahi, and J. Martinez, "Simulation tools for electromagnetic transients in power systems: Overview and challenges," *IEEE Transactions on Power Delivery*, vol. 24, no. 3, pp. 1657 – 1669, Jul. 2009.

[56] M. Bollen and I. Yu-Hua Gu, "On the analysis of voltage and current transients in three-phase power systems," *IEEE Transactions on Power Delivery*, vol. 22, no. 2, pp. 1194 – 1201, Apr. 2007.

[57] B. van Leersum, F. Buesink, J. Bergsma, and F. Leferink, "Ethernet susceptibility to electric fast transients," in *2013 International Symposium on Electromagnetic Compatibility (EMC EUROPE)*, Sep. 2013.

[58] J. Goedbloed, "Transients in low-voltage supply networks," *IEEE Transactions on Electromagnetic Compatibility*, vol. EMC-29, no. 2, pp. 104 – 115, May 1987.

[59] *Testing and measurement techniques – Electrical fast transient/burst immunity test*, International Electrotechnical Commission Std. IEC 61 000-4-4, Rev. ed. 3, 2012.

[60] *Testing and measurement techniques – Surge immunity test*, International Electrotechnical Commission Std. IEC 61 000-4-5, Rev. ed. 2, 2005.

[61] *Electromagnetic compatibility for industrial-process measurement and control equipment – Electrical fast transient/burst requirements*, International Electrotechnical Commission Std. IEC 801-4, Rev. ed. 1, 1988.

[62] M. Brethouwer, "Design of a high-speed multichannel datalogger for power quality measurements," Bachelor thesis, University of Twente, Jul. 2012.

[63] D. Mansson, T. Nilsson, R. Thottappillil, and M. Backstrom, "Propagation of uwb transients in low-voltage installation power cables," *IEEE Transactions on Electromagnetic Compatibility*, vol. 49, no. 3, pp. 585 – 592, 2007.

[64] D. Mansson, R. Thottappillil, and M. Backstrom, "Propagation of uwb transients in low-voltage power installation networks," *IEEE Transactions on Electromagnetic Compatibility*, vol. 50, no. 3, pp. 619 – 629, 2008.

[65] J. Hagmann, S. Dickmann, and S. Potthast, "Application and propagation of transient pulses on power supply networks," in *EMC Europe 2011 York*, 2011, pp. 7 – 12.

[66] P. van Vugt, "Behavioral models of non-linear power consuming loads," Master thesis, University of Twente, Jun. 2013.

[67] F. Canavero, "Behavioral characterization of conducted wideband electromagnetic noise of equipment connected to mains," in *IEEE EMC Benelux Chapter Workshop: EMC Kennismarkt Oost*, Oct. 2012.

[68] Y. Koyama, M. Tanaka, and H. Akagi, "Modeling and analysis for simulation of common-mode noises produced by an inverter-driven air conditioner," *IEEE Transactions on Industry Applications*, vol. 47, no. 5, pp. 2166 – 2174, Sep. 2011.

[69] L. Ran, S. Gokani, J. Clare, K. Bradley, and C. Christopoulos, "Conducted electromagnetic emissions in induction motor drive systems. i. time domain analysis and identification of dominant modes," *IEEE Transactions on Power Electronics*, vol. 13, no. 4, pp. 757 – 767, Jul. 1998.

[70] R. Kahoul, Y. Azzouz, P. Marchal, and B. Mazari, "New behavioral modeling for dc motor armatures applied to automotive emc characterization," *IEEE Transactions on Electromagnetic Compatibility*, vol. 52, no. 4, pp. 888 – 901, Nov. 2010.

[71] H. Bishnoi, A. Baisden, P. Mattavelli, and D. Boroyevich, "Analysis of emi terminal modeling of switched power converters," *IEEE Transactions on Power Electronics*, vol. 27, no. 9, pp. 3924 – 3933, Sep. 2012.

[72] (2013) The spice home page. [Online]. Available: http://bwrcs.eecs.berkeley.edu/Classes/IcBook/SPICE/

[73] (2013) Ibis open forum. [Online]. Available: http://www.eda.org/ibis/

[74] R. Erickson and D. Maksimovic, *Fundamentals of Power Electronics*, 2nd ed. Springer US, 2004.

[75] D. Maksimovic, A. Stanković, V. Thottuvelil, and G. C. Verghese, "Modeling and simulation of power electronic converters," *Proceedings of the IEEE*, vol. 89, no. 6, pp. 898 – 912, Jun. 2001.

[76] (2013) 'sluipmoordenaar' loert op noodstroom ziekenhuizen |cobouw.nl. [Online]. Available: http://www.cobouw.nl/nieuws/techniek/2012/03/07/sluipmoordenaar-loert-opnoodstroom-ziekenhuizen

[77] P. van Vugt, R. Bijman, R. Timens, and F. Leferink, "Impact of grounding and filtering on power insulation monitoring in insulated terrestrial power networks," in *2013 International Symposium on Electromagnetic Compatibility (EMC EUROPE)*, Sep. 2013.

Acknowledgments

It is not possible to personally thank everyone within this section as many, many people helped me, directly or indirectly, through the last $4\frac{1}{2}$ years to complete this work. Nevertheless, I will try and start by thanking my promotor Prof.dr.ir.ing. Frank Leferink and daily advisor and senior researcher ir. Frits Buesink for their academic and social support and fruitful discussions with me. It was not only about 'Ga aan het werk' ('Set to work') and 'Creatief proces en assimilatie' ('Creative process and assimilation') to deliver this book, but also about becoming a researcher and developing professional skills. For this both of you spend a lot of time and effort in reading, reviewing, giving important feedback on presentations, reports, papers and eventually this thesis.

I would like to thank my co-promotor Prof.dr.ir. Sjef Cobben for the cooperation throughout the project and for sharing expertise and giving feedback on the project results. I also would like to thank all members of the Committee for accepting to review my thesis and to share your time and expertise.

I would like to thank Dr.Dipl.Ing.Vladimir Ćuk for the cooperation throughout the project. Furthermore, I would like to thank the IOP-EMVT for sponsoring this project and all members for their interest in the progress and results of the project. I also would like to include here all project partners.

Part of the work are the many measurements performed in the field. For this I have been on a naval vessel, on farms, in residential environment and in industrial laboratories. I would like to thank all the engineers and technicians from the industry and all other people involved for their time, support and contribution.

My special thanks go to the students who collaborated with me in this project: Luuk van der Velde, Christiaan Teerling, Martijn Brethouwer and Pieter van Vugt. In connecting to the work of Pieter van Vugt, I also would like to thank dr. Igor Stievano for contributing on assistance and sharing expertise.

It is great to have been and to be among the members and old members of our TE group. I would like to thank Lilian Hannink for all the nontechnical support ranging from arranging things to giving social support. Furthermore, I would like to thank Eduard Bos for all the technical support which includes trips by car to lumberyards and construction of measurement setups. I also thank all other members of the TE group for all the academic support and socializing events. I should not forget here to extend my thanks to all the

people from the pink coffee corner for the useful social diversion.

Special thanks go to Mark Ruiter who has been a tower of strength for me since the first year of my bachelor study. I would also like to thank all other friends for being part of my live.

My endless gratitude goes to my grandmother, my parents, Henriëtte, Diane, Erik, all other relatives and Wieneke's relatives for commitment and encouragement. And finally, there are no words which can express my gratitude to my girlfriend Wieneke. Wieneke, you have made and still making my life invaluable. It started with a cup of coffee in the pink coffee corner ☺.

Roelof Bernardus Timens
Enschede, The Netherlands
October 11, 2013

Biography

Roelof Bernardus Timens was born in Meppel, The Netherlands, in 1984. He attended secondary school in Diever and Meppel, and obtained his 'Atheneum' diploma from 'Stad en Esch' in 2003.

Subsequently he started studying Electrical Engineering at the University of Twente, Enschede, The Netherlands. He received the BSc degree in September 2006. Afterwards he attended several elective and compulsory courses of the Telecommunication Networks Master track. In 2008 he did an internship at ASTRON, Dwingeloo, The Netherlands, analyzing and further developing microwave photonic link technology. He received the MSc degree in March 2009 for his thesis on the performance evaluation of frequency modulation and slope detection in microwave photonic links.

In April 2009 he started working as a PhD researcher in the Telecommunication Engineering group at the University of Twente. The topic of his PhD project was Power Quality and EMC. The main results of his PhD research is presented in this thesis.

Roelof Bernardus Timens is currently employed as a postdoctoral researcher in the Telecommunication Engineering group at the University of Twente. His work involves improving EMC test methods in industrial environments.

List of publications

Publications related to this thesis

1. R.C.G. Bijman, **R.B. Timens**, and F.B.J. Leferink, 'Effect of Integrated Mast on Power Quality of Naval Vessel in Island Configuration,' *International Symposium on Electromagnetic Compatibility (EMC Europe 2013)*, Brugge, Belgium, 2nd to 6th September 2013.

2. P.K.A. van Vugt, R.C.G. Bijman, **R.B. Timens**, and F.B.J. Leferink, 'Impact of Grounding and Filtering on Power Insulation Monitoring in Insulated Terrestrial Power Networks,' *International Symposium on Electromagnetic Compatibility (EMC Europe 2013)*, Brugge, Belgium, 2nd to 6th September 2013.

3. P.K.A. van Vugt, **R.B. Timens**, I.S. Stievano, F.B.J. Leferink, F.G. Canavero, 'Experimental characterization of CFL bulbs for power quality assessment,' *International Symposium on Electromagnetic Compatibility (EMC 2013)*, Denver, Colorado (USA), 5th to 9th August 2013.

4. **R.B. Timens**, F.J.K. Buesink, and F.B.J. Leferink, 'Effect of Energy Saving Lights on Power Supply,' *International Symposium on Electromagnetic Compatibility (EMC Europe 2012)*, Rome, Italy, 17th to 21th September 2012.

5. **R.B. Timens**, B.J.A.M. van Leersum, R.C.G. Bijman, and F.B.J. Leferink, 'Voltage Quality in a Naval Vessel Power System during Island Configuration,' *International Symposium on Electromagnetic Compatibility (EMC Europe 2012)*, Rome, Italy, 17th to 21th September 2012.

6. **R.B. Timens**, F.J.K. Buesink, and F.B.J. Leferink, 'Voltage Quality in Urban and Rural Areas,' *2012 IEEE International Symposium on Electromagnetic Compatibility (EMC 2012)*, Pittsburgh, Pennsylvania (USA), 5th to 10th August 2012.

7. **R.B. Timens**, F.J.K. Buesink, V. Ćuk, J.F.G. Cobben, and F.B.J. Leferink, 'Diversity and Summation of Large Number of Energy Saving

Lighting,' *IEEE 2012 Asia-Pacific International Symposium on Electromagnetic Compatibility (APEMC 2012)*, Singapore, Singapore, 21th to 24th May 2012.

8. **R.B. Timens**, F.J.K. Buesink, V. Ćuk, J.F.G. Cobben, W.L. Kling, and F.B.J. Leferink, 'Large Number of Small Non-Linear Power Consumers Causing Power Quality Problems,' *Proceedings of the 10th International Symposium on Electromagnetic Compatibility (EMC Europe 2011)*, York, UK, 26th to 30th September 2011.

9. **R.B. Timens**, F.J.K. Buesink, V. Ćuk, J.F.G. Cobben, W.L. Kling, and F.B.J. Leferink, 'High Harmonic Distortion in a New Building due to a Multitude of Electronic Equipment,' *2011 IEEE International Symposium on Electromagnetic Compatibility (EMC 2011)*, Long Beach, California (USA), 14th to 19th August 2011.

10. **R.B. Timens**, F.J.K. Buesink, V. Ćuk, J.F.G. Cobben, W.L. Kling, M. Melenhorst, and F.B.J. Leferink, 'Electromagnetic Interference in Complex Power Supply Networks,' *9th International Symposium on EMC joint with 20th International Wroclaw Symposium on EMC (EMC Europe 2010)*, Wroclaw, Poland, 13th to 17th September 2010.

Other publications

1. F.B.J. Leferink, **R.B. Timens**, and P.K.A. van Vugt, 'Grounding and filtering effects on power insulation monitoring in naval power networks,' *Proceedings of Marine Electrical and Control Systems Safety Conference 2013 (MECSS 2013)*, Amsterdam, The Netherlands, 2nd to 3rd October 2013.

2. C.H. Keyer, **R.B. Timens**, F.J.K. Buesink, and F.B.J. Leferink, 'DC Pollution of AC Mains due to Modern CFL and LED Lamps,' *International Symposium on Electromagnetic Compatibility (EMC Europe 2013)*, Brugge, Belgium, 2nd to 6th September 2013.

3. V. Ćuk, J.F.G. Cobben, W.L. Kling, and **R.B. Timens**, 'Analysis of Current Transients Caused by Voltage Notches,' *Proceedings of IEEE Power and Energy Society General Meeting (PES 2011)*, Detroit, Michigan (USA), 24th to 29th July 2011.

4. V. Ćuk, J.F.G. Cobben, W.L. Kling, and **R.B. Timens**, 'Analysis of Harmonic Current Interaction in an Industrial Plant,' *Proceedings of 21st International Conference on Electricity Distribution (CIRED 2011)*, Frankfurt am Main, Germany, 6th to 9th June 2011.

5. D.A.I. Marpaung, C.G.H. Roeloffzen, **R.B. Timens**, A. Leinse and M. Hoekman, 'Design and Realization of an Integrated Optical Frequency Modulation Discriminator for a High Performance Microwave Photonic Link,'

2010 IEEE International Topical Meeting on Microwave Photonics (MWP 2010), Montreal, Canada, 5th to 9th October 2010.

6. V. Ćuk, J.F.G. Cobben, W.L. Kling, and **R.B. Timens**, 'An Analysis of Diversity Factors applied to Harmonic Emission Limits for Energy Saving Lamps,' *14th International Conference on Harmonics and Quality of Power*, Bergamo, Italy, 26th to 29th September 2010.

7. V. Ćuk, S. Bhattacharyya, J.F.G. Cobben, W.L. Kling, **R.B. Timens**, and F.B.J. Leferink, 'The effect of inrush transients on PV inverter's grid impedance measurement based on inter-harmonic injection,' *International Conference on Renewable Energies and Power Quality (ICREPQ '10)*, Granada, Spain, 23rd to 25th March 2010.

8. V. Ćuk, J.F.G. Cobben, W.L. Kling, **R.B. Timens**, and F.B.J. Leferink, 'A Test Procedure for Determining Models of LV Equipment,' *15th International Symposium on Power Electronics (Ee 2009)*, Novi sad, Republic of Serbia), 28th to 30th October 2009.

9. **R.B. Timens**, D.A.I. Marpaung, C.G.H. Roeloffzen, and F.B.J. Leferink, 'Performance evaluation of frequency modulation and slope detection in analog optical links,' *Master thesis, University of Twente*, Enschede, The Netherlands, March 2009.

10. **R.B. Timens**, D.A.I. Marpaung, C.G.H. Roeloffzen, and W.C. van Etten, 'Design and simulation of an integrated optical ring-resonator based frequency discriminator for analog optical links,' *Proceedings of the 13th Annual Symposium of the IEEE/LEOS Benelux Chapter*, Enschede, The Netherlands), 27th to 28th November 2008.

ISBN: 978-90-365-0719-6
ISSN: 1381-3617
CTIT Ph.D. Thesis Series No. 13-265

CTIT